Landsvirkjun

LV-2025-009

Vatnajökull: Mass balance, meltwater drainage and surface velocity of the glacial year 2023-2024

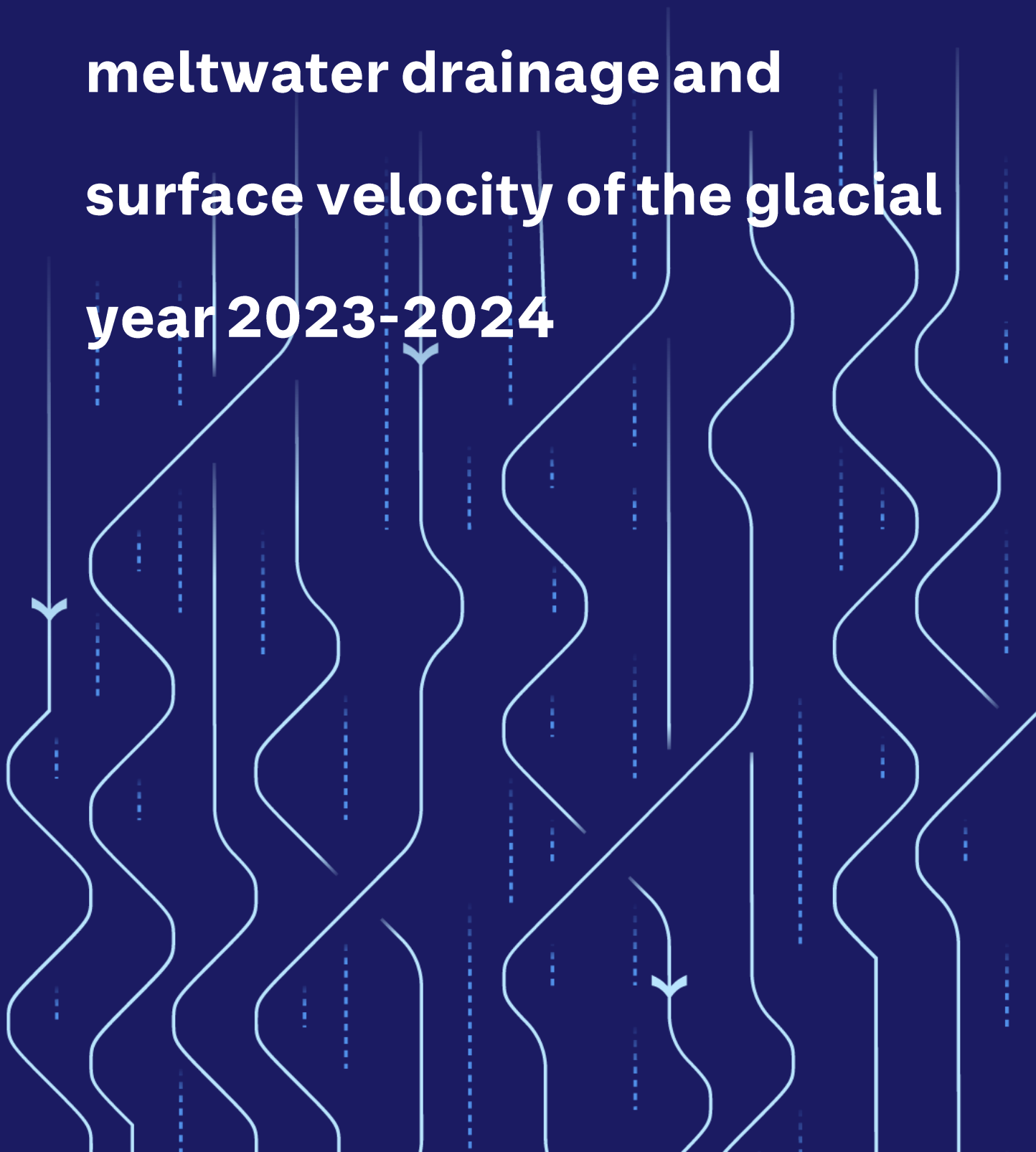

Vatnajökull: Mass balance, meltwater drainage and surface velocity of the glacial year 2023-2024

Höfundar
Finnur Pálsson
Andri Gunnarsson
Eyjólfur Magnússon
Sveinbjörn Steinþórsson
Hlynur Skagfjörð Pálsson

Dagsetning
Janúar 2025

Lykilsíða

Skýrsla LV nr	LV-2025-009	**Dagsetning**	Janúar 2025
Fjöldi síðna	56 s.	**Upplag**	1
Dreifing	[X] Birt á vef LV	[ ] Opin	[ ] Takmörkuð til [Dags.]
Titill	Vatnajökull: Mass balance, meltwater drainage and surface velocity of the glacial year 2023-2024		
Höfundar/fyrirtæki	Finnur Pálsson, Andri Gunnarsson, Eyjólfur Magnússon, Sveinbjörn Steinþórsson, Hlynur Skagfjörð Pálsson		
Verkefnisstjóri	Andri Gunnarsson		
Unnið fyrir	Landsvirkjun		
Samvinnuaðilar	Jarðvísindastofnun Háskólans		
Útdráttur	Vetrarafkoma Vatnajökuls fyrir árið 2023-24 var um 90% af meðaltali frá 1991-92, þar sem flest nýleg ár hafa haft hærri vetrarafkomu en meðaltalið. Sumarleysing yfirborðs var 91% af meðaltali frá 1995 og var meðal lægri leysingarára á mælitímabilinu. Ársafkoma var neikvæð, eða 62% af meðaltali frá 1995. Mælingar á yfirborðshraða benda til þess að Dyngjujökull sé að hefja fyrstu stig jökulhlaups og gæti lokið slíkri hringrás á næstu árum.		
Lykilorð	Vatnajökull, jöklar, jöklarannóknir afkoma, leysing, afrennsli, yfirborðshraði		

Samþykki verkefnisstjóra
Landsvirkjunar

VATNAJÖKULL:
Mass balance, meltwater drainage and surface velocity of the glacial year 2023_24

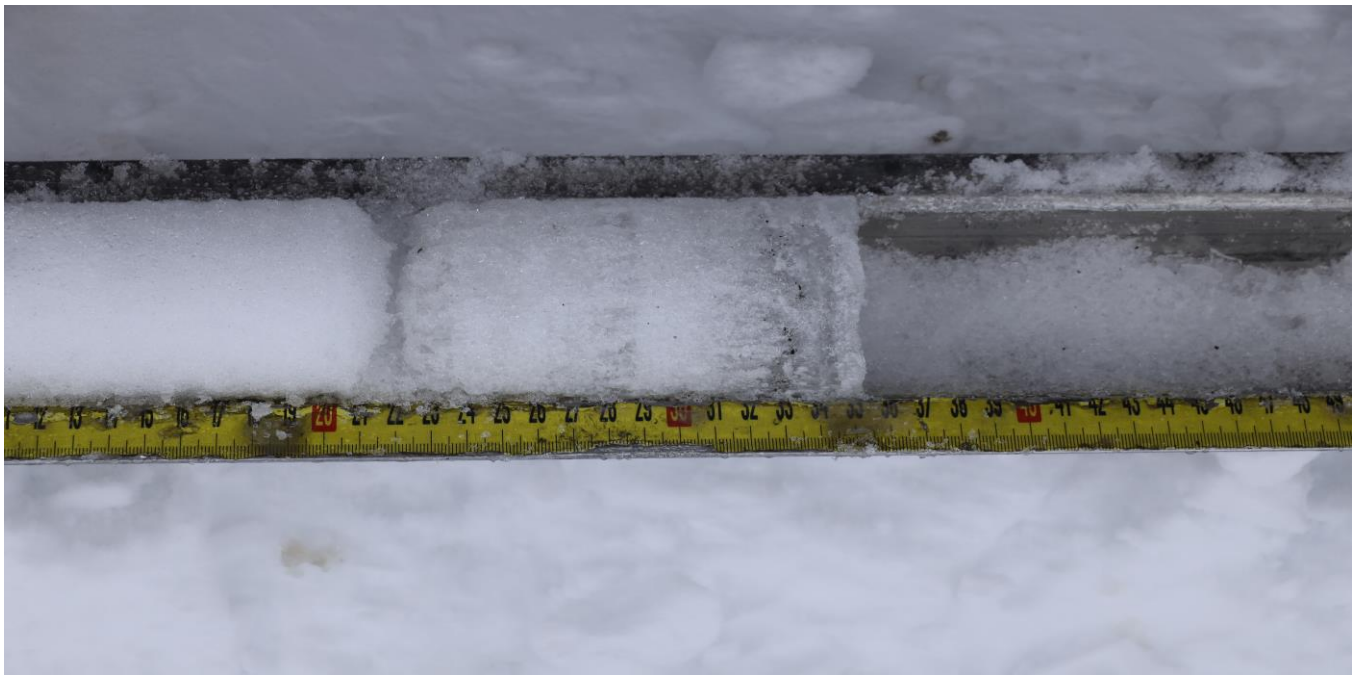

Institute of Earth Sciences
University of Iceland
and
National Power Company

Finnur Pálsson
Andri Gunnarsson
Eyjólfur Magnússon
Sveinbjörn Steinþórsson
Hlynur Skagfjörð Pálsson

RH-09-24

Contents:

Figures:

Tables:

Appendixes:

1. **INTRODUCTION**

In 1992 (glacial year 1991_92) a program of surface mass balance measurements was started for Vatnajökull by the Science Institute University of Iceland (now Institute of Earth Sciences, IES) in collaboration with the National Power Company (NPC). For the first year the program was limited to the western part of the glacier but then expanded to include the northern outlets as well. In 1996 this study was further expanded to include southern outlets, with support from The European Union (Framework IV - Environment and Climate, TEMBA project 1996-1997). This program was extended 1998–2000 with further support from EU (Framework IV - Environment and Climate, ICEMASS project, 1998-2000). In 2000-2002 NPC and IES continued the program. In 2003-2005 IES participated in a multinational research project, which was financially supported by The European Union (EVK2-CT-2002-00152 SPICE). IES was responsible for obtaining data sets for calibration of models of the mass balance and dynamics of Vatnajökull. This work was also supported by The National Power Company of Iceland and The National Road Authority and was a continuation of the TEMBA-project of 1996-97 and ICEMASS project 1998-2001.
Since then, IES and NPC have continued a similar program. Mass balance measurements on the southeast outlet Breiðamerkurjökull is financially supported by the National Road Authority.
The aim of the collaborative work of NPC and IES is to improve understanding of the mass balance and melt water runoff from glaciers. This work in combination with energy balance measurements by NPC and IES on Vatnajökull will is used for calibration of models of the surface energy and mass balance of Vatnajökull.
This report describes the field measurements, mass balance, melt water runoff and GNSS survey, for the glaciological year 2023_24.

2. DIARY

April 30 – May 5, June 9-12: measurements of the winter balance, setup of AWSs.
June 11-12: installation of melt wires and maintenance of the lower AWS on Breiðamerkurjökull.
September 25-28, November 21- 23: summer balance measurements, take down of AWSs.

In all expeditions the locations of mass balance stakes were measured with Kinematic GNSS (or fast static GNSS) for surface velocity calculation.

The following members of staff of the Institute of Earth Sciences, University of Iceland, carried out the fieldwork on Vatnajökull: Finnur Pálsson, Sveinbjörn Steinþórsson, Eyjólfur Magnússon, with Andri Gunnarsson and Franz Fredriksson (National Power Company), Hlynur Skagfjörð (Reykjavík Rescue Team) and Eiríkur Finnur Sigursteinsson.
Volunteers in the Iceland Glaciological Society Spring expedition to Vatnajökull helped in the field work in June.

Field work in spring was done in favorable conditions, except that this time “Svítan” (the cabin on skis) was recently destroyed, so accommodation was the snow track and a pop-up kitchen in a container. The extraordinary autumn weather, dry and at times with high northern wind, set conditions such that the autumn field work was postponed till late November as a last resort. In 4 days of temperatures ~-15 - -20 °C and similar numbers ms^{-1} for wind speed most of the sites were visited, but 8 sites at lower elevation were left out due to lack of snow (not secure for travel). The leftover sites will be visited in early 2025.

3. MASS BALANCE MEASUREMENTS

The purpose of the mass balance measurements is to describe the temporal and spatial distribution of the components of the mass balance. The mean annual values of the components and their variation from year to year are analyzed and related to meteorological conditions and climatic variability. The results are used in studies of changes in the glacier volume, estimates of meltwater contribution to glacial rivers, mass balance modeling, evaluation of altitudinal and regional variations of mass balance in response to climatic variations, and to assess the hydrometeorological and dynamic response of the ice cap to climate change.

The mass balance was determined by a stratigraphic method, measuring changes in thickness and density relative to the summer surface. The winter balance was estimated by drilling ice cores through the winter layer in the spring. Ablation was monitored from markers; snow stakes were put up on the glacier and wires were drilled down in the ablation area. The summer balance was measured in the autumn.

3.1 Methods

Measurements of the surface mass balance on a large ice cap like Vatnajökull are impractical in terms of cost with conventional techniques and sampling density that are typically used on small glaciers. The spatial variability of the mass balance may, however, be predictable on the flat large outlets of such an ice cap given data on several profiles extending over the elevation range of the glacier. The precipitation generally increases with elevation and decreases with the distance from the coast, but both the distribution of snowfall and redistribution of snow by drift depend on the prevailing wind direction during the winter. The summer melting depends mainly on the altitude and the albedo of the glacier surface. Therefore, we have used observations along a limited number of flowlines which span the elevation ranges of the outlets. Each profile describes the variation with elevation, but together they also describe the lateral variation of the mass balance. Recently, modern over-snow vehicles and helicopters have allowed fast traverses to ensure successful fieldwork despite frequently poor weather conditions. The error for individual point measurement is estimated ~30 cm_{we} for both summer and winter balance. The error for the glacier wide specific mass balance, based on area integral of mass balance, is however considered smaller, since the error for individual survey sites is independent.

The winter mass balance (b_w) is defined as the mass of snow accumulated during the winter months, the summer balance (b_s) is the mass balance during the summer, and the net balance (b_n) is defined as their sum. The specific mass balance is expressed in terms of the equivalent thickness of water. All mass balance components apply to a time interval between given measurement dates, which are not fixed from one year to another. The dates in the autumn are separated by approximately one calendar year, which roughly coincides with the glaciological year defined as October 1st to September 30th. Snow cores are drilled in April-May through the winter layer and profiles of the density are measured. The summer balance is derived in the autumn from measurements of the changes in the snow core density during the summer in the accumulation area and from readings at stakes and wires drilled into the ice in the ablation areas.

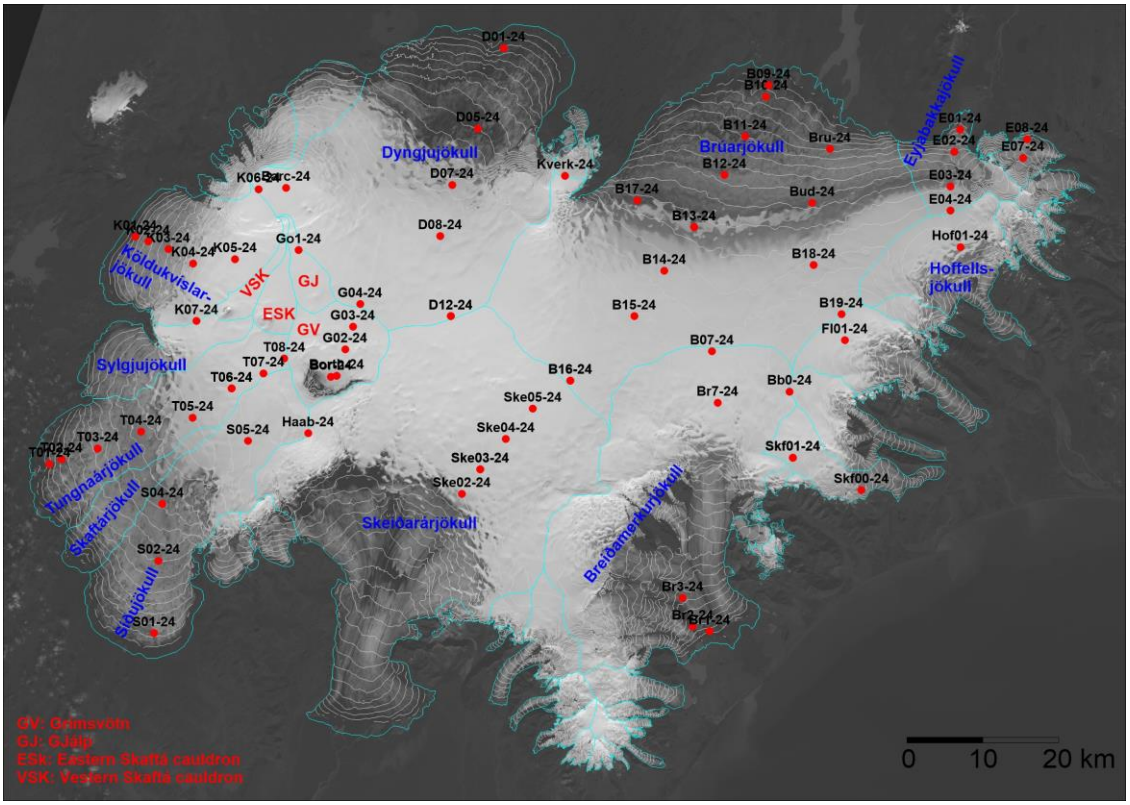

Figure 1. Outlets of Vatnajökull and location of mass balance survey sites 2023_24.

Digital maps are created for winter, summer and net balance for the whole ice cap based on the in-situ measurements. The mass balance is calculated over both the ice and water drainage basins. The summer balance over the water basin is an estimate of meltwater contribution to rivers and groundwater storage. This estimate, however, does not include precipitation that falls as rain on the glacier or snow, which falls and melts during the summer. As conventional for the north hemisphere we define the glaciological year from the start of October to the end of September next year and the period draining meltwater from the glacier during the summer from start of June through September. It would be misleading to include May in the summer period because runoff from the glacier melt in May is delayed due to refreezing during the elimination of the frost in the surface layer.

3.2 Results of mass balance measurements.

Winter mass balance measurements were done at 68 sites in spring 2023 (Fig. 1). The specific mass balance at individual sites is shown in Fig. 2. Most survey sites are on approximate central flow lines at individual outlets. The specific mass balance along the flow lines is given in Fig 3. for the glacier outlets: Síðujökull, Tungnaárjökull, Köldukvíslarjökull, Dyngjujökull, Brúarjökull (west and east), Eyjabakkajökull, Breiðamerkurjökull, SE-Vatnajökull, Skeiðarárjökull accumulation zone and the ice catchment of Grímsvötn.

Digital maps for winter, summer and net balance are shown in Figure 4. The mass balance of individual outlet is discussed in the following subsections.

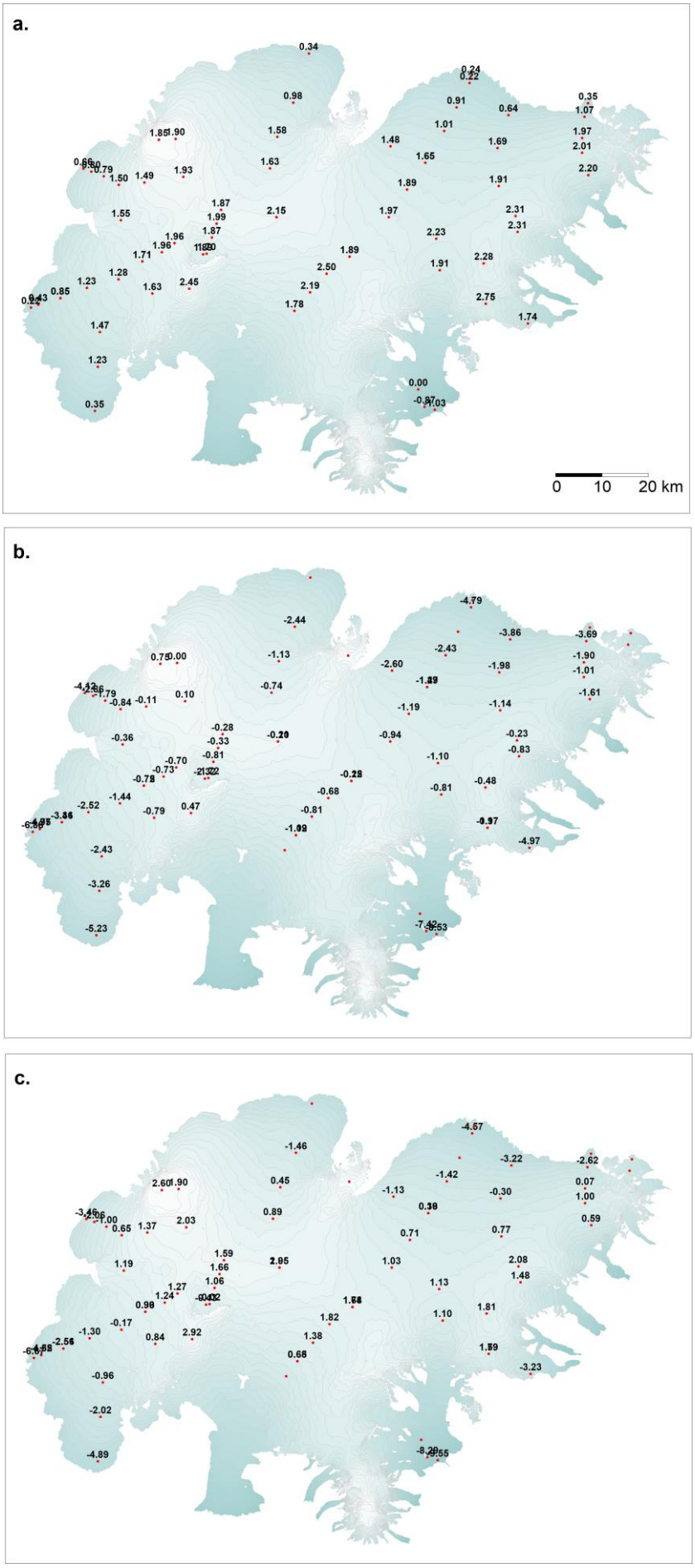

Figure 2. Maps showing point values of specific surface mass balance in m water equivalent (m_{we}), 2023_24. a. winter, b. summer, c. net balance.

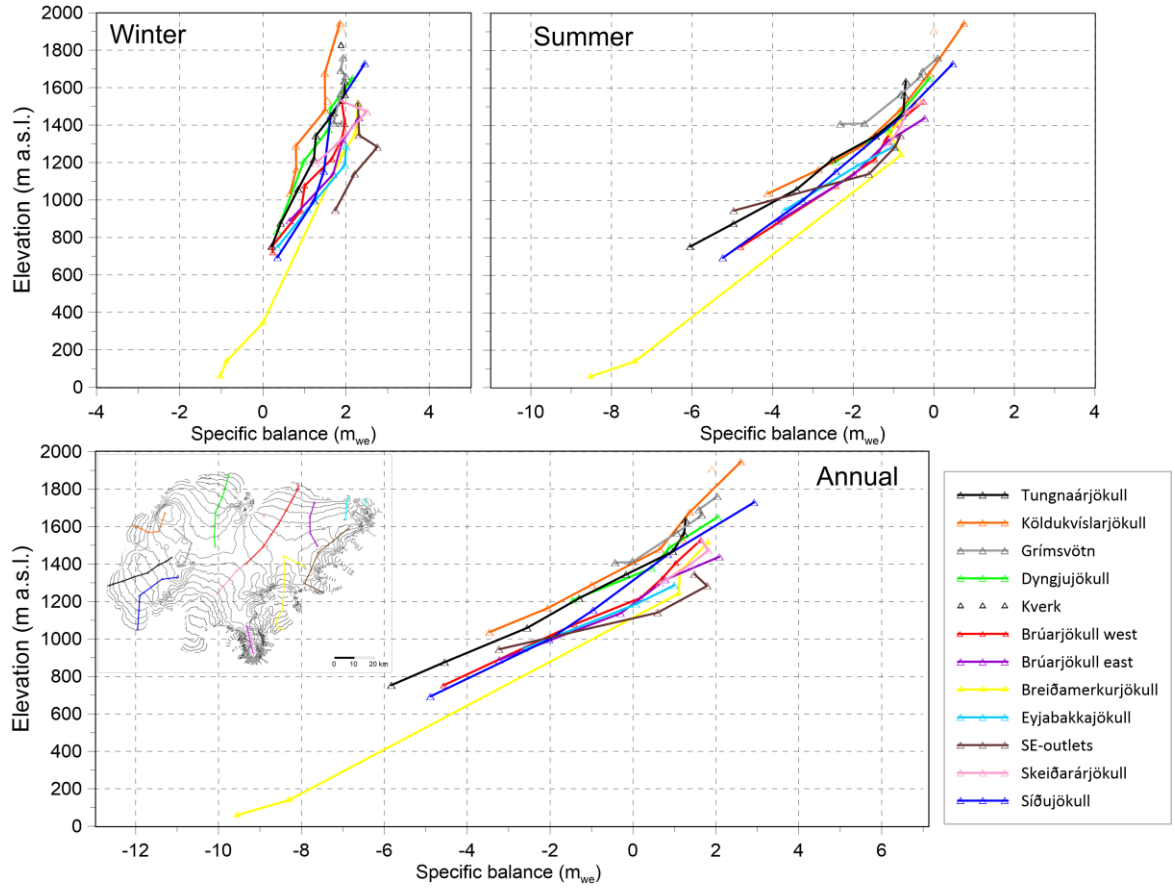

Figure 3. a. Specific mass balance (m_{we}), at survey sites along all mass balance profiles 2023_24.

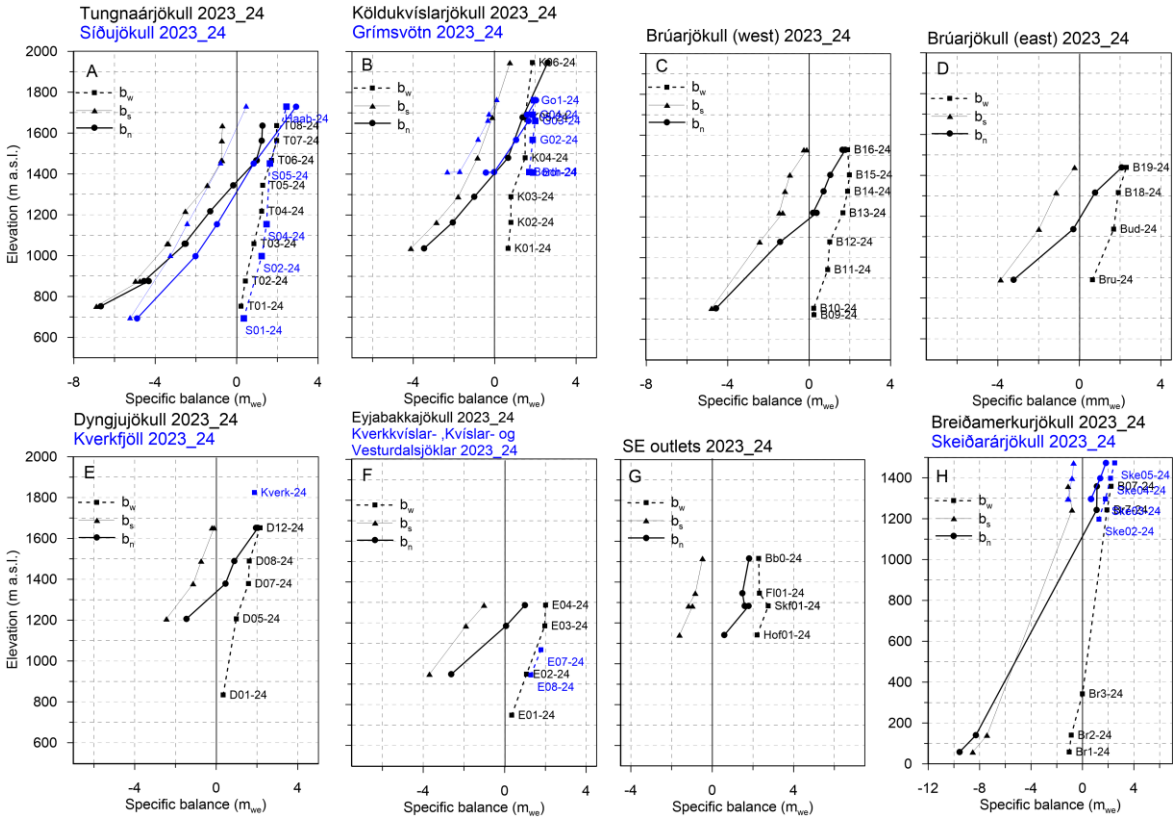

Figure 3. b. Specific point mass balance (m_{we}) 2023_24 as a function of elevation on central flow lines on Vatnajökull outlets.

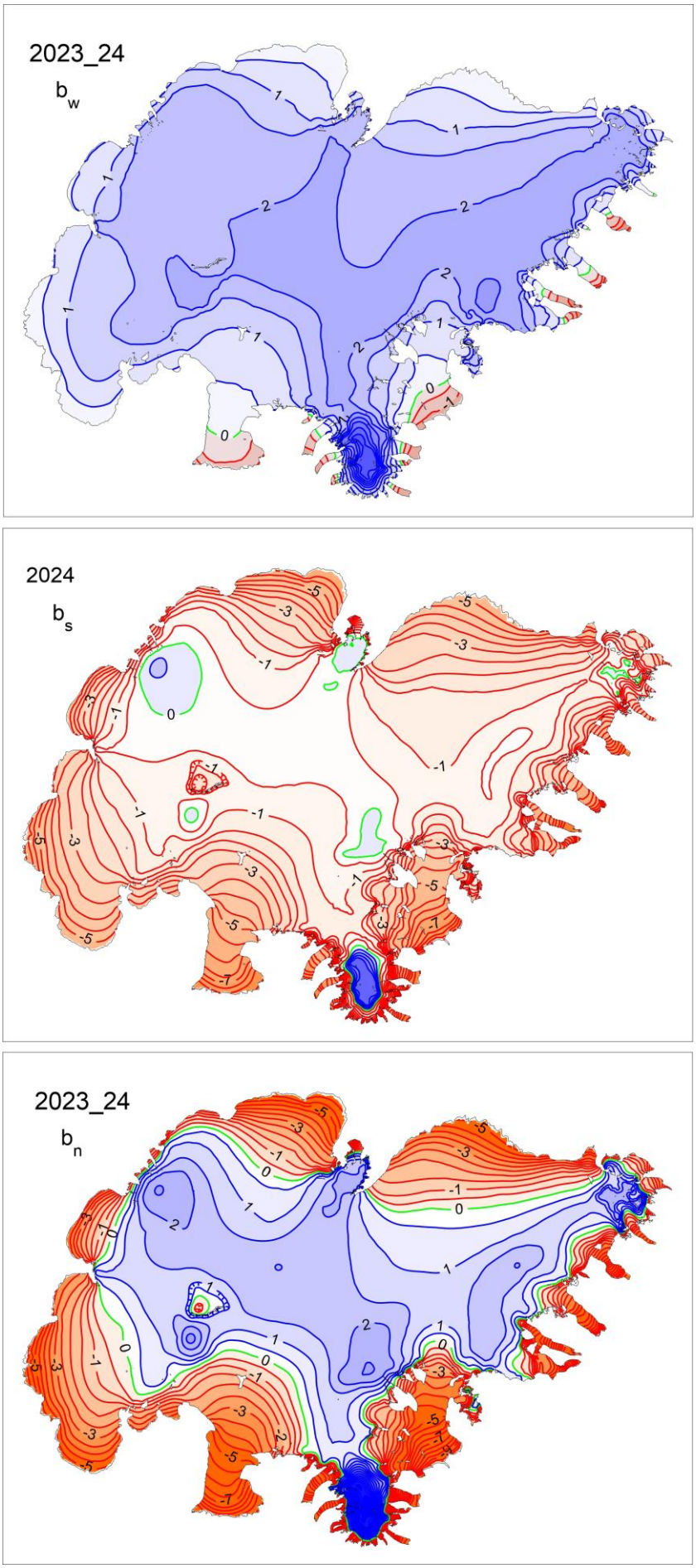

Figure 4. Specific mass balance (m_{we}) maps of Vatnajökull 2023_24. Top: winter, Centre: summer, Bottom: net balance.

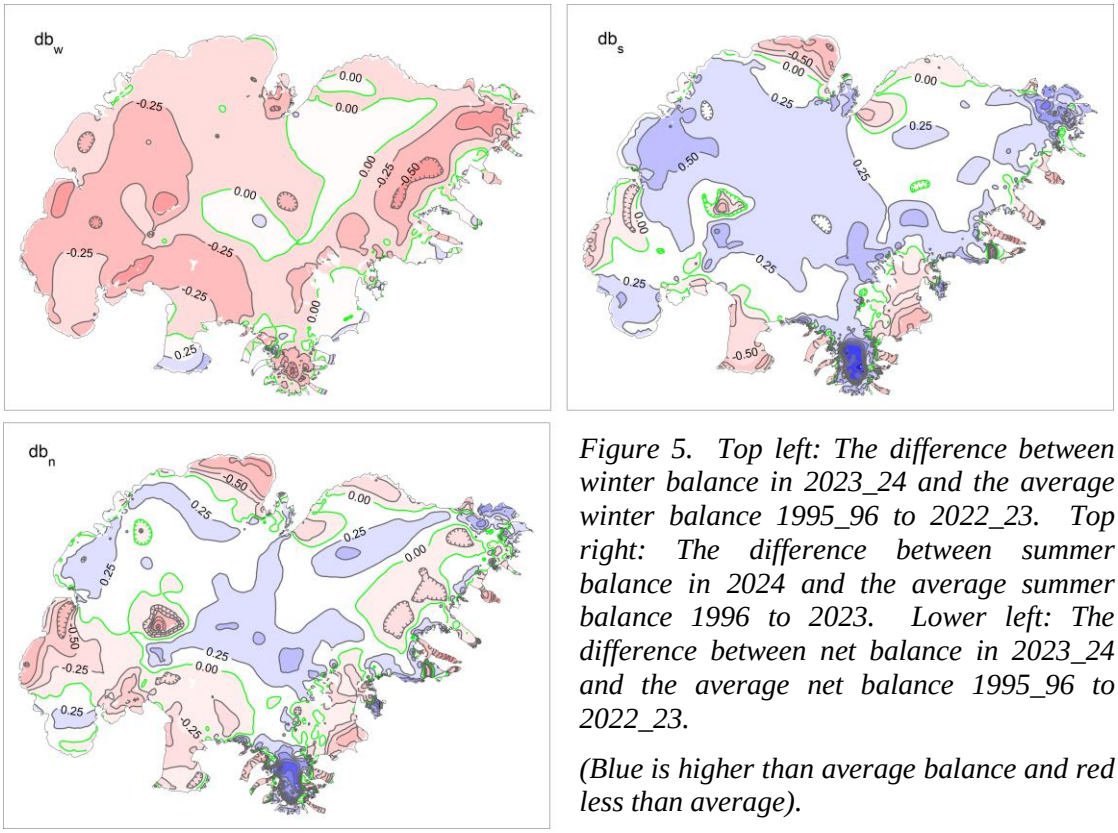

Figure 5. Top left: The difference between winter balance in 2023_24 and the average winter balance 1995_96 to 2022_23. Top right: The difference between summer balance in 2024 and the average summer balance 1996 to 2023. Lower left: The difference between net balance in 2023_24 and the average net balance 1995_96 to 2022_23.

(Blue is higher than average balance and red less than average).

A surface DEM is needed for surface area distribution and delineation of ice divides for individual outlets and catchments. The currently used surface DEM is mostly based on LiDAR survey 2010, -11 and -12 (**Jóhannesson et al. 2013), but the large set of GNSS profiles measured in spring 2023 were used to update the DEM to the 2023 elevation. That DEM cut to the glacier terminus of autumn 2023, was used in all area distributions; ice and water divides were not reworked. Although of variable accuracy locally the DEM reflects fairly accurate elevation distribution.

The winter of 2023-2024 was rather cold, with winter precipitation less than average, very little until end of December 2023.

Distribution of the winter snow was not typical (see fig. 5). In general, there was by far less snow than average in the accumulation zones of the ice cap, and by far less than average at all elevations in the west. Winter melting at the low-lying S-outlets was less than average. The beginning of summer was cold, with snowfall reducing melting, relatively sunny July, but cold and wet August. The autumn months were very dry, most of the N-Atlantic low-pressure systems passed far south of Iceland. Warm and windy days in the autumn contributed markedly to the total melt. In all this resulted in less average summer melting, especially in above ~1000 m elevation, and above ~1650 m the summer balance was positive. The resulting annual balance was close to average in the ~1000-1500 m range, slightly above average above that, but lower than average in many of the ablation zone regions. In total the mass loss was ~60 % of the average since 1995.

**Jóhannesson, T., Björnsson, H., Magnússon, E., Guðmundsson, S.,Pálsson, F., Sigurðsson, O., Thorsteinsson, T., and Berthier, E.: Ice-volume changes, bias estimation of mass-balance measurements and changes in subglacial lakes derived by lidar mapping of the surface Icelandic glaciers, Ann. Glaciol., 54, 63–74, doi:10.3189/2013AoG63A422,2013.

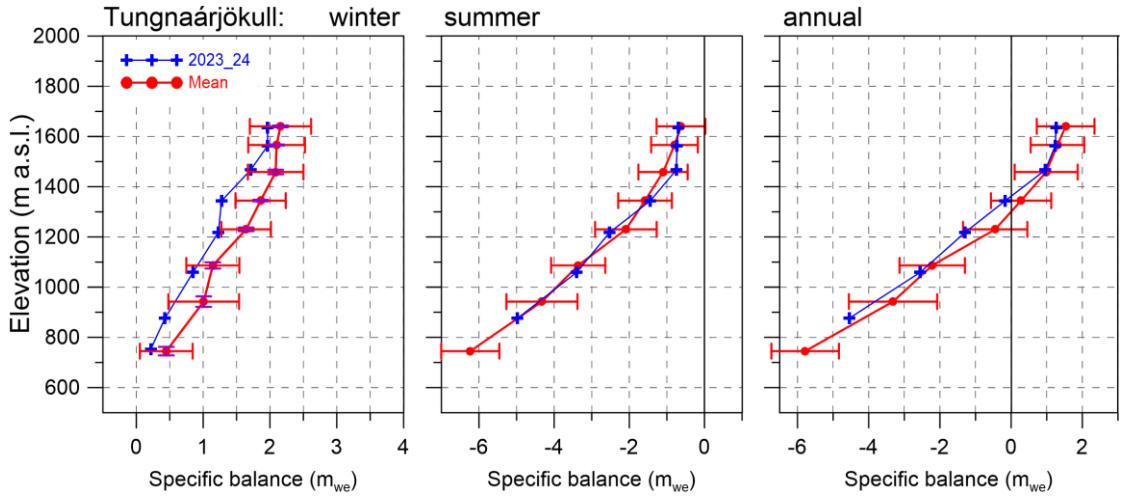

Figure 6. Mass balance at a central flow line of Tungnaárjökull 2023_234 and average mass balance 1991_92 to 2021_22 (the horizontal red lines indicate std. dev of the variability at the survey site during the survey period).

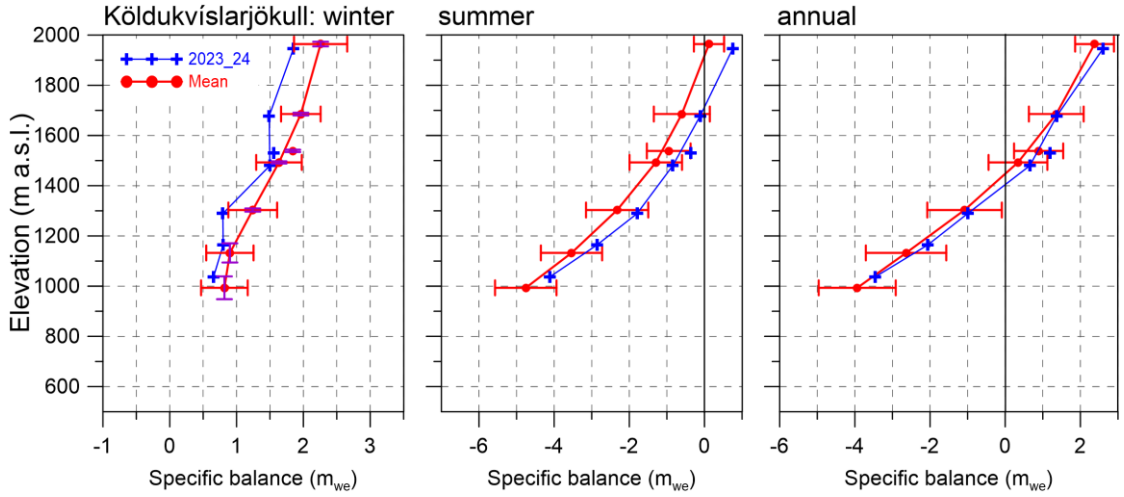

Figure 7. Mass balance at a central flow line of Köldukvíslarjökull 2023_24 and average mass balance 1991_92 to 2021_22.

3.2.1 Tungnaárjökull.

Area = 323 km^2
B_w= 0.37 km^3_{we} ; b_w = 1.15 m_{we}
B_s = -0.81 km^3_{we} ; b_s = -2.52 m_{we}
B_n = -0.44 km^3_{we} ; b_n = -1.37 m_{we}
ELA = 1365 m a.s.l. (at profile)
AAR = 35 %
(The terms are defined at the foot of this page)

Variation of mass balance along a central flow line on Tungnaárjökull is shown in Fig. 6. The winter accumulation was under the average at all survey sites, by far so, in the ablation zone. The total winter balance was only 77% of the average. Summer mass loss was not far from average at all survey sites, in total 5% less than average. This year is the 29th year out of the 32 surveyed with negative net balance on Tungnaárjökull catchment, this time 20 % more mass was lost than at average in the survey period.

3.2.2 Köldukvíslarjökull

Area = 284 km^2
B_w = 0.36 km^3_{we}; b_w = 1.28 m_{we}
B_s = -0.38 km^3_{we}; b_s = -1.36 m_{we}
B_n = -0.02 km^3_{we}; b_n = -0.08 m_{we}
ELA = 1405 m a.s.l. (at profile)
AAR = 58 %
Variation of mass balance along a central flow line on Köldukvíslarjökull is shown in Fig. 7. The winter accumulation was less than average in the accumulation zone by about 1. Std.

For each ice catchment basin, B_w, B_s and B_n are water equivalent volumes of winter, summer and net balance, ELA the equilibrium line altitude, and AAR is the accumulation area ratio.

close to average at close to the ELA zone, but almost ½ std. in the ablation zone. The total winter accumulation was ~86 % of the average. Summer mass loss was ~1 std. less than average in the accumulation zone, but by ½ to ¼ std. in the ablation zone. In total summer mass loss was ~70% of the average. This year Köldukvíslarjökull net balance was negative, as have been 27 years of the 33 surveyed, now only 17% of the mass loss in an average year since 1991-92.

3.2.3 Dyngjujökull

Area = 1026 km^2
B_w = 1.49 km^3_{we} ; b_w= 1.45 m_{we}
B_s = -1.54 km^3_{we} ; b_s = -1.50 m_{we}
B_n = -0.05 km^3_{we} ; b_n = -0.05 m_{we}
ELA = 1340 m a.s.l. (at profile)
AAR = 47 %

Variation of mass balance along a flow line on Dyngjujökull is shown on Fig. 8. At the highest accumulation zone sites snow accumulation was ~l.25 std. under average, but close to average at all other. In the ablation zone snow collection was close to average. The total winter accumulation is estimated 91% of the average of the survey period.
Summer mass loss was almost at average at all survey sites but by about 1 std. under average at the top site. The lowest site has not been visited yet when the report is written.
The net balance was slightly negative, by -0.05 m_{we} not far from the average for Dyngjujökull that is only slightly negative (-0.03 m_{we}).
Dyngjujökull has often had mass balance close to zero, and the net balance has been estimated positive in at least 12 years of the three-decade period of almost continuous mass loss for Vatnajökull as a whole. The inland Dyngjujökull, is the outlet of Vatnajökull closest to mass equilibrium during the survey period.

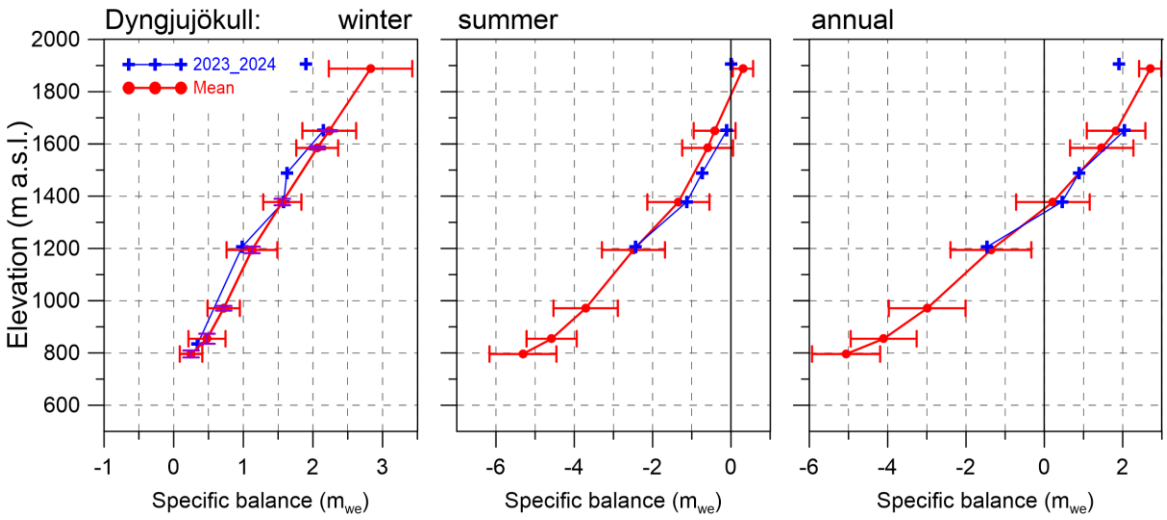

Figure 8. Mass balance at a central flow line on Dyngjujökull 2023_24 and average mass balance 1991_92 to 2021_22 (except 1998_99 – 2003_04 at all but the top elevation).

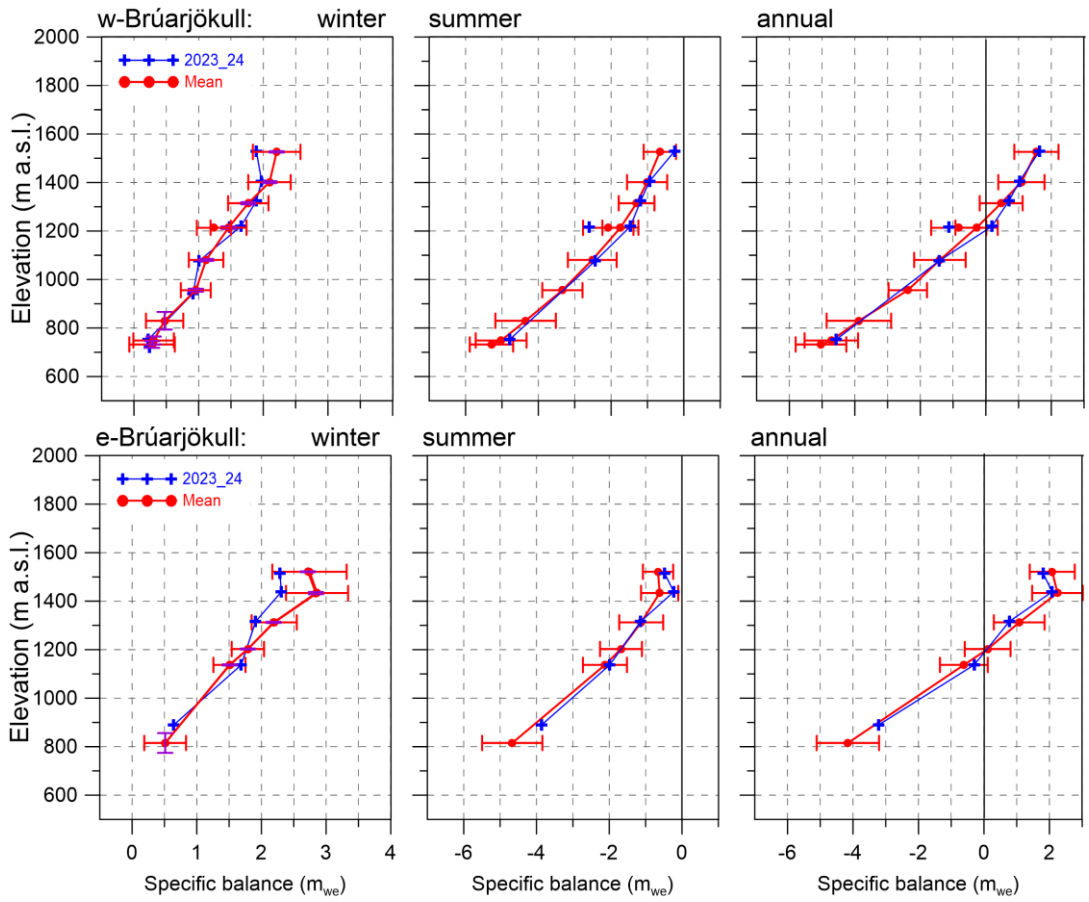

Figure 9. Mass balance at two flow lines on Brúarjökull 2023_24 and average mass balance 1992_93 to 2021_22.

3.2.4 Brúarjökull

Area = 1481 km^2
B_w = 2.40 km^3_{we} ; b_w = 1.62 m_{we}
B_s = -2.49 km^3_{we}; b_s = -1.68 m_{we}
B_n = -0.09 km^3_{we}; b_n = -0.06 m_{we}
ELA = 1280 m a.s.l. (western flow line)
ELA = 1205 m a.s.l. (eastern flow line)
AAR = 53 %

Variation of mass balance along the flow lines on Brúarjökull is shown in Fig. 9. On Brúarjökull winter snow collection was not far from average at most survey sites, except in upper accumulation zone, where it was ~1 std. less than average. The winter accumulation was in total at average. Summer mass loss was close to average at the survey sites below 1400 m elevation, but less than 1 std. over average at sites above. In total the mass loss in summer was 87% of the average.

The net balance was close to average at all survey sites. In total the net balance was slightly negative by ~20% of the average. During the survey period, there have been 9 years of positive balance and 23 years with negative net balance.

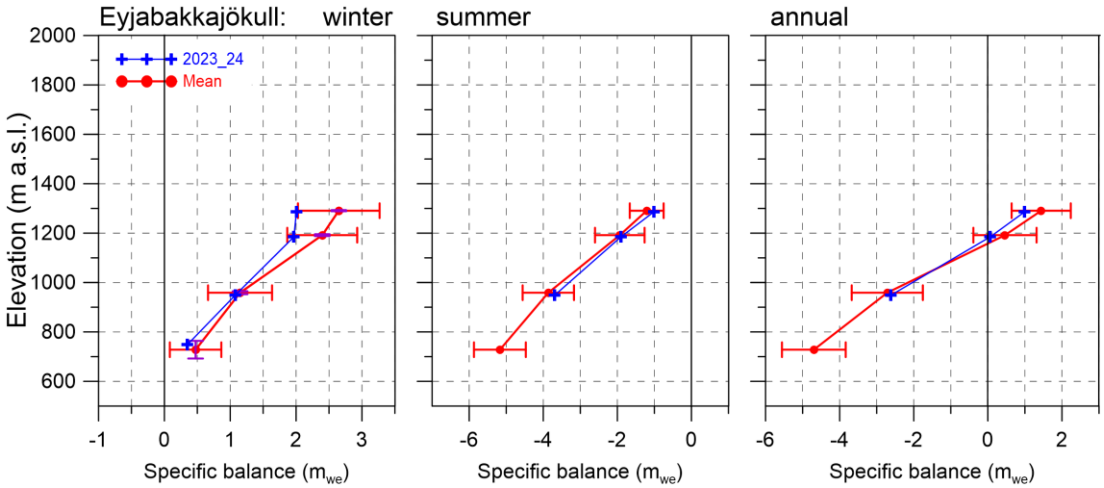

Figure 10. Mass balance at a central flow line of Eyjabakkajökull 2023_24 and average mass balance 1995_96 to 2021_22.

3.2.5 Eyjabakkajökull

Area = 104 km^2
B_w= 0.17 km^3 we; b_w = 1.62 m_{we}
B_s = -0.22 km^3 we; b_s = -2.14 m_{we}
B_n = -0.05 km^3 we; b_n = -0.51 m_{we}
ELA = 1180 m a.s.l. (at profile)
AAR = 46 %

Variation of mass balance along a central flow line on Eyjabakkajökull is shown in Fig. 10. Like Brúarjökull the winter accumulation here was at average at the lower sites but 1 std. less at the higher. The total winter accumulation is estimated 89% of the survey period average. Summer mass loss was slightly less than average at all survey sites. The total summer mass loss was 80% of the average. The net balance was negative by 60% of the average of the survey period and has been negative for all but 3 years of the 29 years of survey.

3.2.6 Breiðamerkurjökull

Area = 875 km^2
B_w = 1.33 km^3we; b_w = 1.52 m_{we}
B_s = -1.98 km^3 we; b_s = -2.27 m_{we}
B_n = -0.65 km^3we; b_n= -0.74 m_{we}
ELA = 1150 m a.s.l. (at profile)
AAR = 58%

Variation of surface mass balance along a central flow line on Breiðamerkurjökull is shown in Fig. 11.
Winter accumulation was less than average at the survey sites in the

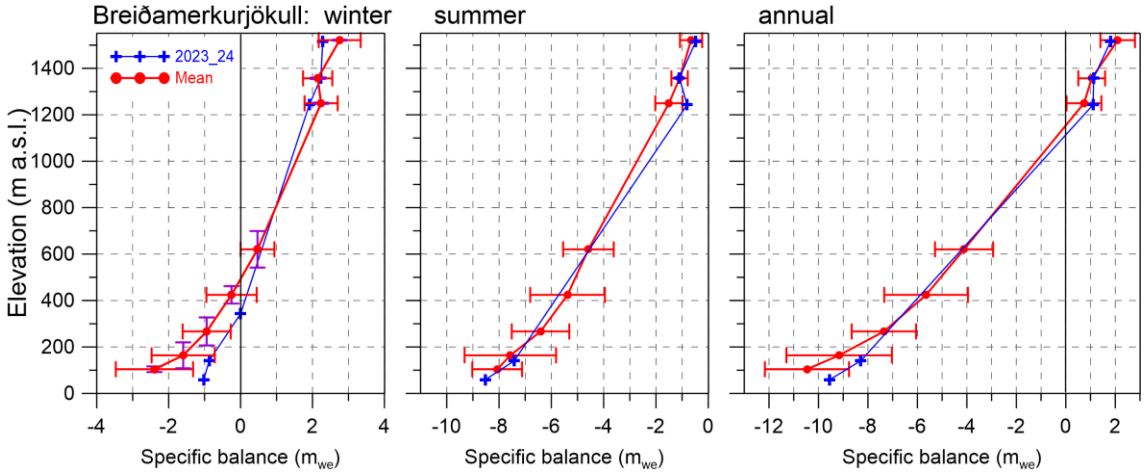

Figure 11. Mass balance at a central flow line of Breiðamerkurjökull 2023_24 and average mass balance 1995_96 to 2021_22.

accumulation zone, but at the lower sites in the ablation zone mass loss in winter was more 1 std. less than average. This led to the total winter balance close to average (2% higher) of the survey period average.
Summer mass loss was not far from the average in the accumulation zone) at all survey sites. The total summer mass loss is estimated 14% less than the average during the survey period. The net surface mass loss this year is estimated about 66% of an average year.
In addition to mass loss due to surface melt Breiðamerkurjökull loses in the order of 0.5 km^3 (~0.6 m) annually via calving into the marginal lake Jökulsárlón; this mass loss is not accounted for here.

3.2.7 Skeiðarárjökull

Area = 1346 km^2
B_w = 1.98 km^3_{we}; b_w = 1.47 m_{we}
B_s = -2.68 km^3_{we}; b_s = -1.99 m_{we}
B_n = -0.70 km^3_{we}; b_n= -0.52 m_{we}
ELA = ~1190 m a.s.l. (at profile)
AAR = 58
The surface mass balance of Skeiðarárjökull is only measured in the accumulation zone due to almost impassable terrain in the ablation zone both in autumn and spring.
The mb-survey program here was initiated in 2002, although sporadic measurements were conducted in the 1990s. Estimation of mb in the ablation zone for the creation of the mb-maps is based on the survey of the neighboring Breiðamerkurjökull in the east (with similar elevation span) and western neighboring outlet Síðujökull.
Variation of mass balance along the survey profile on Skeiðarárjökull is shown in Fig. 12. Winter snow accumulation was 1 std. under average at the lower accumulation zone, but at average at the higher.
Summer mass loss was far less than average at the upper sites, at average at 1250 m but the lowest was not reachable in the autumn due to crevasses.

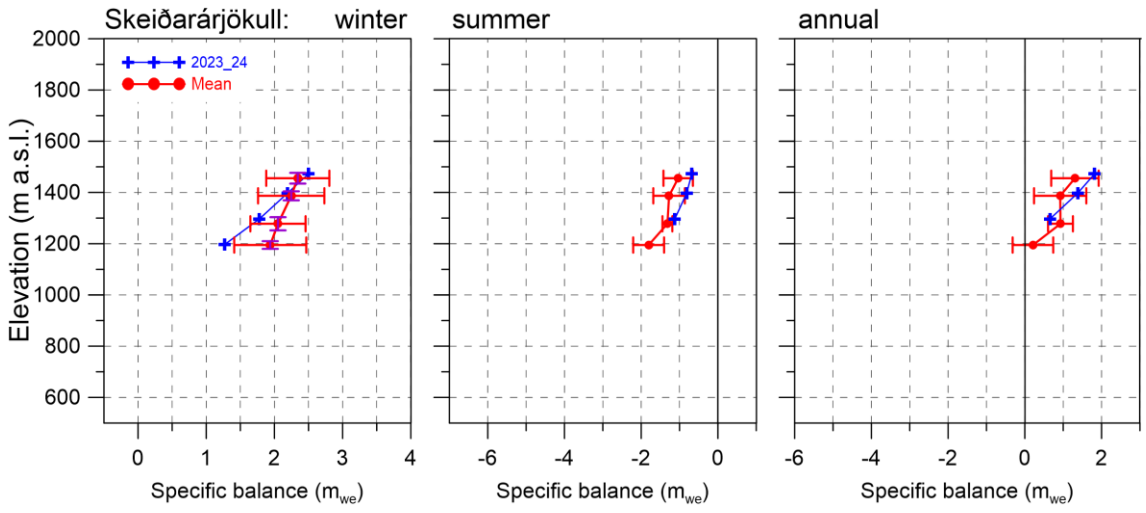

Figure 12. Mass balance at a central flow line of Skeiðarárjökull 2023_24 and average mass balance 2016_17 to 2021_22.

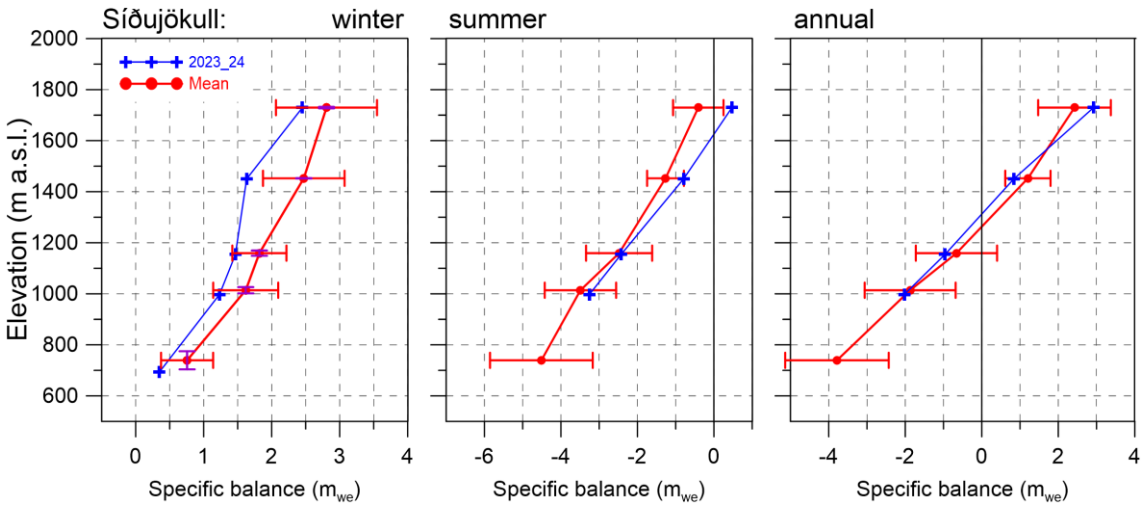

Figure 13. Mass balance at a central flow line of Síðujökull 2023_24 and average mass balance 2004_05 to 2021_22.

3.2.8 Síðujökull

Area = 400 km^2
B_w= 0.52 km^3_{we}; b_w = 1.30 m_{we}
B_s = -1.00 km^3_{we}; b_s = -2.51 m_{we}
B_n = -0.48 km^3_{we}; b_n= -1.20 m_{we}
ELA = 1310 m a.s.l. (at profile)
AAR = 37 %

Variation of mass balance along a central flow line on Síðujökull is shown in Fig. 13.
The winter snow accumulation was between ½ - 1 std. under average at all survey sites. The total winter balance was 82% of the average (since 2004_05). Summer mass loss was at average at the lower sites, but far less at the upper sites, even net mass gain at the summit of Háabunga. (In autumn the route to the lowest site was impassable). The total summer mass loss was 85% of the average of the survey period. Total mass loss was ~90 % of the average during the 19-year survey period. At Síðujökull the only year of surveyed positive net balance was 2014_2015.

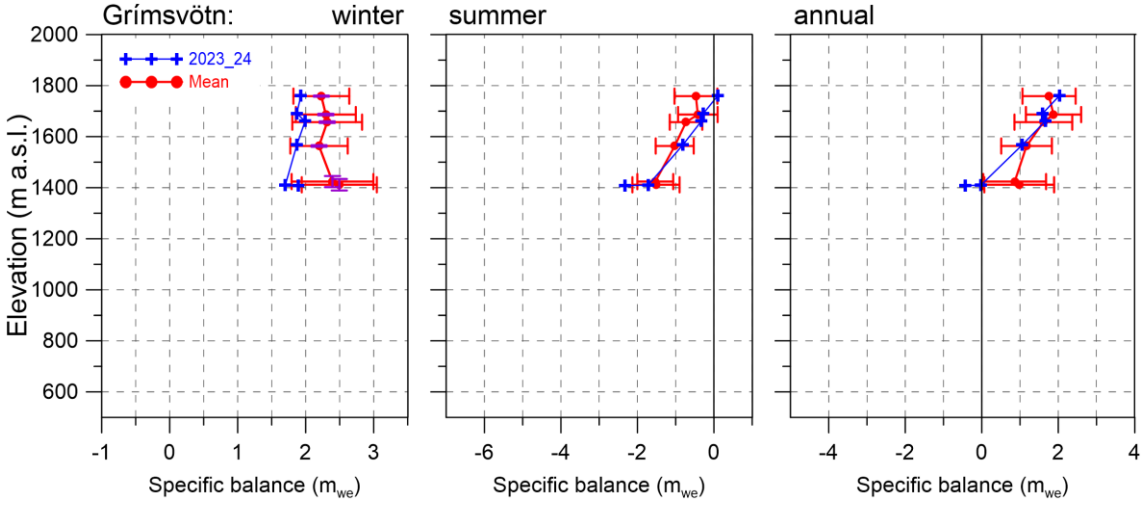

Figure 14. Mass balance at a flow line towards Grímsvötn 2023_24 and average mass balance 1991_92 to 2021_22.

3.2.9 Grímsvötn-Gjálp

Area = 173 km^2
B_w = 0.34 km^3_{we}; b_w = 1.92 m_{we}
B_s = -0.12 km^3_{we}; b_s = -0.70 m_{we}
B_n = 0.21 km^3_{we}; b_n= 1.21 m_{we}

Variation of mass balance at sites close to a flow line from Bárðarbunga towards Grímsvötn center is shown in Fig. 14. Snow accumulation at the survey sites was between ½ - 1 std. less than average, and total winter accumulation 12% less than average. Summer mass loss was at average at the sites on the ice-shelf of Grímsvötn, but far less at the upper sites, even net mass gain at the slopes of Bárðarbunga. Total summer mass loss was ~85 % of the average. Net balance was at average at the survey sites except the one at the center of the ice shelf. As always (except 2010) the total surface balance is positive, now ~82 % of the average.

In addition to surface mass loss in summer, geothermal melt in the Grímsvötn catchment area is on the order of 0.2 km^3 annually. This mass loss is about 1.21 m evenly distributed over the ice catchment, or approximately equal to this year net surface balance. This means that the total balance for the catchment of Grímsvötn is close to zero this year.
The average surface mass balance in the survey period (since 1991-92) is +1.50 m, so assuming the annual 1.21 m loss due to geothermal melt yields an annual surplus of ~0.3 m (0.052 km^3) on average, or ~1.6 km^3. In the Gjálp eruption, within the Grímsvötn ice catchment, over 3.5 km^3 of ice was melted and some, although much less, in the 1998, 2004 and 2011 Grímsvötn eruptions. About half of this has been compensated for by the average total positive surface balance.

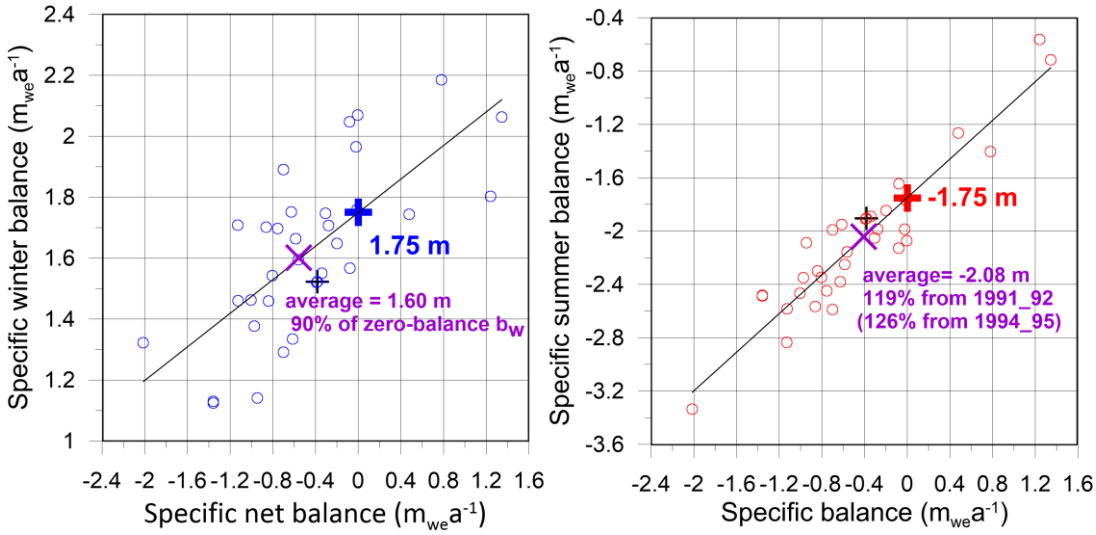

Figure 15. Vatnajökull winter (left) and summer (right) mass balance plotted against net mass balance for the survey period 1991_92 to 2023_24, current point marked with +. The + and + and the accompanying numbers, mark the zero-mass balance mass turnover for Vatnajökull (current topography) as estimated from the linear trends shown with thin black lines.

3.3 Vatnajökull:
Surface mass balance record

From the digital mb maps (Fig. 4) the glacier wide volumes of winter, summer and net balances for Vatnajökull have been calculated by integration and are as follows:

Area = 7593 km^2
B_w = 11.50 km$^3_{we}$; b_w = 1.52 m_{we}
B_s = -14.39 km$^3_{we}$; b_s = -1.90 m_{we}
B_n = -2.88 km$^3_{we}$; b_n = -0.38 m_{we}
AAR = 58%;

(balance values as a function of elevation are tabulated in appendix D)

The winter of 2023-2024 was rather cold, with winter precipitation less than average, very little until end of December 2023.
Distribution of the winter snow was not typical (see fig. 5). In general, there was by far less snow than average in the accumulation zones of the ice cap, and by far less than average at all elevations in the west. Winter melting at the low-lying S-outlets was less than average. The total mass collection in winter was ~95% of the average since 1995.
Early summer was cold with occasional snowfall, reducing melting, relatively sunny July, but cold and wet August. The autumn months were very dry, most of the N-Atlantic low-pressure systems passed far south of Iceland. Warm and windy days in the autumn contributed markedly to the total melt. In all this resulted in less average summer melting, especially in above ~1000 m elevation, and above ~1650 m the summer balance was positive. This resulted in a summer mass loss ~86% of the average since 1995.

The resulting annual balance was close to average in the ~1000-1500 m range, slightly above average above that, but lower than average in many of the ablation zone regions. In total the mass loss was ~62 % of the average since 1995.
The zero-mass balance mass turnover (mbt) for Vatnajökull (current topography) is estimated from the zero net balance crossover of the linear trend of b_w plotted against b_n and equivalently b_s against b_n (see fig 15.) and found to be close to 1.75 m_{we} (13.4 km$^3_{we}$). The winter balance 2023_24 is ~93% of the estimated zero-mass balance turnover (0-mbt), while the average b_w of the survey period is ~92% of the 0-mbt.
The summer balance of 2024 is -0.19 m (or 22%) more negative than 0-mbt. On average the summer mass loss has been 19% (average of summers 1992-2022) higher than 0-mbt, (27% for the period of 1995-2023).
This clearly shows that the high mass loss of the past 3 decades is governed by too much mass loss during summer rather than too little snow accumulation during winter.
Since 2010, after the 15-year period of high mass loss, the summer and net balance have been highly variable (figure 16.), one year with definite positive mass balance, 2014_15, and a few close to zero or slightly positive: 2010_11, 2016_17, 2017_18 and 2021_22.
The variability of the winter balance is by far more prominent for the outlets closest to sea. That section of the glacier receives precipitation in all south and east wind directions and thus has high snow accumulation in winters when prevailing paths of the North Atlantic low-pressure systems are just south and east of Iceland.

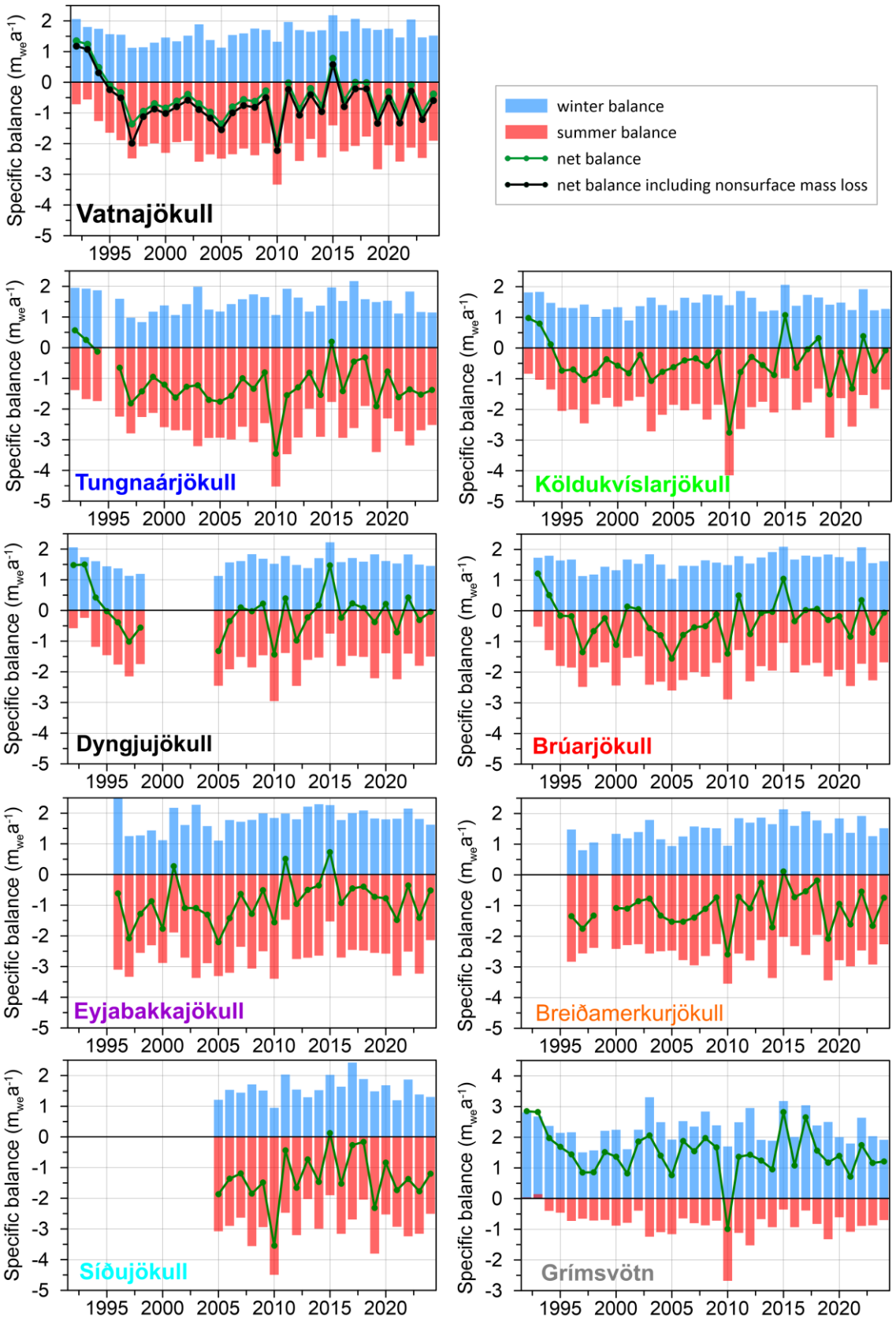

Figure 16. Specific mass balance record for Vatnajökull (top), and selected Vatnajökull outlets 1991_92-2023_24.

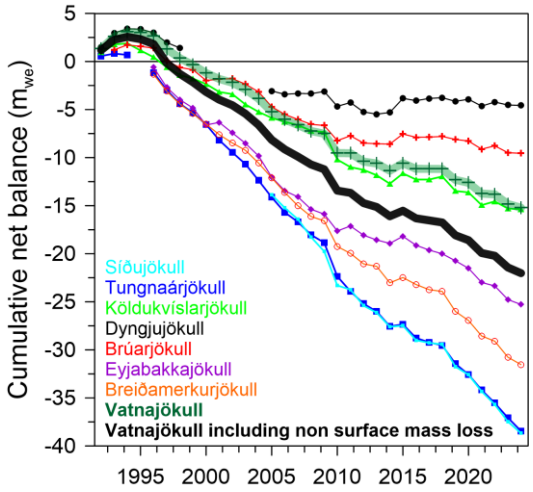

Figure 17. Cumulative specific surface mass balance Vatnajökull and selected Vatnajökull outlets 1991_92 – 2023_24.

The cumulative net balance curves for the outlets of Vatnajökull in Fig. 17 show that all outlets have been losing mass since in most years since 1994_95. In the period of high mass loss, the loss rate is about -0.5 to -0.6 $m_{we}a^{-1}$ for the northern outlets but -1.1 to -1.5 $m_{we}a^{-1}$ for the south and western outlets. After 2010 there is a distinct difference between the north inland (Dyngjujökull and Brúarjökull) and the south and west coastal outlets (Breiðamerkurjökull, Tungnaárjökull and Síðujökull) in that there is a sudden change in the mass balance trend for the northern. The trend changes from -0.5 $m_{we}a^{-1}$ to about zero for the northern while there is little change for the others. The east outlet Eyjabakkajökull behaves like the coastal and is in fact close to sea, while Köldukvíslarjökull in the NV is more like the northern.

The cumulative mb for Vatnajökull is very similar to Köldukvíslarjökull, with a slope of -0.75 $m_{we}a^{-1}$ in the period of high mass loss, but -0.35 $m_{we}a^{-1}$ after 2010.

During the survey period starting in 1991_92 Vatnajökull lost ~134 km^3 of ice or thinned ~15 m due to surface mass loss (summing from the start of high mass loss in 1994_95 yields 162 km^3 or 19 m thinning).

In addition, non-surface mass loss is estimated (calving, geothermal melt, internal friction, eruptions) ~0.21 m_{we} for Vatnajökull in a paper by Tómas Jóhannesson and others (Jóhannesson, T., Pálmason, B., Hjartarson, Á., Jarosch, A., Magnússon, E., Belart,J., et al. (2020). Non-surface mass 1balance of glaciers in Iceland. J. Glaciol. 66,685–697. doi:10.1017/jog.2020.37) which amounts to an ice loss of ~60.3 km^3 or 7.7 m average thinning since 1994_95.

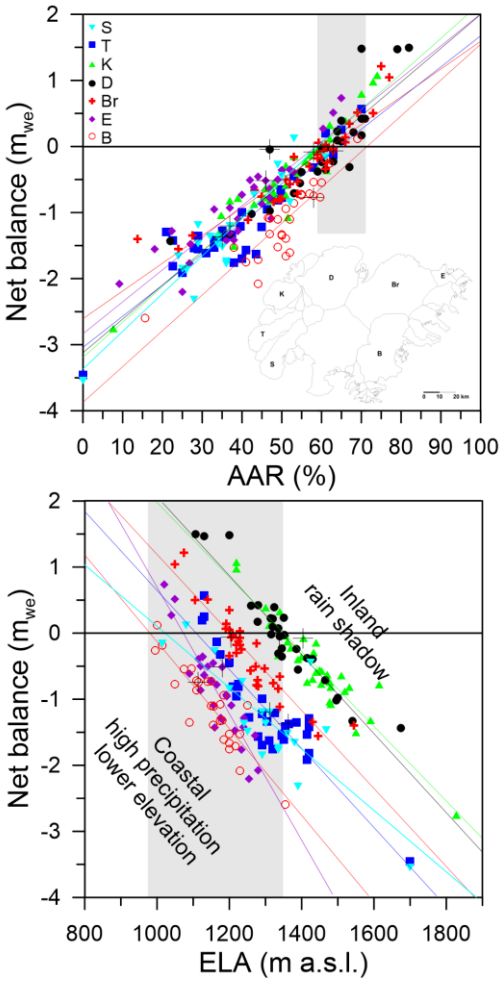

Figure 18. The relation between net annual balance (b_n) and accumulation area ratio (AAR) (upper) and b_n and equilibrium line altitude (ELA), for Vatnajökull outlets during the survey period. (This year's points are marked with a black +).

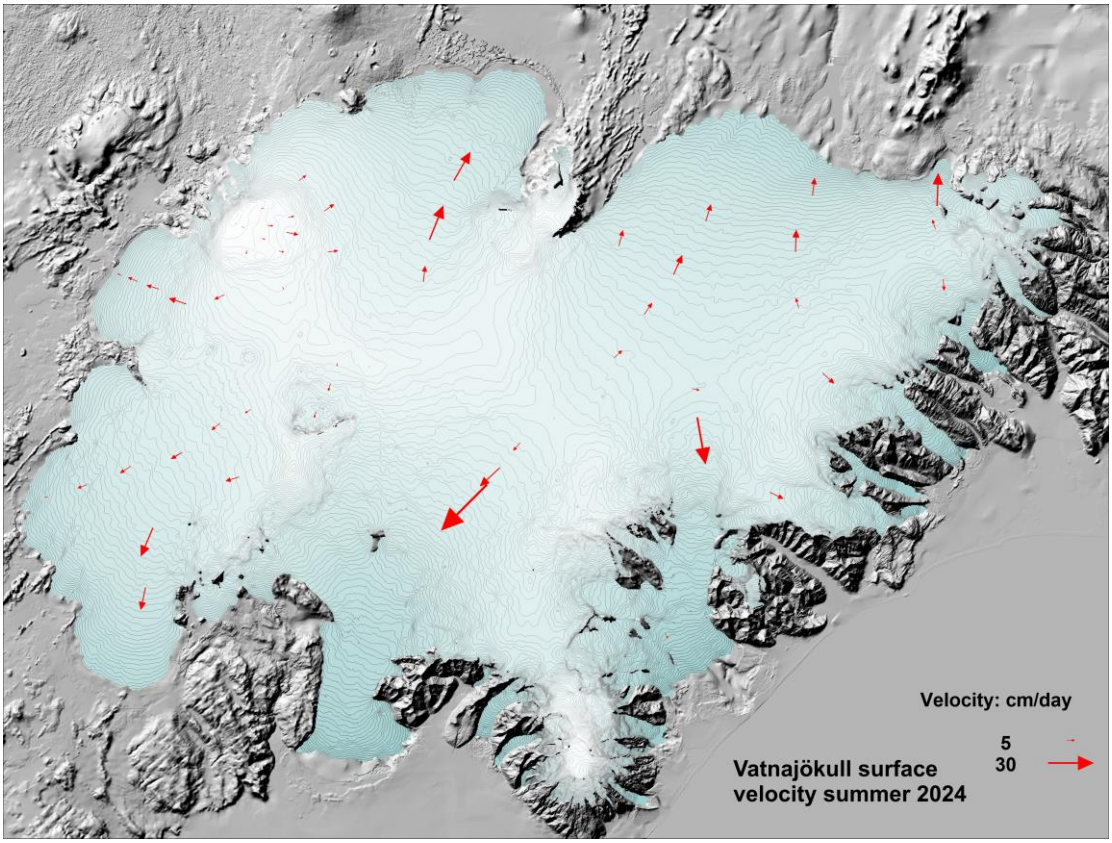

Figure 19. Average summer velocity at survey sites in 2024.

In Fig. 17 the relation of the annual net balance to the accumulation area ratio (AAR) and equilibrium line altitude (ELA) is shown for different outlets over the survey period. The bn-AAR gradient is similar for all outlets, about 0.5 m_{we} for 10% change in AAR. The zero-balance AAR varies for different outlets in the range 60-65%, similar for all outlets except for the southern outlet Breiðamerkurjökull. Breiða-merkurjökull is far from equilibrium, the ablation area is too large. A large part of the outlet has carved 200-300 m deep valley into the former sediment bed, and the surface and bed elevation has lowered accordingly. Similarly, the zero-balance ELA varies from about 1000-1100 m a.s.l. for the southern outlets to 1400 m a.s.l. for the NW outlets. The bn-ELA slope is similar for all outlets -0.6 m_{we} per 100 m, except Eyjabakkajökull with a slope of -1.0 m_{we} per 100 m and Síðujökull with a slope of -.45 m_{we} per 100 m (for Síðujökull possibly due to outliers in the data set).

4. SURFACE VELOCITY MEASUREMENTS

The average summer surface velocity of the glacier surface at the survey sites was calculated from fast static or kinematic GNSS positioning of the ablation stakes/wires (accuracy about ~10 cm). In 2024 nearly all sites were surveyed in spring and autumn and many in June. At a few sites, stakes from previous years were found and resurveyed, making it possible to calculate surface velocity over a year or longer time span. The average summer surface velocity is shown in Figure 19.

At sites close to the glacier terminus very small lateral movement is generally measured. This indicates that the glacier snouts are almost stagnant. In the centre areas of some of the outlets especially close to the equilibrium line, there is an increase in velocity during summer compared to winter. The summer velocity is

typically in the order of two-fold the winter velocity. This suggests that basal sliding is increased in the melting season and is of often at the same magnitude as the deformation velocity.
To better understand the variable velocity continuous GNSS has been run during summer at several sites.
From previous velocity measurements, surging of outlets has been predicted. Currently the increase in velocity at sites D05 and D07 (Fig. 20.) persists and suggests that Dyngjujökull may surge within a few years. The velocity at sites D07 and D05 is now similar that in 1997 prior to the surge in 1998-2000 and the accumulation zone has thickened. To monitor velocity changes leading up to a surge GNSS instruments were set up in spring to continuously monitor movement at sites D05 and D07.
The data collected allows for post-processing to acquire more accuracy (~dm instead of ~m), but the processing has not been finished when this report is written.

Figure 21. shows the average summer velocity and elevation change record at the survey sites on Eyjabakkajökull. There is a steady increase in velocity at sites E01 and E02 since about 2018. This may be caused by the rapid recession of the glacier snout, and thus steeper surface slopes, formation of a frontal lake and the floating of the ice front. This might be signs of a starting surge, but then speed up at E03 would be expected, which is not the case.
Images of velocity and elevation records for other mb survey sites are displayed in Appendix F.
Most vehicles used in the survey expeditions are equipped with survey type GNSS instruments that collect data while driving. These are post-processed, to yield surface profiles with an accuracy of ~dm in horizontal and vertical. Location of all profiles surveyed in 2024 is shown in figure 22. The profiles have proved of high importance to increase accuracy of remote sensing-based surface DEMs.

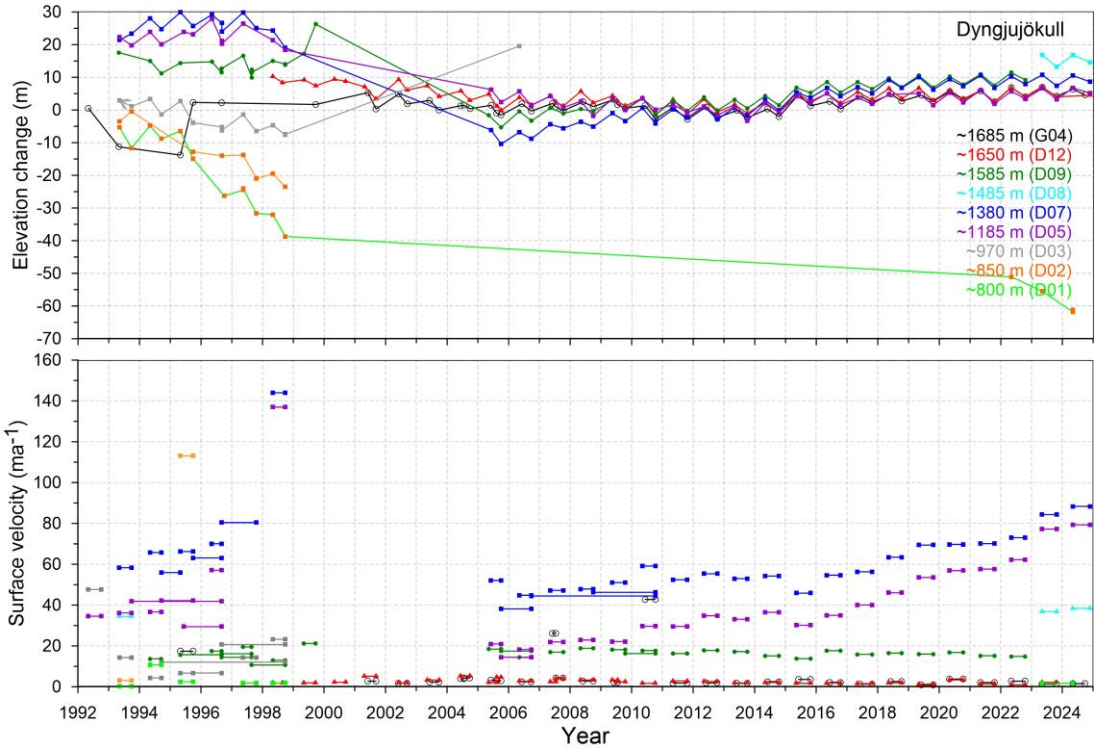

Figure 20. Surface elevation change relative to summer 2011 (upper panel) and average surface velocity (lower panel) at mb sites on Dyngjujökull in 1992 to 2024.

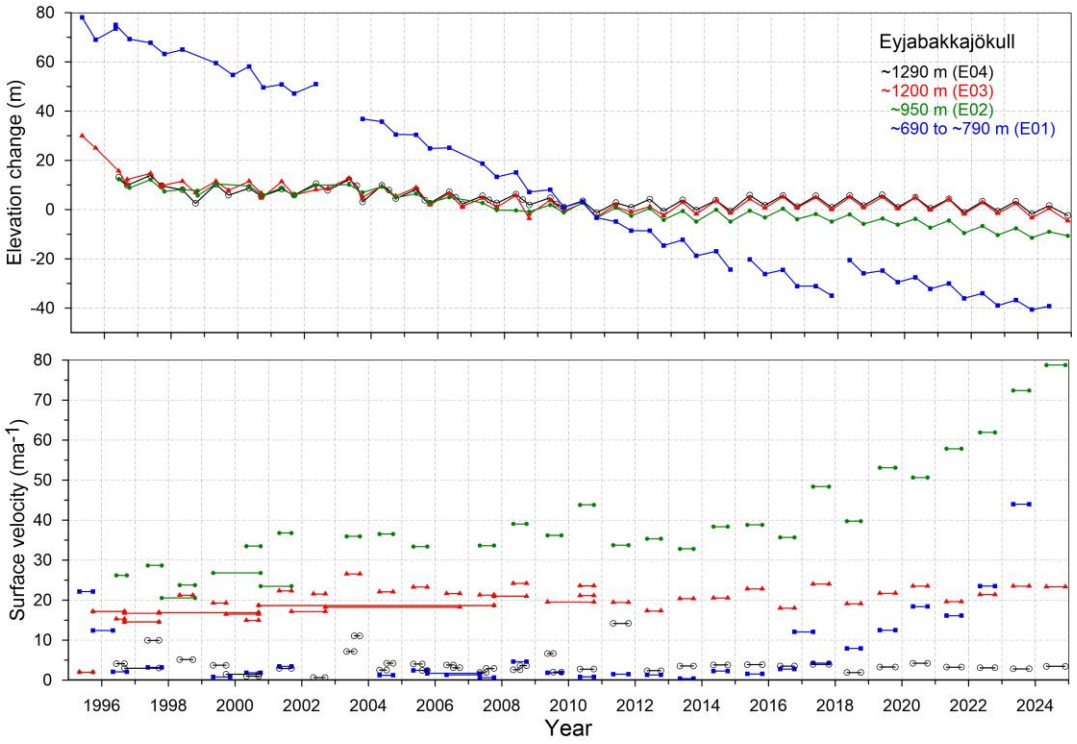

Figure 21. Surface elevation change relative to summer 2010 (upper panel) and average surface velocity (lower panel) at mb sites on Eyjabakkajökull in 1995 to 2024.

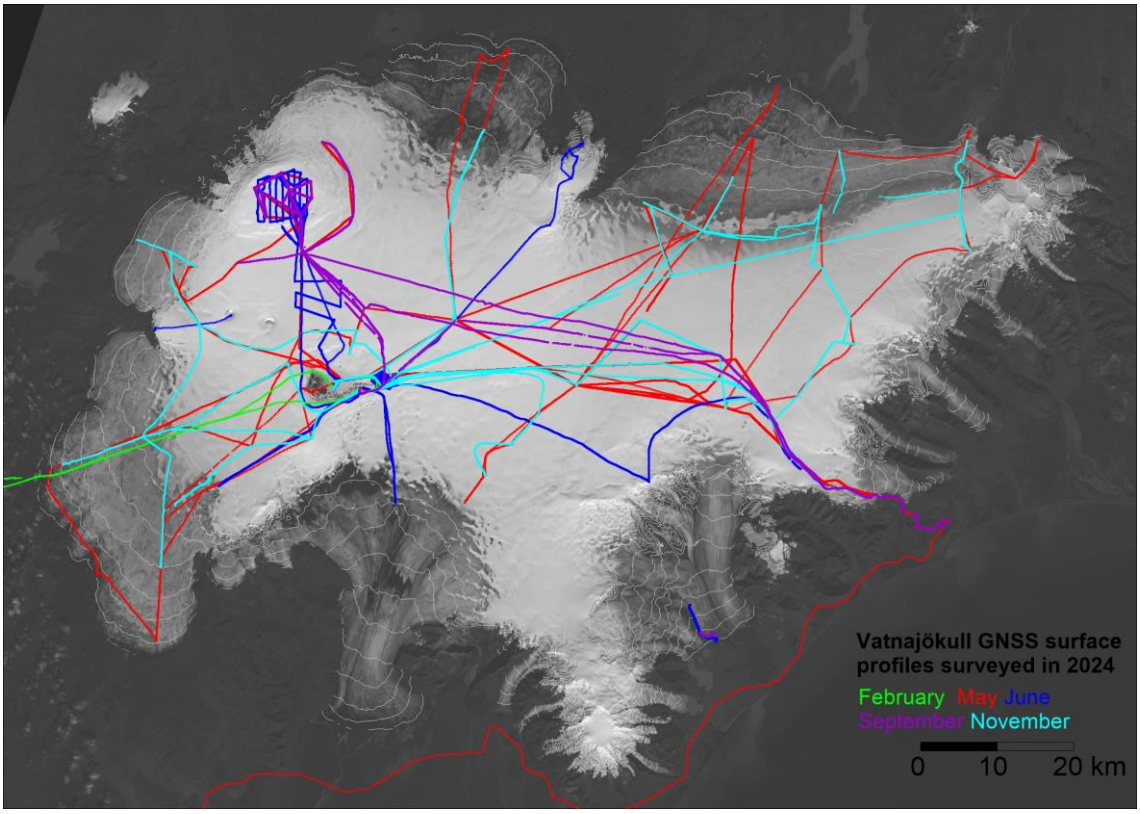

Figure 22. Location of surface elevation profiles surveyed in field trips on Vatnajökull in 2024.

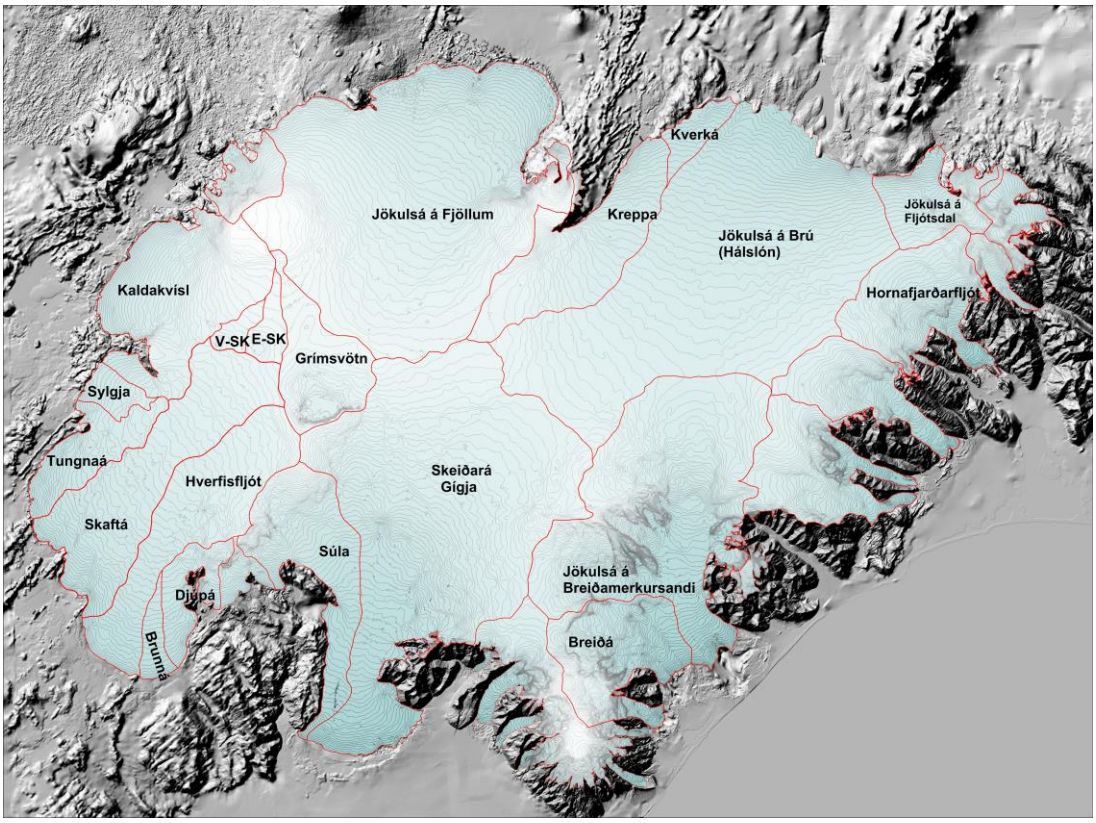

Figure 23. Water divides and drainage basins of selected rivers draining water from Vatnajökull, Súla is since summer 2016 diverted to Gígja.

5. Melt water runoff.

Water divides and drainage basins for rivers draining water from Vatnajökull have been defined from water pressure potential maps. The potential maps were produced from surface (year 2010) and bedrock DEMs.

Figure 23. shows the water divides and drainage areas for selected rivers draining melt water from Vatnajökull. The summer balance over the water basin is an estimate of meltwater contribution to rivers and groundwater storage. This estimate, however, does not include precipitation that falls as rain on the glacier, or snow that falls and melts during the summer. The meltwater contribution can be compared with river runoff at stream flow gauges closest to the glacier. For this comparison, we define the glaciological year from the start of October to the end of September and the period draining meltwater from the glacier during the summer from June through September. It would be misleading to include May in the summer period because runoff from the glacier melt in May is delayed due

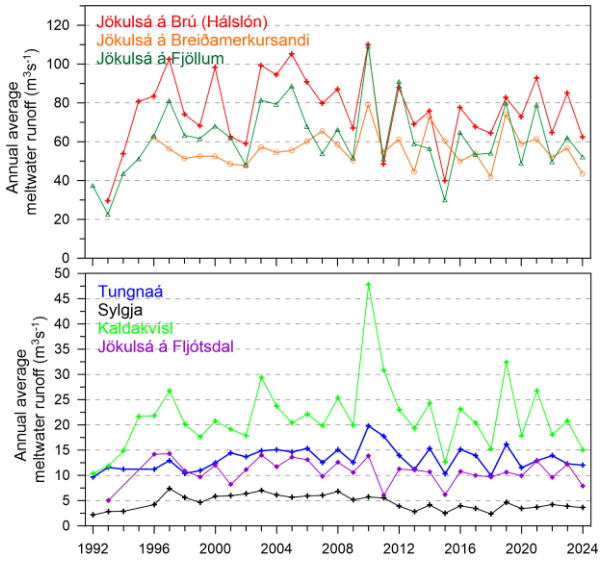

Figure 24. The temporal variation of average annual meltwater runoff to selected river catchments.

Table I. Melt water drainage to selected rivers in summer 2024.

Water Catchment:	Area (km^2)	ΣQ_s ($10^6 m^3$)	Q_s ($m^3 s^{-1}$)	Q_a ($m^3 s^{-1}$)	q_s ($ls^{-1}km^{-2}$)
Vatnajökull	7570	14545	1379.9	461.2	60.9
Tungnaá	104	379	35.9	12.0	115.0
Sylgja	38	114	10.8	3.6	95.6
Kaldakvísl	328	474	45.0	15.0	45.9
Jökulsá á Fjöllum	1109	1647	156.2	52.2	47.1
Kreppa	287	398	37.8	12.6	44.0
Kverka	34	139	13.2	4.4	129.3
Hálslón	1186	1968	186.7	62.4	52.6
Jökulsá á Fljótsdal	121	249	23.6	7.9	65.5
Jökulsá í Lóni	92	179	17.0	5.7	61.6
Hornafjarðarfljót	227	463	43.9	14.7	64.5
Jökulsá á Breiðamerkursandi	686	1371	130.1	43.5	63.4
Breiðá-Fjallsá	220	770	73.0	24.4	110.9
Gígja	1383	2785	264.2	88.3	63.8
Brunná	30	129	12.2	4.1	137.2
Djúpá	70	230	21.8	7.3	104.0
Hverfisfljót	306	617	58.5	19.6	64.0
Skaftá	380	902	85.6	28.6	75.3
Grímsvötn	171	122	11.6	3.9	22.6
Eystri Skaftárketill	39	8	0.8	0.3	6.7
Vestari Skaftárketill	25	5	0.5	0.2	6.5
Hólmsá	157	364	34.5	11.5	73.7
Heinabergsvötn	214	515	48.9	16.3	76.5
Skjálfandafljót	89	79	7.4	2.5	27.9

ΣQ_s: total summer melt water; Q_s: average runoff (averaged over summer, 4 months, June – September)
Q_a: average runoff (averaged over a whole year); q_s: average runoff per km^2 (averaged over a whole year)

to refreezing during elimination of the cold wave and because of the contribution of the spring snow melt from the highlands to the runoff. Some melting also occurs during winter, especially in the terminus regions of the southern outlets.

Average melt water runoff to different rivers is given in Table I, and temporal variation of the average meltwater runoff in Fig. 24. The average specific runoff (q_s) differs from basin to basin from ~31 to ~176 $ls^{-1}km^{-2}$. This is mainly due to different elevation distributions, for example, the water drainage basins for Tungnaá, Brunná and Kverká are within the ablation zone, while that of Grímsvötn and Skaftárkatlar are high in the accumulation zone.

Runoff as function of elevation, estimated from summer balance, is tabulated for individual water catchments in Appendix E.

6. Conclusions

In the glaciological year 2022_23 the winter balance for Vatnajökull was ~90% of the average in the observation period from 1991_92. 11 winters of the survey period have had lower winter balance, but 9 out the 12 recent years have had higher than average winter balance. The average winter balance is 1.6 m_{we} and standard variability is 0.27 m_{we}.

The total summer surface mass loss was 91% of the average since 1995 (86% than average since 1992). During the survey period, only 8 summers have had less surface mass loss. The average summer balance is -2.08 m_{we}, and the standard variability 0.55 m_{we}.

The net balance was negative by 62% of the average since 1995 (83% of the average since 1992), and only 8 glaciological years have had less annual surface mass loss.

The average net balance of the survey period is -0.46 m_{we}, and the standard variability 0.71 m_{we}

Since 2010, after the 15-year period of high mass loss, the summer and net balance have been highly variable, even one year with distinct positive mass balance in 2014_15 and close to zero in 2010_11, 2016_17, 2017_18 and 2021_22.

In contrast 2018_19 and 2020_21 are both among years with highest surface mass loss of the survey period. It is also noteworthy that 4 years of the last decade have had more mass loss than the average of the whole survey period

The cumulative mb for Vatnajökull is very similar to that of Köldukvíslarjökull, with a slope of -0.75 $m_{we}a^{-1}$ in the period of high mass loss, but -0.35 $m_{we}a^{-1}$ in the period after 2010.

During the survey period starting in 1991_92 Vatnajökull has lost ~134 km^3 of ice or thinned ~15 m due to surface mass loss (summing from the start of high mass loss in 1994_95 yields 162 km^3 or 19 m thinning).

In addition, non-surface mass loss is estimated (calving, geothermal melt, internal friction, eruptions) ~0.21 m_{we} for Vatnajökull in a paper by Tómas Jóhannesson and others (Jóhannesson, T., Pálmason, B., Hjartarson, Á., Jarosch, A., Magnússon, E., Belart,J., et al. (2020). Non-surface mass 1balance of glaciers in Iceland. J. Glaciol. 66,685–697. doi:10.1017/jog.2020.37) which amounts to an ice loss of ~60 km^3 or 7.7 m average thinning since 1994_95.

Glacier surface meltwater runoff in summer 2024 (estimated from summer surface balance only, summer rain and snow that falls and melts during summer, calving and geothermal and internal melting, is not included):

to Tungnaá 94% of the average, 70% of the average to Kaldakvísl, 88% of the average to Jökulsá á Fjöllum, 88% of the average to Hálslón, 78% to Jökulsá í Fljótsdal and 83% to Jökulsá á Breiðamerkursandi.

(Averages refer to the survey period of each outlet.)

Surface velocity measurements suggest that Dyngjujökull is in the first phase of a surge and may complete a surge cycle within the next few years.

Surface mass balance summary 2023_24:

B_w = 11.50 km^3_{we}
B_s = -14.39 km^3_{we}
B_n = -2.88 km^3_{we}
AAR = 58%

Specific Values:

b_w = 1.52 m_{we}
b_s = -1.90 m_{we}
b_n = -0.38 m_{we}
$b_{n(\text{including other mass loss})}$ = -0.59 m_{we}

Appendix A: Surface mass balance at measurement sites 2023_24.

b_w: specific winter balance, **b_s**: specific summer balance, **b_n**: specific net balance,
l_a: new snow in autumn (all in water equivalent).

Site	Position				Elévation	Date	Date	b_w	b_s	b_n	la
	Latitude		Longitude		(m a.s.l.)	in spring	in autumn	(m)	(m)	(m)	(m)
B09-23	64	44.4833	16	6.1882	726.3	20230505	20231024	0.09	-6.44	-6.35	0.02
B07-24	64	25.7965	16	17.4809	1358.8	20240430	20240925	2.23	-1.10	1.13	0.00
B09-24	64	44.4841	16	6.1878	720.2	20240502	20240000	0.24			0.00
B10-24	64	43.6842	16	6.7027	752.2	20240502	20241001	0.22	-4.79	-4.57	0.00
B11-24	64	40.9390	16	10.4800	942.0	20240501	20240000	0.91			0.00
B12-24	64	38.2629	16	14.1506	1077.2	20240501	20241123	1.01	-2.43	-1.42	0.08
B13-24	64	34.6584	16	19.5610	1219.2	20240502	20241001	1.65	-1.47	0.19	0.00
B14-24	64	31.6498	16	24.7708	1324.8	20240501	20241121	1.89	-1.19	0.71	0.15
B15-24	64	28.5128	16	30.0324	1405.7	20240501	20241121	1.97	-0.94	1.03	0.21
B16-24	64	24.1239	16	40.9139	1528.9	20240501	20241001	1.89	-0.25	1.64	0.10
B17-24	64	36.7326	16	28.7959	1216.6	20240501	20241121	1.48	-2.60	-1.13	0.05
B18-24	64	31.5817	16	0.1196	1316.2	20240501	20241121	1.91	-1.14	0.77	0.17
B19-24	64	28.0098	15	55.9862	1438.6	20240501	20241121	2.31	-0.23	2.08	0.23
Barc-24	64	38.4207	17	26.7611	1906.6	20240609	20240927	1.90	0.00	1.90	0.18
Bb0-24	64	22.7065	16	5.0575	1515.5	20240501	20241121	2.28	-0.48	1.81	0.18
Bor-24	64	24.9353	17	20.1523	1408.0	20240609	20241123	1.89	-2.32	-0.43	0.26
Borth-24	64	24.9910	17	19.2025	1410.4	20240502	20240930	1.70	-1.72	-0.02	0.00
Br1-24	64	5.9573	16	19.8247	58.7	20240501	20240928	-1.03	-8.53	-9.55	0.00
Br2-24	64	6.3538	16	22.5234	140.3	20240501	20240928	-0.87	-7.42	-8.29	0.00
Br3-24	64	8.4069	16	23.9626	342.9	20240501	20240000	0.00			0.00
Br7-24	64	22.1413	16	16.9309	1243.1	20240501	20241121	1.91	-0.81	1.10	0.27
Bru-24	64	39.7561	15	56.5333	889.3	20240501	20241123	0.64	-3.86	-3.22	0.06
Bud-24	64	35.9920	15	59.8869	1137.4	20240501	20241121	1.69	-1.98	-0.30	0.12
D01-24	64	47.8680	16	49.9738	833.7	20240503	20240000	0.34			0.00
D05-24	64	42.2298	16	54.6827	1206.7	20240503	20241123	0.98	-2.44	-1.46	0.03
D07-24	64	38.2946	16	59.2556	1378.4	20240503	20241123	1.58	-1.13	0.45	0.22
D08-24	64	34.6858	17	1.5208	1488.8	20240503	20241123	1.63	-0.74	0.89	0.27
D12-24	64	28.9748	17	0.1844	1651.6	20240502	20241123	2.15	-0.20	1.95	0.34
E01-24	64	40.6633	15	34.8317	747.8	20240501	20240000	0.35			0.00
E02-24	64	39.1111	15	36.0021	948.5	20240501	20241123	1.07	-3.69	-2.62	0.05
E03-24	64	36.6643	15	36.9262	1185.2	20240501	20241123	1.97	-1.90	0.07	0.17
E04-24	64	34.9530	15	37.1465	1286.7	20240501	20241123	2.01	-1.01	1.00	0.17
E07-24	64	38.4128	15	24.6995	1067.9	20240501	20240000	1.78			0.00
E08-24	64	39.7220	15	23.8488	945.6	20240501	20240000	1.29			0.00
Fl01-24	64	26.1578	15	55.6246	1346.0	20240501	20241121	2.31	-0.83	1.48	0.13
G02-24	64	26.8495	17	17.7109	1567.5	20240503	20241121	1.87	-0.81	1.06	0.26
G03-24	64	28.4432	17	16.3317	1660.9	20240503	20241122	1.99	-0.33	1.66	0.26
G04-24	64	30.0218	17	15.0384	1690.7	20240503	20240927	1.87	-0.28	1.59	0.03
Go1-24	64	33.9740	17	24.9254	1761.3	20240504	20240926	1.93	0.10	2.03	0.03
Haab-24	64	20.9661	17	24.1103	1729.6	20240504	20241122	2.45	0.47	2.92	0.48
Hof01-24	64	32.3434	15	35.8545	1140.6	20240501	20241123	2.20	-1.61	0.59	0.06

K01-24	64	35.1697	17	51.8566	1036.5	20240504	20241122	0.66	-4.12	-3.47	0.03
K02-24	64	34.8167	17	49.7080	1164.2	20240504	20241122	0.80	-2.86	-2.06	0.06
K03-24	64	34.2393	17	46.4293	1289.2	20240504	20241122	0.79	-1.79	-1.00	0.03
K04-24	64	33.2070	17	42.3638	1479.9	20240504	20241122	1.50	-0.84	0.65	0.16
K05-24	64	33.4449	17	35.4525	1677.9	20240504	20240926	1.49	-0.11	1.37	0.02
K06-24	64	38.3574	17	31.3104	1946.3	20240504	20240926	1.85	0.75	2.60	0.23
K07-24	64	29.1116	17	42.0174	1530.5	20240504	20241122	1.55	-0.36	1.19	0.21
Kverk-24	64	38.6640	16	40.5191	1824.6	20240612	20240000	1.88			0.00
S01-24	64	7.0173	17	49.9724	693.3	20240504		0.35			
S02-24	64	12.1659	17	48.9957	997.4	20240504	20241122	1.23	-3.26	-2.03	0.00
S04-24	64	16.1761	17	48.1993	1153.9	20240504	20241122	1.47	-2.43	-0.96	0.03
S05-24	64	20.5172	17	33.9922	1450.4	20240503	20241122	1.63	-0.79	0.84	0.24
Ske02-24	64	16.3571	16	59.2968	1196.9	20240502	20240000	1.27			0.00
Ske03-24	64	18.0542	16	56.1678	1296.6	20240502	20241001	1.78	-1.12	0.65	0.00
Ske04-24	64	20.1442	16	51.8033	1397.7	20240502	20241121	2.19	-0.81	1.38	0.15
Ske05-24	64	22.2338	16	47.2258	1472.6	20240502	20241121	2.50	-0.68	1.82	0.22
Skf00-24	64	15.4813	15	54.0959	945.0	20240430	20240925	1.74	-4.97	-3.23	0.00
Skf01-24	64	18.0173	16	5.0229	1283.4	20240430	20240925	2.76	-0.97	1.79	0.00
T01-24	64	19.1551	18	6.5258	753.1	20240505	20240129	0.22			
T02-24	64	19.4775	18	4.5569	876.1	20240504	20241022	0.43	-4.97	-4.55	0.03
T03-24	64	20.1986	17	58.6135	1058.9	20240504	20241001	0.85	-3.41	-2.56	0.00
T04-24	64	21.3299	17	51.5161	1217.8	20240503	20241122	1.23	-2.52	-1.30	0.11
T05-24	64	22.2627	17	42.9974	1343.9	20240503	20241122	1.28	-1.44	-0.17	0.17
T06-24	64	24.2655	17	36.5159	1466.9	20240504	20241122	1.71	-0.72	0.99	0.19
T06-24	64	24.2655	17	36.5159	1466.9	20240504	20240930	1.71	-0.75	0.96	0.03
T07-24	64	25.2953	17	31.2118	1562.8	20240503	20241122	1.96	-0.73	1.24	0.24
T08-24	64	26.3007	17	27.7483	1635.9	20240503	20241122	1.96	-0.70	1.27	0.27

Appendix B: Surface mass balance distribution by elevation in 2023_24.

ΔS : area in elevation range, ∑ΔS: cumulative area above given elevation, b_w: specific winter balance, b_s: specific summer balance. b_n: specific winter balance, ΔB_w: winter balance at a given elevation range, $\sum\Delta B_w$: cumulative winter balance above given elevation, ΔB_s summer balance at a given elevation range, $\sum\Delta B_s$: cumulative summer balance above given elevation, ΔB_n: net annual balance in a given elevation range, $\sum B_n$: cumulative net annual balance above given elevation.

Vatnajökull

Elevation (m a.s.l.)			ΔS (km^2)	∑ΔS (km^2)	b_w (mm)	b_s (mm)	b_n (mm)	ΔB_w ($10^6 m^3$)	$\sum\Delta B_w$ ($10^6 m^3$)	ΔB_s ($10^6 m^3$)	$\sum\Delta B_s$ ($10^6 m^3$)	ΔB_n ($10^6 m^3$)	$\sum B_n$ ($10^6 m^3$)
2000	2050	2025	0.3	0.3	4851	2470	7322	1.7	1.7	0.9	0.9	2.6	2.6
1950	2000	1975	6.9	7.3	2549	967	3517	17.6	19.3	6.7	7.6	24.3	26.9
1900	1950	1925	41.3	48.6	2070	529	2599	85.6	104.9	21.9	29.4	107.4	134.3
1850	1900	1875	44.3	92.9	2288	526	2815	101.5	206.4	23.3	52.8	124.8	259.1
1800	1850	1825	45.6	138.6	2555	737	3292	116.6	323.0	33.7	86.4	150.3	409.4
1750	1800	1775	54.8	193.4	2266	417	2684	124.3	447.3	22.9	109.3	147.2	556.6
1700	1750	1725	114.4	307.8	2025	73	2099	231.7	679.0	8.5	117.8	240.2	796.8
1650	1700	1675	217.3	525.1	2016	-185	1830	438.1	1117.2	-40.3	77.4	397.8	1194.6
1600	1650	1625	373.6	898.7	2060	-250	1809	770.0	1887.1	-93.8	-16.3	676.2	1870.8
1550	1600	1575	357.9	1256.6	2036	-345	1691	728.8	2616.0	-123.6	-139.9	605.2	2476.0
1500	1550	1525	421.2	1677.8	1983	-475	1507	835.7	3451.7	-200.5	-340.4	635.2	3111.2
1450	1500	1475	452.5	2130.4	1968	-656	1311	890.8	4342.5	-297.3	-637.7	593.5	3704.8
1400	1450	1425	502.9	2633.3	1982	-800	1182	996.8	5339.3	-402.4	-1040.1	594.4	4299.2
1350	1400	1375	540.3	3173.6	1958	-961	997	1058.1	6397.4	-519.3	-1559.4	538.8	4838.0
1300	1350	1325	531.3	3704.8	1868	-1140	728	992.9	7390.3	-606.0	-2165.4	386.9	5224.9
1250	1300	1275	496.7	4201.6	1758	-1353	405	873.5	8263.8	-672.1	-2837.6	201.3	5426.2
1200	1250	1225	435.5	4637.1	1597	-1680	-83	695.8	8959.6	-732.1	-3569.6	-36.2	5390.0
1150	1200	1175	387.9	5025.0	1448	-2031	-583	561.8	9521.4	-788.0	-4357.6	-226.2	5163.8
1100	1150	1125	344.1	5369.1	1324	-2349	-1025	455.8	9977.2	-808.5	-5166.1	-352.7	4811.1
1050	1100	1075	296.5	5665.6	1214	-2670	-1456	360.1	10337.3	-791.8	-5957.9	-431.7	4379.4
1000	1050	1025	276.5	5942.1	1101	-3023	-1921	304.5	10641.8	-835.9	-6793.8	-531.4	3848.0
950	1000	975	247.4	6189.5	1010	-3311	-2301	249.9	10891.8	-819.4	-7613.2	-569.4	3278.6
900	950	925	214.0	6403.6	911	-3575	-2663	195.2	11086.9	-765.2	-8378.4	-570.1	2708.5
850	900	875	184.3	6587.9	792	-3854	-3061	146.1	11233.0	-710.4	-9088.8	-564.3	2144.2
800	850	825	166.7	6754.6	689	-4153	-3463	114.9	11347.9	-692.2	-9781.0	-577.4	1566.9
750	800	775	145.4	6899.9	594	-4388	-3793	86.5	11434.4	-637.9	-10418.9	-551.4	1015.4
700	750	725	114.8	7014.8	519	-4550	-4030	59.7	11494.1	-522.5	-10941.5	-462.8	552.6
650	700	675	95.1	7109.9	516	-4641	-4125	49.1	11543.2	-441.4	-11382.9	-392.3	160.3
600	650	625	64.3	7174.2	537	-4770	-4232	34.6	11577.8	-306.9	-11689.8	-272.3	-112.0
550	600	575	52.7	7226.9	455	-5024	-4568	24.0	11601.8	-264.9	-11954.7	-240.9	-352.9
500	550	525	53.6	7280.5	353	-5296	-4942	18.9	11620.7	-283.8	-12238.5	-264.9	-617.8
450	500	475	37.9	7318.4	253	-5546	-5292	9.6	11630.3	-210.2	-12448.7	-200.5	-818.4
400	450	425	34.7	7353.2	149	-5776	-5626	5.2	11635.5	-200.7	-12649.3	-195.5	-1013.8
350	400	375	38.9	7392.0	14	-6034	-6020	0.5	11636.1	-234.6	-12883.9	-234.0	-1247.8
300	350	325	35.2	7427.2	-155	-6373	-6528	-5.5	11630.6	-224.1	-13108.0	-229.6	-1477.4
250	300	275	31.9	7459.1	-336	-6721	-7058	-10.8	11619.9	-214.5	-13322.5	-225.2	-1702.6
200	250	225	30.7	7489.8	-526	-7082	-7608	-16.1	11603.7	-217.2	-13539.7	-233.4	-1936.0
150	200	175	29.6	7519.4	-692	-7449	-8141	-20.5	11583.2	-220.7	-13760.4	-241.2	-2177.2
100	150	125	28.2	7547.6	-859	-7885	-8744	-24.2	11559.0	-222.3	-13982.8	-246.6	-2423.8
50	100	75	22.2	7569.8	-1035	-8341	-9376	-23.0	11536.0	-185.1	-14167.9	-208.1	-2631.9
0	50	25	24.1	7593.9	-1352	-9124	-10477	-32.6	11503.4	-219.7	-14387.6	-252.3	-2884.1

Tungnaárjökull

Elevation (m a.s.l.)			ΔS (km^2)	∑ΔS (km^2)	b_w (mm)	b_s (mm)	b_n (mm)	ΔB_w ($10^6 m^3$)	$\sum\Delta B_w$ ($10^6 m^3$)	ΔB_s ($10^6 m^3$)	$\sum\Delta B_s$ ($10^6 m^3$)	ΔB_n ($10^6 m^3$)	$\sum B_n$ ($10^6 m^3$)
1650	1700	1675	1.7	1.7	1899	-525	1374	3.3	3.3	-0.9	-0.9	2.4	2.4
1600	1650	1625	12.3	14.0	1922	-577	1345	23.7	27.0	-7.1	-8.0	16.6	18.9
1550	1600	1575	16.3	30.4	1863	-558	1304	30.4	57.4	-9.1	-17.1	21.3	40.2
1500	1550	1525	16.1	46.4	1788	-619	1169	28.7	86.1	-9.9	-27.1	18.8	59.0
1450	1500	1475	18.3	64.7	1670	-711	958	30.6	116.7	-13.0	-40.1	17.5	76.6
1400	1450	1425	23.0	87.8	1540	-932	608	35.5	152.1	-21.5	-61.6	14.0	90.6
1350	1400	1375	21.0	108.8	1401	-1186	214	29.4	181.6	-24.9	-86.5	4.5	95.1
1300	1350	1325	27.1	135.9	1316	-1499	-183	35.7	217.3	-40.6	-127.1	-5.0	90.1
1250	1300	1275	20.3	156.2	1283	-1934	-651	26.1	243.3	-39.3	-166.4	-13.2	76.9
1200	1250	1225	22.2	178.4	1207	-2418	-1211	26.8	270.1	-53.7	-220.2	-26.9	50.0
1150	1200	1175	21.0	199.4	1110	-2759	-1649	23.3	293.4	-57.9	-278.0	-34.6	15.4
1100	1150	1125	17.6	217.0	977	-3047	-2069	17.3	310.7	-53.8	-331.8	-36.5	-21.1
1050	1100	1075	16.4	233.4	871	-3364	-2492	14.3	325.0	-55.3	-387.1	-41.0	-62.1
1000	1050	1025	16.7	250.2	770	-3775	-3005	12.9	337.9	-63.1	-450.3	-50.3	-112.4
950	1000	975	15.6	265.8	647	-4209	-3561	10.1	348.0	-65.8	-516.1	-55.7	-168.1
900	950	925	16.0	281.8	526	-4615	-4088	8.4	356.4	-74.0	-590.1	-65.6	-233.6
850	900	875	12.4	294.3	425	-4984	-4558	5.3	361.7	-61.9	-652.0	-56.6	-290.2
800	850	825	12.1	306.3	351	-5303	-4951	4.2	366.0	-63.9	-715.9	-59.7	-349.9
750	800	775	9.7	316.0	287	-5689	-5401	2.8	368.8	-54.9	-770.9	-52.2	-402.1
700	750	725	6.1	322.0	239	-6032	-5792	1.5	370.2	-36.5	-807.4	-35.1	-437.2
650	700	675	1.2	323.2	229	-6116	-5887	0.3	370.5	-7.1	-814.5	-6.9	-444.0

Sylgjujökull

Elevation (m a.s.l.)			ΔS (km^2)	∑ΔS (km^2)	b_w (mm)	b_s (mm)	b_n (mm)	ΔB_w ($10^6 m^3$)	$\sum\Delta B_w$ ($10^6 m^3$)	ΔB_s ($10^6 m^3$)	$\sum\Delta B_s$ ($10^6 m^3$)	ΔB_n ($10^6 m^3$)	$\sum B_n$ ($10^6 m^3$)
1600	1650	1625	1.4	1.4	1790	-320	1469	2.5	2.5	-0.4	-0.4	2.0	2.0
1550	1600	1575	5.1	6.5	1732	-372	1359	8.9	11.3	-1.9	-2.3	7.0	9.0
1500	1550	1525	18.8	25.3	1612	-436	1176	30.4	41.7	-8.2	-10.6	22.1	31.1
1450	1500	1475	13.4	38.7	1536	-618	917	20.6	62.3	-8.3	-18.9	12.3	43.4
1400	1450	1425	8.3	47.1	1497	-872	625	12.5	74.8	-7.3	-26.1	5.2	48.6
1350	1400	1375	5.6	52.6	1428	-1094	334	8.0	82.7	-6.1	-32.2	1.9	50.5
1300	1350	1325	5.1	57.7	1362	-1434	-72	6.9	89.7	-7.3	-39.5	-0.4	50.1
1250	1300	1275	9.6	67.3	1227	-1991	-763	11.8	101.5	-19.1	-58.7	-7.3	42.8
1200	1250	1225	11.4	78.7	1048	-2559	-1511	11.9	113.4	-29.2	-87.9	-17.2	25.6
1150	1200	1175	12.8	91.5	867	-2907	-2039	11.1	124.5	-37.2	-125.1	-26.1	-0.5
1100	1150	1125	12.1	103.6	726	-3141	-2415	8.8	133.3	-38.0	-163.1	-29.2	-29.7
1050	1100	1075	11.2	114.8	638	-3379	-2740	7.1	140.4	-37.7	-200.7	-30.6	-60.3
1000	1050	1025	9.9	124.7	576	-3654	-3077	5.7	146.2	-36.3	-237.1	-30.6	-90.9
950	1000	975	3.1	127.8	538	-3825	-3287	1.7	147.8	-11.9	-248.9	-10.2	-101.1
900	950	925	1.2	129.1	506	-3998	-3492	0.6	148.5	-4.9	-253.8	-4.3	-105.4

Köldukvíslarjökul

Elevation (m a.s.l.)			ΔS (km^2)	∑ΔS (km^2)	b_w (mm)	b_s (mm)	b_n (mm)	ΔB_w ($10^6 m^3$)	$\sum\Delta B_w$ ($10^6 m^3$)	ΔB_s ($10^6 m^3$)	$\sum\Delta B_s$ ($10^6 m^3$)	ΔB_n ($10^6 m^3$)	$\sum B_n$ ($10^6 m^3$)
1950	2000	1975	0.6	0.6	1892	648	2540	1.2	1.2	0.4	0.4	1.6	1.6
1900	1950	1925	13.7	14.4	1869	461	2331	25.7	26.9	6.3	6.8	32.0	33.6
1850	1900	1875	6.6	20.9	1821	291	2113	12.0	38.9	1.9	8.7	13.9	47.5
1800	1850	1825	6.2	27.1	1810	213	2024	11.2	50.1	1.3	10.0	12.5	60.1
1750	1800	1775	10.1	37.3	1790	160	1950	18.2	68.2	1.6	11.6	19.8	79.9
1700	1750	1725	17.3	54.6	1715	48	1763	29.6	97.9	0.8	12.5	30.5	110.3
1650	1700	1675	16.0	70.5	1648	-110	1538	26.3	124.2	-1.8	10.7	24.6	134.9
1600	1650	1625	14.3	84.8	1615	-261	1353	23.1	147.3	-3.7	6.9	19.4	154.3
1550	1600	1575	18.4	103.3	1600	-425	1175	29.5	176.8	-7.8	-0.9	21.7	176.0
1500	1550	1525	19.9	123.2	1530	-582	947	30.5	207.3	-11.6	-12.5	18.9	194.8
1450	1500	1475	19.2	142.4	1460	-791	668	28.1	235.4	-15.2	-27.7	12.9	207.7
1400	1450	1425	14.8	157.2	1361	-1000	360	20.2	255.6	-14.8	-42.5	5.3	213.0
1350	1400	1375	14.7	172.0	1217	-1265	-48	18.0	273.5	-18.7	-61.2	-0.7	212.3
1300	1350	1325	16.3	188.3	1064	-1591	-526	17.3	290.9	-25.9	-87.1	-8.6	203.7
1250	1300	1275	17.3	205.6	948	-2001	-1053	16.4	307.3	-34.7	-121.8	-18.2	185.5
1200	1250	1225	16.5	222.1	860	-2447	-1587	14.2	321.5	-40.5	-162.3	-26.2	159.2
1150	1200	1175	15.9	238.0	784	-2891	-2107	12.5	334.0	-46.0	-208.3	-33.5	125.7
1100	1150	1125	14.1	252.1	702	-3324	-2622	9.9	343.9	-46.8	-255.1	-36.9	88.8
1050	1100	1075	12.7	264.8	616	-3786	-3170	7.8	351.7	-47.9	-303.0	-40.1	48.7
1000	1050	1025	10.2	275.0	543	-4226	-3682	5.6	357.2	-43.2	-346.2	-37.6	11.0
950	1000	975	7.2	282.2	494	-4529	-4034	3.6	360.8	-32.8	-379.0	-29.2	-18.2
900	950	925	1.2	283.5	460	-4702	-4242	0.6	361.4	-5.7	-384.7	-5.1	-23.4

Dyngjujökull

Elevation (m a.s.l.)			ΔS (km^2)	∑ΔS (km^2)	b_w (mm)	b_s (mm)	b_n (mm)	ΔB_w ($10^6 m^3$)	$\sum\Delta B_w$ ($10^6 m^3$)	ΔB_s ($10^6 m^3$)	$\sum\Delta B_s$ ($10^6 m^3$)	ΔB_n ($10^6 m^3$)	$\sum B_n$ ($10^6 m^3$)
1950	2000	1975	2.4	2.4	1889	519	2409	4.5	4.5	1.2	1.2	5.7	5.7
1900	1950	1925	17.7	20.1	1899	385	2285	33.6	38.1	6.8	8.0	40.4	46.1
1850	1900	1875	21.7	41.8	1899	153	2053	41.3	79.4	3.3	11.4	44.6	90.8
1800	1850	1825	13.2	55.0	1897	126	2023	25.0	104.5	1.7	13.0	26.7	117.5
1750	1800	1775	15.6	70.7	1899	68	1967	29.7	134.2	1.1	14.1	30.8	148.3
1700	1750	1725	32.7	103.3	1907	-54	1853	62.3	196.5	-1.8	12.3	60.5	208.8
1650	1700	1675	74.5	177.8	1952	-206	1746	145.5	342.0	-15.4	-3.1	130.1	338.9
1600	1650	1625	120.5	298.3	1955	-255	1699	235.7	577.6	-30.8	-33.9	204.8	543.7
1550	1600	1575	96.3	394.6	1839	-400	1438	177.2	754.8	-38.6	-72.5	138.6	682.3
1500	1550	1525	86.8	481.4	1740	-570	1169	151.1	905.9	-49.6	-122.1	101.5	783.8
1450	1500	1475	72.6	554.0	1672	-740	932	121.4	1027.3	-53.7	-175.8	67.7	851.5
1400	1450	1425	60.3	614.3	1599	-896	703	96.4	1123.7	-54.0	-229.8	42.4	893.9
1350	1400	1375	47.7	661.9	1526	-1172	353	72.7	1196.5	-55.9	-285.7	16.8	910.8
1300	1350	1325	36.1	698.0	1404	-1551	-147	50.7	1247.2	-56.0	-341.7	-5.3	905.5
1250	1300	1275	39.2	737.2	1265	-1910	-645	49.6	1296.7	-74.8	-416.5	-25.3	880.2
1200	1250	1225	43.5	780.7	1093	-2273	-1180	47.6	1344.3	-98.9	-515.4	-51.3	828.9
1150	1200	1175	43.3	824.0	906	-2726	-1819	39.3	1383.5	-118.0	-633.5	-78.8	750.1
1100	1150	1125	42.3	866.3	760	-3198	-2437	32.2	1415.8	-135.4	-768.9	-103.2	646.9
1050	1100	1075	30.2	896.6	642	-3709	-3067	19.4	1435.2	-112.2	-881.1	-92.8	554.1
1000	1050	1025	30.6	927.2	560	-4239	-3679	17.1	1452.3	-129.7	-1010.9	-112.6	441.5
950	1000	975	28.4	955.6	477	-4741	-4263	13.6	1465.9	-134.8	-1145.7	-121.3	320.2
900	950	925	24.3	979.9	405	-5150	-4744	9.9	1475.8	-125.1	-1270.8	-115.3	204.9
850	900	875	20.4	1000.4	346	-5560	-5214	7.1	1482.9	-113.6	-1384.4	-106.5	98.4
800	850	825	16.5	1016.9	305	-5976	-5671	5.0	1487.9	-98.7	-1483.1	-93.7	4.8
750	800	775	8.5	1025.4	270	-6287	-6016	2.3	1490.2	-53.5	-1536.6	-51.2	-46.4
700	750	725	0.3	1025.7	245	-6402	-6156	0.1	1490.3	-2.2	-1538.8	-2.1	-48.5

Brúarjökull

Elevation (m a.s.l.)			ΔS (km^2)	∑ΔS (km^2)	b_w (mm)	b_s (mm)	b_n (mm)	ΔB_w ($10^6 m^3$)	$\sum\Delta B_w$ ($10^6 m^3$)	ΔB_s ($10^6 m^3$)	$\sum\Delta B_s$ ($10^6 m^3$)	ΔB_n ($10^6 m^3$)	$\sum B_n$ ($10^6 m^3$)
1900	1950	1925	0.0	0.0	1899	259	2159	0.1	0.1	0.0	0.0	0.1	0.1
1850	1900	1875	1.2	1.3	1890	316	2207	2.3	2.4	0.4	0.4	2.7	2.8
1800	1850	1825	4.4	5.6	1878	318	2197	8.2	10.6	1.4	1.8	9.6	12.4
1750	1800	1775	2.8	8.5	1923	173	2097	5.5	16.1	0.5	2.3	5.9	18.4
1700	1750	1725	4.0	12.5	1973	47	2021	7.9	23.9	0.2	2.5	8.1	26.4
1650	1700	1675	5.6	18.1	1993	-40	1953	11.2	35.1	-0.2	2.3	11.0	37.4
1600	1650	1625	51.6	69.6	2056	-182	1873	106.0	141.1	-9.4	-7.1	96.6	134.0
1550	1600	1575	47.7	117.3	2039	-229	1810	97.2	238.4	-10.9	-18.1	86.3	220.3
1500	1550	1525	73.6	190.9	1972	-308	1663	145.1	383.5	-22.7	-40.8	122.4	342.7
1450	1500	1475	80.1	271.0	1956	-519	1436	156.7	540.2	-41.6	-82.4	115.1	457.7
1400	1450	1425	114.0	385.0	2071	-706	1364	236.1	776.2	-80.5	-162.9	155.6	613.3
1350	1400	1375	157.5	542.4	2060	-934	1126	324.5	1100.8	-147.1	-310.1	177.4	790.7
1300	1350	1325	147.2	689.7	1963	-1125	837	289.0	1389.8	-165.7	-475.7	123.4	914.1
1250	1300	1275	137.9	827.6	1869	-1304	564	257.8	1647.6	-180.0	-655.7	77.9	991.9
1200	1250	1225	115.8	943.4	1739	-1603	135	201.4	1849.0	-185.6	-841.3	15.7	1007.7
1150	1200	1175	99.5	1042.9	1572	-1970	-397	156.5	2005.5	-196.0	-1037.3	-39.5	968.2
1100	1150	1125	80.2	1123.1	1386	-2295	-908	111.2	2116.7	-184.1	-1221.4	-72.9	895.3
1050	1100	1075	64.9	1188.0	1200	-2557	-1356	77.9	2194.6	-166.0	-1387.4	-88.1	807.2
1000	1050	1025	57.2	1245.2	1053	-2842	-1788	60.2	2254.8	-162.5	-1549.9	-102.3	704.9
950	1000	975	51.6	1296.8	932	-3181	-2249	48.1	2303.0	-164.3	-1714.2	-116.2	588.7
900	950	925	44.6	1341.4	802	-3548	-2745	35.8	2338.8	-158.2	-1872.5	-122.4	466.3
850	900	875	38.4	1379.8	636	-3889	-3252	24.4	2363.2	-149.2	-2021.7	-124.8	341.5
800	850	825	34.2	1414.0	464	-4233	-3769	15.9	2379.1	-145.0	-2166.7	-129.1	212.4
750	800	775	30.9	1444.9	304	-4613	-4308	9.4	2388.5	-142.7	-2309.4	-133.3	79.1
700	750	725	26.1	1471.0	205	-4951	-4745	5.4	2393.9	-129.2	-2438.6	-123.8	-44.7
650	700	675	9.5	1480.6	132	-5188	-5056	1.3	2395.1	-49.5	-2488.1	-48.3	-93.0
600	650	625	0.5	1481.1	96	-5311	-5215	0.0	2395.2	-2.6	-2490.7	-2.5	-95.5

Eyjabakkajökull

Elevation (m a.s.l.)			ΔS (km^2)	∑ΔS (km^2)	b_w (mm)	b_s (mm)	b_n (mm)	ΔB_w ($10^6 m^3$)	$\sum\Delta B_w$ ($10^6 m^3$)	ΔB_s ($10^6 m^3$)	$\sum\Delta B_s$ ($10^6 m^3$)	ΔB_n ($10^6 m^3$)	$\sum B_n$ ($10^6 m^3$)
1550	1600	1575	0.0	0.0	2299	-31	2268	0.0	0.0	0.0	0.0	0.0	0.0
1500	1550	1525	0.1	0.1	2299	11	2311	0.2	0.2	0.0	0.0	0.2	0.2
1450	1500	1475	1.1	1.2	2299	13	2313	2.6	2.8	0.0	0.0	2.6	2.8
1400	1450	1425	2.0	3.3	2299	-30	2269	4.7	7.5	-0.1	0.0	4.6	7.5
1350	1400	1375	2.6	5.9	2289	-182	2107	6.0	13.5	-0.5	-0.5	5.5	13.0
1300	1350	1325	4.2	10.1	2262	-452	1809	9.5	23.0	-1.9	-2.4	7.6	20.6
1250	1300	1275	13.4	23.5	2083	-980	1102	27.9	50.9	-13.1	-15.5	14.7	35.3
1200	1250	1225	12.4	35.9	2018	-1302	715	25.1	76.0	-16.2	-31.8	8.9	44.2
1150	1200	1175	13.9	49.8	1889	-1626	263	26.2	102.2	-22.6	-54.3	3.7	47.9
1100	1150	1125	11.4	61.2	1720	-1980	-260	19.7	121.9	-22.7	-77.0	-3.0	44.9
1050	1100	1075	9.8	71.1	1518	-2425	-907	14.9	136.8	-23.8	-100.8	-8.9	36.0
1000	1050	1025	9.1	80.2	1310	-2809	-1498	12.0	148.8	-25.7	-126.5	-13.7	22.3
950	1000	975	7.6	87.8	1117	-3285	-2168	8.5	157.3	-25.0	-151.5	-16.5	5.8
900	950	925	5.0	92.8	919	-3839	-2920	4.6	161.9	-19.4	-170.8	-14.7	-8.9
850	900	875	3.9	96.7	774	-4226	-3452	3.0	165.0	-16.5	-187.4	-13.5	-22.4
800	850	825	2.9	99.6	641	-4577	-3935	1.8	166.8	-13.1	-200.4	-11.2	-33.6
750	800	775	1.8	101.4	465	-4988	-4523	0.8	167.6	-8.7	-209.2	-7.9	-41.6
700	750	725	1.6	103.0	317	-5356	-5038	0.5	168.1	-8.8	-218.0	-8.3	-49.8
650	700	675	0.6	103.6	200	-5660	-5459	0.1	168.3	-3.6	-221.6	-3.5	-53.3

Hoffellsjökull

Elevation (m a.s.l.)			ΔS (km^2)	∑ΔS (km^2)	b_w (mm)	b_s (mm)	b_n (mm)	ΔB_w ($10^6 m^3$)	$\sum\Delta B_w$ ($10^6 m^3$)	ΔB_s ($10^6 m^3$)	$\sum\Delta B_s$ ($10^6 m^3$)	ΔB_n ($10^6 m^3$)	$\sum B_n$ ($10^6 m^3$)
1450	1500	1475	1.2	1.2	2299	45	2345	2.7	2.7	0.1	0.1	2.7	2.7
1400	1450	1425	7.3	8.4	2235	-368	1867	16.3	18.9	-2.7	-2.6	13.6	16.3
1350	1400	1375	9.8	18.3	2227	-509	1717	21.9	40.9	-5.0	-7.6	16.9	33.2
1300	1350	1325	16.1	34.4	2207	-704	1502	35.5	76.4	-11.3	-19.0	24.2	57.4
1250	1300	1275	34.4	68.7	2151	-952	1198	73.9	150.3	-32.7	-51.7	41.2	98.6
1200	1250	1225	25.5	94.3	2190	-1081	1109	55.9	206.2	-27.6	-79.3	28.3	126.9
1150	1200	1175	17.6	111.9	2184	-1336	847	38.4	244.7	-23.5	-102.8	14.9	141.8
1100	1150	1125	16.6	128.4	2148	-1653	494	35.6	280.2	-27.4	-130.2	8.2	150.0
1050	1100	1075	12.4	140.8	2042	-2008	34	25.4	305.6	-25.0	-155.2	0.4	150.5
1000	1050	1025	9.4	150.3	1937	-2286	-348	18.3	323.9	-21.6	-176.7	-3.3	147.2
950	1000	975	8.6	158.9	1821	-2558	-736	15.7	339.6	-22.1	-198.8	-6.4	140.8
900	950	925	6.7	165.6	1668	-2811	-1143	11.1	350.7	-18.7	-217.5	-7.6	133.2
850	900	875	4.2	169.7	1522	-3089	-1567	6.4	357.1	-12.9	-230.4	-6.5	126.6
800	850	825	3.4	173.2	1408	-3327	-1919	4.8	361.9	-11.4	-241.8	-6.6	120.1
750	800	775	2.9	176.1	1316	-3454	-2138	3.8	365.7	-10.1	-251.9	-6.2	113.8
700	750	725	2.9	179.0	1111	-3849	-2737	3.3	369.0	-11.3	-263.2	-8.0	105.8
650	700	675	3.2	182.2	914	-4327	-3412	2.9	371.9	-13.7	-276.9	-10.8	95.0
600	650	625	2.5	184.7	800	-4625	-3824	2.0	373.9	-11.6	-288.5	-9.6	85.4
550	600	575	1.8	186.5	698	-4861	-4163	1.3	375.2	-8.7	-297.2	-7.5	78.0
500	550	525	1.5	188.0	596	-5125	-4529	0.9	376.1	-7.7	-304.9	-6.8	71.1
450	500	475	1.1	189.0	429	-5478	-5049	0.5	376.5	-5.8	-310.7	-5.4	65.8
400	450	425	0.7	189.8	258	-5720	-5462	0.2	376.7	-4.1	-314.9	-3.9	61.8
350	400	375	0.7	190.5	-1	-6003	-6004	0.0	376.7	-4.3	-319.1	-4.3	57.5
300	350	325	0.5	191.0	-245	-6346	-6591	-0.1	376.6	-3.2	-322.3	-3.3	54.2
250	300	275	0.6	191.6	-442	-6684	-7126	-0.3	376.3	-4.0	-326.4	-4.3	49.9
200	250	225	0.9	192.4	-596	-7050	-7647	-0.5	375.8	-6.0	-332.4	-6.5	43.4
150	200	175	1.8	194.2	-751	-7469	-8221	-1.3	374.5	-13.4	-345.8	-14.7	28.7
100	150	125	2.4	196.6	-916	-7950	-8866	-2.2	372.3	-18.8	-364.6	-21.0	7.7
50	100	75	2.2	198.8	-1231	-8453	-9684	-2.7	369.6	-18.5	-383.1	-21.2	-13.5
0	50	25	2.9	201.7	-1720	-9302	-11022	-5.0	364.6	-26.9	-409.9	-31.8	-45.3

Breiðamerkurjökull

Elevation (m a.s.l.)			ΔS (km^2)	∑ΔS (km^2)	b_w (mm)	b_s (mm)	b_n (mm)	ΔB_w ($10^6 m^3$)	$\sum\Delta B_w$ ($10^6 m^3$)	ΔB_s ($10^6 m^3$)	$\sum\Delta B_s$ ($10^6 m^3$)	ΔB_n ($10^6 m^3$)	$\sum B_n$ ($10^6 m^3$)
1900	1950	1925	0.0	0.0	4715	2299	7015	0.2	0.2	0.1	0.1	0.3	0.3
1850	1900	1875	0.4	0.4	4692	2338	7030	1.7	2.0	0.9	1.0	2.6	3.0
1800	1850	1825	0.5	0.9	4565	2266	6831	2.2	4.2	1.1	2.1	3.3	6.2
1750	1800	1775	0.9	1.8	4392	1974	6367	4.0	8.2	1.8	3.9	5.8	12.0
1700	1750	1725	2.6	4.4	3423	917	4340	8.8	17.0	2.4	6.2	11.2	23.2
1650	1700	1675	6.0	10.4	2726	333	3060	16.3	33.3	2.0	8.2	18.3	41.6
1600	1650	1625	18.0	28.3	2515	98	2613	45.2	78.5	1.8	10.0	46.9	88.5
1550	1600	1575	26.4	54.7	2397	-96	2300	63.2	141.7	-2.5	7.5	60.6	149.1
1500	1550	1525	31.8	86.5	2321	-316	2005	73.9	215.5	-10.1	-2.6	63.8	212.9
1450	1500	1475	46.6	133.1	2261	-523	1737	105.3	320.8	-24.4	-27.0	80.9	293.8
1400	1450	1425	57.5	190.6	2234	-695	1539	128.5	449.3	-40.0	-67.0	88.5	382.3
1350	1400	1375	88.2	278.8	2200	-868	1332	194.1	643.5	-76.6	-143.6	117.5	499.9
1300	1350	1325	94.3	373.1	2128	-917	1210	200.6	844.1	-86.5	-230.1	114.1	614.0
1250	1300	1275	56.9	430.0	1991	-978	1012	113.3	957.3	-55.7	-285.7	57.6	671.6
1200	1250	1225	38.2	468.2	1852	-1154	698	70.9	1028.2	-44.2	-329.9	26.7	698.3
1150	1200	1175	30.7	498.9	1736	-1414	322	53.3	1081.5	-43.4	-373.4	9.9	708.2
1100	1150	1125	25.1	524.1	1625	-1690	-64	40.8	1122.4	-42.5	-415.8	-1.6	706.6
1050	1100	1075	21.6	545.7	1527	-1953	-426	33.1	1155.4	-42.3	-458.1	-9.2	697.3
1000	1050	1025	18.7	564.4	1438	-2201	-762	26.9	1182.4	-41.2	-499.3	-14.3	683.0
950	1000	975	20.3	584.7	1320	-2549	-1229	26.8	1209.1	-51.7	-551.0	-24.9	658.1
900	950	925	21.9	606.6	1244	-2817	-1572	27.3	1236.4	-61.7	-612.7	-34.4	623.7
850	900	875	17.9	624.5	1155	-3104	-1949	20.7	1257.1	-55.7	-668.4	-35.0	588.7
800	850	825	20.8	645.4	1030	-3414	-2384	21.5	1278.6	-71.2	-739.6	-49.7	539.0
750	800	775	21.8	667.2	896	-3752	-2855	19.5	1298.1	-81.8	-821.3	-62.2	476.8
700	750	725	16.7	683.8	798	-4042	-3244	13.3	1311.4	-67.3	-888.6	-54.0	422.8
650	700	675	22.4	706.3	714	-4326	-3611	16.0	1327.5	-97.1	-985.7	-81.0	341.8
600	650	625	25.4	731.6	614	-4618	-4004	15.6	1343.1	-117.2	-1102.9	-101.6	240.1
550	600	575	22.5	754.2	508	-4917	-4409	11.5	1354.5	-110.9	-1213.8	-99.4	140.7
500	550	525	21.2	775.4	405	-5125	-4719	8.6	1363.1	-108.7	-1322.5	-100.1	40.7
450	500	475	12.1	787.5	297	-5352	-5054	3.6	1366.7	-64.9	-1387.4	-61.3	-20.6
400	450	425	13.3	800.8	182	-5632	-5449	2.4	1369.2	-74.8	-1462.2	-72.4	-93.0
350	400	375	14.7	815.5	46	-5982	-5936	0.7	1369.8	-87.8	-1550.0	-87.2	-180.2
300	350	325	11.6	827.1	-128	-6380	-6508	-1.5	1368.4	-74.2	-1624.2	-75.6	-255.8
250	300	275	9.8	836.9	-379	-6723	-7103	-3.7	1364.6	-66.1	-1690.2	-69.8	-325.6
200	250	225	9.9	846.8	-631	-7020	-7651	-6.3	1358.4	-69.7	-1759.9	-75.9	-401.6
150	200	175	8.9	855.7	-823	-7340	-8164	-7.3	1351.0	-65.1	-1825.0	-72.4	-474.0
100	150	125	9.1	864.8	-952	-7811	-8764	-8.7	1342.4	-71.0	-1896.0	-79.6	-553.6
50	100	75	7.0	871.8	-1078	-8384	-9462	-7.6	1334.8	-58.9	-1954.9	-66.5	-620.1
0	50	25	3.0	874.8	-1187	-9067	-10255	-3.5	1331.3	-26.9	-1981.8	-30.4	-650.5

Síðujökull

Elevation (m a.s.l.)			ΔS (km^2)	∑ΔS (km^2)	b_w (mm)	b_s (mm)	b_n (mm)	ΔB_w ($10^6 m^3$)	$\sum\Delta B_w$ ($10^6 m^3$)	ΔB_s ($10^6 m^3$)	$\sum\Delta B_s$ ($10^6 m^3$)	ΔB_n ($10^6 m^3$)	$\sum B_n$ ($10^6 m^3$)
1700	1750	1725	0.9	0.9	2386	248	2635	2.2	2.2	0.2	0.2	2.4	2.4
1650	1700	1675	5.9	6.9	2281	-290	1991	13.6	15.8	-1.7	-1.5	11.8	14.3
1600	1650	1625	11.3	18.1	2136	-549	1586	24.0	39.8	-6.2	-7.7	17.9	32.1
1550	1600	1575	11.7	29.8	2101	-615	1485	24.5	64.3	-7.2	-14.9	17.3	49.5
1500	1550	1525	21.4	51.2	1998	-722	1276	42.8	107.1	-15.5	-30.3	27.4	76.8
1450	1500	1475	38.0	89.2	1786	-837	948	67.9	175.0	-31.8	-62.2	36.1	112.9
1400	1450	1425	24.8	114.0	1671	-956	715	41.4	216.4	-23.7	-85.9	17.7	130.6
1350	1400	1375	21.0	135.0	1631	-1240	391	34.2	250.7	-26.0	-111.9	8.2	138.8
1300	1350	1325	17.1	152.0	1574	-1542	31	26.9	277.6	-26.3	-138.2	0.5	139.3
1250	1300	1275	15.1	167.2	1540	-1800	-259	23.3	300.9	-27.2	-165.5	-3.9	135.4
1200	1250	1225	21.1	188.3	1521	-2005	-483	32.1	333.0	-42.3	-207.8	-10.2	125.2
1150	1200	1175	17.5	205.8	1472	-2293	-820	25.8	358.9	-40.3	-248.1	-14.4	110.8
1100	1150	1125	16.6	222.5	1405	-2583	-1177	23.4	382.2	-43.0	-291.1	-19.6	91.2
1050	1100	1075	15.0	237.5	1338	-2900	-1561	20.1	402.4	-43.6	-334.7	-23.5	67.7
1000	1050	1025	18.5	256.0	1252	-3158	-1906	23.1	425.5	-58.3	-393.0	-35.2	32.5
950	1000	975	19.4	275.4	1121	-3379	-2258	21.7	447.2	-65.4	-458.5	-43.7	-11.2
900	950	925	19.6	294.9	960	-3605	-2645	18.8	466.0	-70.5	-529.0	-51.7	-63.0
850	900	875	18.8	313.7	829	-3848	-3019	15.6	481.6	-72.3	-601.2	-56.7	-119.7
800	850	825	17.7	331.4	697	-4097	-3399	12.3	493.9	-72.4	-673.6	-60.1	-179.7
750	800	775	20.1	351.5	558	-4399	-3841	11.2	505.1	-88.5	-762.1	-77.3	-257.0
700	750	725	20.0	371.5	428	-4702	-4273	8.6	513.7	-94.3	-856.4	-85.7	-342.7
650	700	675	19.9	391.4	305	-5018	-4713	6.1	519.8	-99.9	-956.3	-93.8	-436.5
600	650	625	8.9	400.3	231	-5281	-5050	2.1	521.8	-47.0	-1003.3	-45.0	-481.5
550	600	575	0.0	400.4	201	-5400	-5198	0.0	521.8	-0.2	-1003.6	-0.2	-481.7

Skaftárjökull

Elevation (m a.s.l.)			ΔS (km^2)	∑ΔS (km^2)	b_w (mm)	b_s (mm)	b_n (mm)	ΔB_w ($10^6 m^3$)	$\sum\Delta B_w$ ($10^6 m^3$)	ΔB_s ($10^6 m^3$)	$\sum\Delta B_s$ ($10^6 m^3$)	ΔB_n ($10^6 m^3$)	$\sum B_n$ ($10^6 m^3$)
1400	1450	1425	0.0	0.0	1500	-1100	399	0.0	0.0	0.0	0.0	0.0	0.0
1350	1400	1375	2.5	2.5	1471	-1260	211	3.6	3.6	-3.1	-3.1	0.5	0.5
1300	1350	1325	5.2	7.7	1421	-1526	-105	7.4	11.1	-8.0	-11.1	-0.6	0.0
1250	1300	1275	4.0	11.7	1400	-1868	-468	5.5	16.6	-7.4	-18.5	-1.9	-1.9
1200	1250	1225	6.3	17.9	1393	-2253	-860	8.7	25.4	-14.1	-32.6	-5.4	-7.3
1150	1200	1175	7.4	25.3	1356	-2550	-1194	10.0	35.3	-18.8	-51.4	-8.8	-16.1
1100	1150	1125	10.6	35.9	1275	-2832	-1557	13.5	48.9	-30.1	-81.5	-16.5	-32.6
1050	1100	1075	11.7	47.6	1174	-3130	-1955	13.7	62.6	-36.6	-118.1	-22.9	-55.5
1000	1050	1025	12.7	60.4	1048	-3425	-2376	13.4	76.0	-43.6	-161.8	-30.3	-85.8
950	1000	975	8.8	69.2	895	-3698	-2802	7.9	83.9	-32.6	-194.4	-24.7	-110.5
900	950	925	5.8	75.0	781	-3926	-3144	4.5	88.4	-22.7	-217.2	-18.2	-128.7
850	900	875	4.7	79.7	668	-4173	-3505	3.2	91.6	-19.7	-236.8	-16.5	-145.2
800	850	825	4.8	84.5	561	-4426	-3864	2.7	94.3	-21.2	-258.0	-18.5	-163.7
750	800	775	4.5	88.9	461	-4656	-4194	2.1	96.3	-20.8	-278.8	-18.8	-182.5
700	750	725	3.9	92.9	365	-4886	-4521	1.4	97.8	-19.1	-297.9	-17.7	-200.2
650	700	675	2.8	95.7	280	-5088	-4807	0.8	98.5	-14.2	-312.2	-13.5	-213.6
600	650	625	0.5	96.2	236	-5187	-4951	0.1	98.7	-2.7	-314.8	-2.5	-216.2

Vestari Skaftárketill

Elevation (m a.s.l.)			ΔS (km^2)	∑ΔS (km^2)	b_w (mm)	b_s (mm)	b_n (mm)	ΔB_w ($10^6 m^3$)	$\sum\Delta B_w$ ($10^6 m^3$)	ΔB_s ($10^6 m^3$)	$\sum\Delta B_s$ ($10^6 m^3$)	ΔB_n ($10^6 m^3$)	$\sum B_n$ ($10^6 m^3$)
1900	1950	1925	0.5	0.5	1899	258	2158	1.0	1.0	0.1	0.1	1.1	1.1
1850	1900	1875	0.7	1.2	1899	227	2127	1.2	2.3	0.1	0.3	1.4	2.5
1800	1850	1825	0.8	2.0	1899	208	2108	1.5	3.7	0.2	0.4	1.6	4.2
1750	1800	1775	2.5	4.4	1887	144	2031	4.7	8.4	0.4	0.8	5.0	9.2
1700	1750	1725	5.4	9.9	1772	20	1793	9.6	18.0	0.1	0.9	9.7	18.9
1650	1700	1675	6.5	16.3	1705	-116	1588	11.0	29.0	-0.8	0.2	10.3	29.2
1600	1650	1625	7.3	23.6	1711	-221	1489	12.4	41.5	-1.6	-1.4	10.8	40.0
1550	1600	1575	5.0	28.6	1688	-289	1399	8.4	49.9	-1.4	-2.9	7.0	47.0
1500	1550	1525	2.7	31.2	1685	-317	1367	4.5	54.4	-0.8	-3.7	3.6	50.7

Eystri Skaftárketill

Elevation (m a.s.l.)			ΔS (km^2)	∑ΔS (km^2)	b_w (mm)	b_s (mm)	b_n (mm)	ΔB_w ($10^6 m^3$)	$\sum\Delta B_w$ ($10^6 m^3$)	ΔB_s ($10^6 m^3$)	$\sum\Delta B_s$ ($10^6 m^3$)	ΔB_n ($10^6 m^3$)	$\sum B_n$ ($10^6 m^3$)
1750	1800	1775	1.1	1.1	1899	109	2009	2.1	2.1	0.1	0.1	2.2	2.2
1700	1750	1725	10.0	11.1	1818	-59	1759	18.2	20.3	-0.6	-0.5	17.6	19.8
1650	1700	1675	15.5	26.6	1837	-247	1589	28.5	48.7	-3.8	-4.3	24.6	44.4
1600	1650	1625	9.2	35.8	1821	-306	1515	16.8	65.5	-2.8	-7.1	14.0	58.4
1550	1600	1575	4.2	39.9	1799	-327	1472	7.5	73.0	-1.4	-8.5	6.1	64.5

Gjálp

Elevation (m a.s.l.)			ΔS (km^2)	∑ΔS (km^2)	b_w (mm)	b_s (mm)	b_n (mm)	ΔB_w ($10^6 m^3$)	$\sum\Delta B_w$ ($10^6 m^3$)	ΔB_s ($10^6 m^3$)	$\sum\Delta B_s$ ($10^6 m^3$)	ΔB_n ($10^6 m^3$)	$\sum B_n$ ($10^6 m^3$)
1900	1950	1925	0.4	0.4	1899	251	2151	0.7	0.7	0.1	0.1	0.8	0.8
1850	1900	1875	0.8	1.1	1899	206	2106	1.4	2.1	0.2	0.2	1.6	2.3
1800	1850	1825	1.2	2.3	1899	177	2077	2.3	4.4	0.2	0.5	2.5	4.8
1750	1800	1775	5.5	7.8	1899	105	2005	10.5	14.9	0.6	1.0	11.1	15.9
1700	1750	1725	23.7	31.5	1899	-125	1774	45.1	59.9	-3.0	-1.9	42.1	58.0
1650	1700	1675	7.8	39.4	1899	-263	1636	14.9	74.8	-2.1	-4.0	12.8	70.8

Grímsvötn

Elevation (m a.s.l.)			ΔS (km^2)	∑ΔS (km^2)	b_w (mm)	b_s (mm)	b_n (mm)	ΔB_w ($10^6 m^3$)	$\sum\Delta B_w$ ($10^6 m^3$)	ΔB_s ($10^6 m^3$)	$\sum\Delta B_s$ ($10^6 m^3$)	ΔB_n ($10^6 m^3$)	$\sum B_n$ ($10^6 m^3$)
1700	1750	1725	1.3	1.3	1900	-281	1618	2.6	2.6	-0.4	-0.4	2.2	2.2
1650	1700	1675	40.7	42.1	1947	-401	1546	79.3	81.9	-16.3	-16.7	63.0	65.2
1600	1650	1625	30.7	72.8	1935	-628	1307	59.4	141.3	-19.3	-36.0	40.1	105.3
1550	1600	1575	19.6	92.4	1920	-805	1115	37.7	178.9	-15.8	-51.8	21.9	127.2
1500	1550	1525	16.3	108.7	1903	-1176	726	31.0	210.0	-19.2	-71.0	11.8	139.0
1450	1500	1475	9.5	118.2	1840	-1662	177	17.5	227.4	-15.8	-86.7	1.7	140.7
1400	1450	1425	13.7	131.9	1850	-2050	-200	25.4	252.8	-28.1	-114.9	-2.7	137.9
1350	1400	1375	1.2	133.1	1818	-2059	-241	2.3	255.1	-2.6	-117.4	-0.3	137.6

Appendix C: Coordinates of the velocity measurement stakes in 2024.

Position of the velocity measurement stakes determined by GPS sub-metre differential (I), fast static (FS) and kinematic (K). (Accuracy of horizontal position 0.5 – 1.0 m, and vertical accuracy 1-2 m for DGPS, about 1cm for fast static, and 3 cm for kinematic).
The station Hofn in Höfn í Hornafirði is used as a stationary reference for all measurements, ÍSN93 datum, h_l is elevation above ellipsoid, dL antenna height, N estimated difference between ellipsoid and sea-level, H elevation in metres above sea level (H= h_l+N+dL). X and Y are ÍSN93 Lambert conformal conic projected coordinates. M is a quality marker.

Site	time	Date	Calender Day #	Year	Latitude	Longitude	h_l (m a. e.)	dL (m)	N (m)	H (m a. s. l.)	X	Y	M
B07-23	11.72	4	5	124	2023	64	25.79652	16	17.48091	1425.86	0.00	-67.05	1358.81	630454.15	439244.78	K
B07-24	16.856	25	9	269	2024	64	25.79490	16	17.48586	1424.18	-2.15	-67.05	1354.98	630450.30	439241.60	K
B07-24	13.926	21	11	326	2024	64	25.79450	16	17.48241	1424.10	-2.10	-67.05	1354.95	630453.10	439240.99	K
B09-24	15.421	2	5	123	2024	64	44.48405	16	6.18781	786.85	0.00	-66.68	720.17	637922.46	474331.61	K
B10-24	14.651	2	5	123	2024	64	43.68419	16	6.70273	818.93	0.00	-66.71	752.22	637582.03	472828.32	K
B11-24	18.871	1	5	122	2024	64	40.93900	16	10.48002	1008.78	0.00	-66.81	941.97	634813.11	467597.34	K
B12-24	17.885	1	5	122	2024	64	38.26292	16	14.15062	1144.05	0.00	-66.90	1077.15	632113.23	462500.89	K
B12-24	16.665	23	11	328	2024	64	38.27489	16	14.14049	1140.73	0.00	-66.90	1073.83	632120.32	462523.46	K
B13-24	17.897	2	5	123	2024	64	34.65838	16	19.56103	1286.24	0.00	-67.01	1219.23	628089.19	455624.28	K
B13-24	14.758	21	11	326	2024	64	34.66970	16	19.54725	1283.46	0.00	-67.01	1216.45	628099.29	455645.75	K
B13ror15	11.3	10	6	162	2024	64	34.66375	16	19.56016	1285.52	0.00	-67.01	1218.51	628089.46	455634.27	K
B13ror15	14.611	21	11	326	2024	64	34.67479	16	19.54760	1285.73	0.00	-67.01	1218.72	628098.61	455655.19	K
B14-24	15.161	1	5	122	2024	64	31.64983	16	24.77075	1391.92	0.00	-67.11	1324.82	624160.98	449866.02	K
B14-24	16.372	21	11	326	2024	64	31.65792	16	24.75669	1388.92	0.00	-67.11	1321.81	624171.60	449881.49	K
B15-24	14.334	1	5	122	2024	64	28.51275	16	30.03235	1472.92	0.00	-67.21	1405.71	620185.09	443872.57	K
B15-24	14.754	21	11	326	2024	64	28.51800	16	30.01885	1471.87	-1.84	-67.21	1402.82	620195.51	443882.74	K
B16-24	12.993	1	5	122	2024	64	24.12385	16	40.91390	1596.25	0.00	-67.33	1528.92	611767.56	435391.19	K
B16-24	15.699	21	11	326	2024	64	24.12424	16	40.91212	1595.91	-1.70	-67.33	1526.87	611768.95	435391.97	K
B17-24	16.261	1	5	122	2024	64	36.73258	16	28.79586	1283.68	0.00	-67.12	1216.56	620566.84	459172.19	K
B17-24	15.789	21	11	326	2024	64	36.74379	16	28.78844	1279.65	0.00	-67.12	1212.53	620571.93	459193.24	K
B18-24	18.625	1	5	122	2024	64	31.58165	16	0.11955	1383.15	0.00	-66.92	1316.22	643870.62	450610.43	K
B18-24	13.282	21	11	326	2024	64	31.58882	16	0.12351	1379.28	0.00	-66.92	1312.36	643866.82	450623.60	K
B19-24	11.796	1	5	122	2024	64	28.00978	15	55.98620	1505.53	0.00	-66.89	1438.64	647495.79	444140.30	K
B19-24	12.659	21	11	326	2024	64	28.01009	15	55.98630	1502.00	0.00	-66.89	1435.11	647495.69	444140.88	K
Bb0-24	10.401	1	5	122	2024	64	22.70650	16	5.05749	1583.38	0.00	-66.85	1515.51	640684.32	433953.23	K
Bb0-24	11.575	21	11	326	2024	64	22.70632	16	5.05832	1579.97	0.00	-66.85	1513.12	640683.67	433952.86	K
Barc-24	15.627	9	6	161	2024	64	38.42065	17	26.76110	1974.48	0.00	-67.87	1906.61	574281.75	460818.20	K
Barc-24	11.462	27	9	271	2024	64	38.42037	17	26.75646	1973.85	-1.25	-67.87	1904.73	574285.46	460817.77	K
BARS-24	19.631	10	5	131	2024	64	33.96845	17	24.94570	1831.66	-1.15	-67.84	1762.66	575935.03	452584.53	K
BB01-24	13.15	10	5	131	2024	64	37.82246	17	23.14747	1922.82	-1.15	-67.85	1853.82	577188.43	459779.27	K
BB01-24	9.762	27	9	271	2024	64	37.82112	17	23.13418	1921.55	-1.50	-67.85	1852.21	577199.08	459777.05	K
BB02-24	11.683	10	5	131	2024	64	38.42285	17	26.76238	1975.35	-1.15	-67.87	1906.33	574280.63	460822.26	K
BB02-24	18.831	26	9	270	2024	64	38.42255	17	26.75643	1974.66	-1.40	-67.87	1905.39	574285.39	460821.83	K
BB05-24	15.642	10	5	131	2024	64	36.58709	17	30.79372	1981.33	-1.15	-67.87	1912.31	571149.76	457335.13	K
BB05-24	14.235	27	9	271	2024	64	36.58519	17	30.79528	1979.96	-1.30	-67.87	1910.79	571148.60	457331.56	K
BB07-24	19.912	9	5	130	2024	64	36.56393	17	25.04691	1951.21	-1.15	-67.86	1882.21	575733.49	457403.38	K
BB07-24	16.218	26	9	270	2024	64	36.56332	17	25.04123	1950.37	-1.10	-67.86	1881.42	575738.04	457402.36	K
BB08-24	12.457	10	5	131	2024	64	39.00630	17	23.29569	1940.50	-1.15	-67.84	1871.50	577014.26	461975.11	K
BB08-24	10.737	27	9	271	2024	64	39.00682	17	23.28887	1939.37	-1.60	-67.84	1869.93	577019.66	461976.22	K
BB09-24	17.146	10	5	131	2024	64	39.66720	17	28.02056	1983.77	-1.15	-67.87	1914.75	573222.41	463109.11	K
BB09-24	11.758	27	9	271	2024	64	39.66697	17	28.01804	1982.85	-1.40	-67.87	1913.58	573224.42	463108.72	K
BB10-24	16.421	10	5	131	2024	64	38.63950	17	32.51580	2029.03	-1.15	-67.87	1960.01	569688.55	461115.50	K
BB10-24	13.179	27	9	271	2024	64	38.63911	17	32.51501	2028.09	-1.70	-67.87	1958.52	569689.19	461114.78	K
BB11-24	11.166	10	5	131	2024	64	37.49393	17	27.96813	1982.18	-1.15	-67.87	1913.16	573362.10	459073.38	K
BB11-24	17.64	26	9	270	2024	64	37.49361	17	27.96396	1981.47	-1.40	-67.87	1912.20	573365.43	459072.86	K
BB12-24	20.751	10	5	131	2024	64	36.48235	17	16.52334	1698.50	-1.15	-67.74	1629.61	582534.30	457429.68	K
BB12-24	14.63	26	9	270	2024	64	36.48282	17	16.51204	1695.74	-0.35	-67.74	1627.65	582543.29	457430.80	K

BB13-24	21.72	10	5	131	2024	64	39.57969	17	16.97270	1620.64	-1.15	-67.71	1551.78	582019.68	463172.66	K
BB13-24	12.453	26	9	270	2024	64	39.58301	17	16.96094	1617.45	-0.30	-67.71	1549.44	582028.87	463179.08	K
BB14-24	22.625	10	5	131	2024	64	41.74082	17	21.22675	1627.88	-1.15	-67.76	1558.97	578529.28	467096.58	K
BB14-24	11.391	26	9	270	2024	64	41.74331	17	21.21862	1624.67	-0.25	-67.76	1556.66	578535.62	467101.38	K
Bor-24	13.362	9	6	161	2024	64	24.93529	17	20.15227	1475.72	0.00	-67.70	1408.02	580205.20	435905.13	K
Bor-24	16.859	23	11	328	2024	64	24.93166	17	20.15528	1492.15	-1.80	-67.70	1422.65	580202.96	435898.34	K
Br1-23	16.216	12	6	164	2024	64	5.96323	16	19.82099	126.98	-1.95	-65.90	59.13	630132.63	402347.09	K
Br1-24	16.269	12	6	164	2024	64	5.95725	16	19.82470	126.58	-1.95	-65.90	58.73	630130.08	402335.86	K
Br1n-24	14.581	28	9	272	2024	64	6.31510	16	20.10596	183.14	-0.20	-65.95	117.00	629873.70	402990.52	K
Br2-23	13.82	12	6	164	2024	64	6.35333	16	22.52293	208.21	-1.95	-66.03	140.23	627908.71	402979.36	K
Br2-24	14.75	12	6	164	2024	64	6.35384	16	22.52342	207.38	-1.03	-66.03	140.32	627908.27	402980.29	K
Br2-24	14.959	28	9	272	2024	64	6.35332	16	22.52402	200.51	-0.20	-66.03	134.28	627907.82	402979.31	K
Br3-23	12.111	12	6	164	2024	64	8.40616	16	23.96131	410.93	-1.95	-66.26	342.72	626584.20	406742.11	K
Br3-24	12.159	12	6	164	2024	64	8.40686	16	23.96260	411.08	-1.95	-66.26	342.87	626583.09	406743.36	K
Br7-24	19.314	1	5	122	2024	64	22.14129	16	16.93093	1310.12	0.00	-67.01	1243.11	631187.23	432478.58	K
Br7-24	12.101	21	11	326	2024	64	22.10726	16	16.92040	1307.69	-2.00	-67.01	1238.68	631198.42	432415.78	K
Bru-24	17.322	1	5	122	2024	64	39.75607	15	56.53328	956.12	0.00	-66.78	889.34	646002.39	465918.10	K
Bru-24	15.311	23	11	328	2024	64	39.76875	15	56.52821	952.88	0.00	-66.78	886.09	646005.29	465941.83	K
Bud-24	17.846	1	5	122	2024	64	35.99204	15	59.88686	1204.24	0.00	-66.88	1137.36	643667.61	458804.51	K
Bud-24	13.887	21	11	326	2024	64	36.00788	15	59.88352	1200.22	0.00	-66.88	1133.34	643668.88	458834.05	K
D01-23	13	3	5	124	2024	64	47.86880	16	49.97568	900.14	0.00	-67.05	833.09	602976.52	479225.05	K
D01-24	13.177	3	5	124	2024	64	47.86803	16	49.97378	900.72	0.00	-67.05	833.67	602978.08	479223.67	K
D05-24	12.186	3	5	124	2024	64	42.22978	16	54.68273	1274.01	0.00	-67.35	1206.66	599596.12	468627.96	K
D05-24	14.064	23	11	328	2024	64	42.24995	16	54.65293	1272.60	-1.40	-67.35	1203.85	599618.56	468666.18	K
D07-24	11.108	3	5	124	2024	64	38.29462	16	59.25557	1445.86	0.00	-67.50	1378.36	596195.81	461202.26	K
D07-24	12.829	23	11	328	2024	64	38.31895	16	59.23063	1443.90	-1.60	-67.50	1374.80	596214.23	461248.07	K
D08-24	10.425	3	5	124	2024	64	34.68584	17	1.52077	1556.37	0.00	-67.56	1488.81	594601.15	454443.50	K
D08-24	12.179	23	11	328	2024	64	34.69727	17	1.51699	1555.64	-1.80	-67.56	1486.28	594603.50	454464.83	K
D12-24	21.55	23	11	328	2024	64	28.97199	17	0.18388	1717.73	-1.13	-67.55	1649.05	596003.55	443866.04	K
E01-24	16.575	1	5	122	2024	64	40.66327	15	34.83165	814.48	0.00	-66.72	747.77	663165.41	468485.92	K
E02-24	16.029	1	5	122	2024	64	39.11108	15	36.00208	1015.27	0.00	-66.79	948.48	662390.53	465555.92	K
E02-24	13.53	23	11	328	2024	64	39.13490	15	35.99671	1011.36	0.00	-66.79	944.58	662392.43	465600.34	K
E03-24	13.991	1	5	122	2024	64	36.66427	15	36.92615	1252.01	0.00	-66.85	1185.16	661898.92	460976.78	K
E03-24	13.127	23	11	328	2024	64	36.67112	15	36.93034	1246.69	0.00	-66.85	1179.84	661894.90	460989.32	K
E04-24	13.429	1	5	122	2024	64	34.95301	15	37.14648	1353.49	0.00	-66.83	1286.66	661893.40	457792.42	K
E04-24	12.272	23	11	328	2024	64	34.95402	15	37.14575	1349.44	0.00	-66.83	1282.61	661893.87	457794.32	K
E07-24	14.725	1	5	122	2024	64	38.41275	15	24.69953	1134.54	0.00	-66.62	1067.93	671452.01	464757.80	K
E08-24	15.261	1	5	122	2024	64	39.72195	15	23.84883	1012.11	0.00	-66.55	945.56	671990.19	467224.88	K
Fl01-24	11.186	1	5	122	2024	64	26.15781	15	55.62463	1412.82	0.00	-66.82	1345.99	647952.58	440717.48	K
Fl01-24	12.259	21	11	326	2024	64	26.14973	15	55.60586	1408.31	0.00	-66.82	1341.49	647968.36	440703.22	K
G02-24	12.544	3	5	124	2024	64	26.84949	17	17.71085	1635.25	0.00	-67.73	1567.53	582069.96	439512.68	K
G02-24	19.355	22	11	327	2024	64	26.84429	17	17.71470	1632.71	0.00	-67.73	1564.98	582067.14	439502.95	K
G03-24	11.722	3	5	124	2024	64	28.44321	17	16.33172	1728.67	0.00	-67.74	1660.94	583095.29	442502.75	K
G03-24	19.03	22	11	327	2024	64	28.44088	17	16.33252	1726.48	0.00	-67.74	1658.74	583094.77	442498.40	K
G04-24	10.901	3	5	124	2024	64	30.02181	17	15.03839	1758.40	0.00	-67.73	1690.67	584050.54	445463.17	K
G04-24	17.844	27	9	271	2024	64	30.02206	17	15.03789	1757.62	-1.00	-67.73	1688.89	584050.94	445463.65	K
Go1-24	11.947	4	5	125	2024	64	33.97403	17	24.92539	1829.16	0.00	-67.84	1761.32	575951.00	452595.29	K
Go1-24	9.567	26	9	270	2024	64	33.97275	17	24.92451	1827.94	-0.40	-67.84	1759.70	575951.76	452592.93	K
GvVi-24	16.829	11	6	163	2024	64	24.39652	17	20.42740	1446.05	0.00	-67.68	1378.36	580010.53	434898.64	K
Haab-24	21.857	4	5	125	2024	64	20.96610	17	24.11026	1797.09	0.00	-67.54	1729.56	577212.96	428450.69	K
Haab-24	18.017	22	11	327	2024	64	20.96654	17	24.10883	1795.86	-0.43	-67.54	1727.89	577214.10	428451.54	K
Hof01-24	12.771	1	5	122	2024	64	32.34335	15	35.85454	1207.25	0.00	-66.67	1140.57	663184.31	453006.02	K
Hof01-24	12.75	23	11	328	2024	64	32.33510	15	35.85387	1203.26	0.00	-66.67	1136.59	663185.68	452990.75	K
K01-24	19.119	4	5	125	2024	64	35.16968	17	51.85664	1104.07	0.00	-67.58	1036.49	554399.65	454353.54	K
K01-24	17.179	22	11	327	2024	64	35.17103	17	51.86375	1099.66	0.00	-67.58	1032.08	554393.92	454355.96	K
K02-24	18.733	4	5	125	2024	64	34.81674	17	49.70803	1231.85	0.00	-67.61	1164.24	556126.86	453729.20	K
K02-24	16.901	22	11	327	2024	64	34.81965	17	49.72358	1228.47	0.00	-67.61	1160.86	556114.35	453734.39	K
K03-24	17.894	4	5	125	2024	64	34.23933	17	46.42930	1356.88	0.00	-67.67	1289.21	558765.36	452706.23	K
K03-24	15.805	22	11	327	2024	64	34.24218	17	46.44956	1354.60	0.00	-67.67	1286.93	558749.07	452711.20	K
K04-24	16.976	4	5	125	2024	64	33.20699	17	42.36377	1547.61	0.00	-67.73	1479.88	562051.56	450853.27	K
K04-24	16.357	22	11	327	2024	64	33.21133	17	42.39233	1544.49	0.00	-67.73	1476.76	562028.57	450860.86	K
K05-24	15.282	4	5	125	2024	64	33.44493	17	35.45251	1745.73	0.00	-67.82	1677.91	567564.72	451413.35	K
K05-24	15.196	26	9	270	2024	64	33.44270	17	35.46428	1744.64	-0.45	-67.82	1676.37	567555.41	451408.99	K
K06-24	13.854	4	5	125	2024	64	38.35738	17	31.31036	2014.13	0.00	-67.88	1946.26	570660.87	460613.75	K
K06-24	15.956	27	9	271	2024	64	38.35698	17	31.30812	2014.61	-1.67	-67.88	1945.06	570662.66	460613.06	K
K07-24	21.055	4	5	125	2024	64	29.11159	17	42.01737	1598.19	0.00	-67.68	1530.51	562484.81	443251.33	K
K07-24	15.093	22	11	327	2024	64	29.11180	17	42.01960	1596.15	0.00	-67.68	1528.47	562483.02	443251.67	K

Kverk-24	13.204	12	6	164	2024	64	38.66399	16	40.51911	1891.95	0.00	-67.38	1824.57	611091.44	462400.10	K
S01-24	20.403	4	5	125	2024	64	7.01727	17	49.97243	760.11	0.00	-66.84	693.28	556869.32	402082.38	K
S02-24	19.496	4	5	125	2024	64	12.16594	17	48.99572	1064.44	0.00	-67.05	997.40	557483.34	411661.87	K
S02-24	13.14	22	11	327	2024	64	12.15008	17	49.00411	1060.04	0.00	-67.04	992.99	557477.10	411632.27	K
S04-24	12.75	4	5	124	2024	64	16.17608	17	48.19933	1221.12	0.00	-67.21	1153.91	557986.97	419123.59	K
S04-24	12.75	22	11	327	2024	64	16.15596	17	48.22035	1216.87	0.00	-67.21	1149.66	557970.70	419085.89	K
S045-auk	12.568	22	11	327	2024	64	16.44727	17	46.50468	1245.45	0.00	-67.23	1178.22	559345.65	419653.59	K
S05-24	17.693	3	5	124	2024	64	20.51715	17	33.99216	1517.93	0.00	-67.51	1450.41	569276.14	427425.96	K
S05-24	11.887	22	11	327	2024	64	20.51440	17	34.01438	1514.65	0.00	-67.51	1447.14	569258.37	427420.45	K
Ske02-24	14.666	2	5	123	2024	64	16.35713	16	59.29677	1263.97	0.00	-67.09	1196.88	597459.85	420461.97	K
Ske03-24	13.919	2	5	123	2024	64	18.05421	16	56.16782	1363.84	0.00	-67.20	1296.64	599882.46	423694.93	K
Ske03-24	18.157	21	11	326	2024	64	18.02240	16	56.24667	1357.65	0.00	-67.20	1290.45	599820.82	423633.78	K
Ske04-24	12.105	2	5	123	2024	64	20.14421	16	51.80334	1464.99	0.00	-67.30	1397.70	603270.29	427692.90	K
Ske04-24	17.759	21	11	326	2024	64	20.13141	16	51.83679	1461.13	0.00	-67.30	1393.83	603244.16	427668.21	K
Ske05-24	11.459	2	5	123	2024	64	22.23379	16	47.22575	1539.90	0.00	-67.35	1472.55	606820.47	431699.83	K
Ske05-24	17.309	21	11	326	2024	64	22.22828	16	47.23753	1536.76	0.00	-67.35	1469.42	606811.35	431689.26	K
Skf00-24	15.862	25	9	269	2024	64	15.46669	15	54.05167	1004.44	-0.20	-66.03	938.21	650187.22	420938.79	K
Skf01-24	16.342	25	9	269	2024	64	18.01655	16	5.00634	1345.98	-2.15	-66.64	1277.19	641127.31	425250.43	K
Skf01-24	11.032	21	11	326	2024	64	18.01510	16	5.00011	1343.27	0.00	-66.64	1276.64	641132.45	425247.98	K
T01-24	11.832	5	5	126	2024	64	19.15510	18	6.52581	820.32	0.00	-67.25	753.07	543109.43	424413.69	K
T02-24	15.914	4	5	125	2024	64	19.47747	18	4.55689	943.41	0.00	-67.27	876.14	544687.86	425035.36	K
T02-24	15.857	22	11	327	2024	64	19.47772	18	4.56198	939.84	-1.25	-67.27	871.33	544683.75	425035.77	K
T03-24	13.751	4	5	125	2024	64	20.19863	17	58.61349	1126.17	0.00	-67.30	1058.87	549456.23	426448.89	K
T03-24	15.034	22	11	327	2024	64	20.19630	17	58.62903	1124.07	-1.35	-67.30	1055.42	549443.78	426444.36	K
T04-24	16.657	3	5	124	2024	64	21.32992	17	51.51609	1285.15	0.00	-67.36	1217.79	555135.73	428648.38	K
T04-24	14.291	22	11	327	2024	64	21.32518	17	51.53348	1283.49	-1.45	-67.36	1214.67	555121.89	428639.34	K
T05-24	15.751	3	5	124	2024	64	22.26272	17	42.99740	1411.35	0.00	-67.47	1343.88	561957.97	430512.70	K
T05-24	12.953	22	11	327	2024	64	22.25821	17	43.01495	1409.90	-1.78	-67.47	1340.65	561944.03	430504.03	K
T05rorh	13.083	22	11	327	2024	64	22.21754	17	43.27393	1405.11	-2.10	-67.46	1335.55	561737.20	430424.28	K
T06-24	11.387	4	5	125	2024	64	24.26551	17	36.51589	1534.48	0.00	-67.61	1466.87	567090.43	434343.32	K
T06-24	11.599	22	11	327	2024	64	24.26071	17	36.53036	1534.22	-2.17	-67.61	1464.44	567079.00	434334.15	K
T07-24	14.397	3	5	124	2024	64	25.29527	17	31.21182	1630.47	0.00	-67.70	1562.77	571307.41	436352.89	K
T07-24	11.023	22	11	327	2024	64	25.29292	17	31.22112	1630.09	-1.98	-67.70	1560.41	571300.05	436348.35	K
T08-24	13.643	3	5	124	2024	64	26.30065	17	27.74827	1703.66	0.00	-67.75	1635.91	574043.09	438286.72	K
T08-24	10.633	22	11	327	2024	64	26.30050	17	27.74920	1703.92	-2.20	-67.75	1633.97	574042.35	438286.43	K

Appendix D: Measured surface velocity at marked sites on Vatnajökull in 2024.

Site	Calendar day date	#	Calendar day date	#	# of days	translation (m)	(°)	velocity (cm/day)	(m/annum)
B07-24	240925	269	241121	326	57	2.87	105	5.03	18.35
B12-24	240501	122	241123	328	206	23.59	20	11.45	41.80
B13-24	240502	123	241121	326	203	23.68	28	11.66	42.57
B13ror15	231026	299	240610	162	228	5.97	41	2.62	9.57
B13ror15	240610	162	241121	326	164	22.77	26	13.89	50.68
B14-24	240501	122	241121	326	204	18.73	37	9.18	33.52
B15-24	240501	122	241121	326	204	14.54	48	7.13	26.02
B16-24	240501	122	241121	326	204	1.60	63	0.79	2.87
B17-24	240501	122	241121	326	204	21.59	16	10.58	38.62
B18-24	240501	122	241121	326	204	13.65	347	6.69	24.43
B19-24	240501	122	241121	326	204	0.58	352	0.28	1.04
Bb0-24	240501	122	241121	326	204	0.75	243	0.37	1.33
Barc-24	240609	161	240927	271	110	3.73	98	3.39	12.38
BB01-24	240510	131	240927	271	140	10.88	103	7.77	28.35
BB02-24	240510	131	240926	270	139	4.77	97	3.43	12.53
BB05-24	240510	131	240927	271	140	3.73	199	2.67	9.73
BB07-24	240509	130	240926	270	140	4.67	104	3.33	12.17
BB08-24	240510	131	240927	271	140	5.51	80	3.94	14.38
BB09-24	240510	131	240927	271	140	2.05	102	1.46	5.34
BB10-24	240510	131	240927	271	140	0.96	139	0.68	2.50
BB11-24	240510	131	240926	270	139	3.38	100	2.43	8.86
BB12-24	240510	131	240926	270	139	9.05	84	6.51	23.77
BB13-24	240510	131	240926	270	139	11.20	57	8.06	29.40
BB14-24	240510	131	240926	270	139	7.94	54	5.71	20.85
Bor-24	240609	161	241123	328	167	7.14	200	4.28	15.61
Br1-23	231022	295	240612	164	234	0.08	198	0.03	0.12
Br2-23	231022	295	240612	164	234	0.46	178	0.20	0.72
Br2-24	240612	164	240928	272	108	1.08	207	1.00	3.65
Br3-23	231022	295	240612	164	234	8.45	151	3.61	13.18
Br7-24	240501	122	241121	326	204	63.59	172	31.17	113.78
Bru-24	240501	122	241123	328	206	23.83	10	11.57	42.22
Bud-24	240501	122	241121	326	204	29.46	5	14.44	52.70
D01-23	230505	125	240503	124	364	1.68	339	0.46	1.69
D05-24	240503	124	241123	328	204	44.23	32	21.68	79.13
D07-24	240503	124	241123	328	204	49.24	24	24.14	88.11
D08-24	240503	124	241123	328	204	21.38	8	10.48	38.26
E02-24	240501	122	241123	328	206	44.32	6	21.52	78.53
E03-24	240501	122	241123	328	206	13.12	345	6.37	23.24
E04-24	240501	122	241123	328	206	1.96	17	0.95	3.47
Fl01-24	240501	122	241121	326	204	21.23	135	10.41	37.99
G02-24	240503	124	241122	327	203	10.11	198	4.98	18.18
G03-24	240503	124	241122	327	203	4.36	188	2.15	7.84
G04-24	240503	124	240927	271	147	0.61	41	0.42	1.52
Go1-24	240504	125	240926	270	145	2.47	163	1.71	6.22
Haab-24	240504	125	241122	327	202	1.41	55	0.70	2.55
Hof01-24	240501	122	241123	328	206	15.29	178	7.42	27.09

K01-24	240504	125	241122	327	202	6.20	294	3.07	11.20
K02-24	240504	125	241122	327	202	13.53	293	6.70	24.45
K03-24	240504	125	241122	327	202	17.02	288	8.42	30.75
K04-24	240504	125	241122	327	202	24.19	289	11.98	43.71
K05-24	240504	125	240926	270	145	10.27	246	7.08	25.85
K06-24	240504	125	240927	271	146	1.93	113	1.32	4.83
K07-24	240504	125	241122	327	202	1.83	282	0.90	3.30
S01-24	240504	125	250129	0	240	0.15	12	0.06	0.23
S02-24	240504	125	241122	327	202	30.15	193	14.92	54.47
S04-24	240504	124	241122	327	203	40.94	204	20.17	73.62
S05-24	240503	124	241122	327	203	18.60	254	9.16	33.45
Ske03-24	240502	123	241121	326	203	86.68	227	42.70	155.86
Ske04-24	240502	123	241121	326	203	35.88	229	17.68	64.52
Ske05-24	240502	123	241121	326	203	13.93	223	6.86	25.04
Skf01-24	240925	269	241121	326	57	5.70	118	9.99	36.48
T02-24	240504	125	241122	327	202	4.13	276	2.04	7.46
T03-24	240504	125	241122	327	202	13.24	251	6.55	23.92
T04-24	240503	124	241122	327	203	16.52	238	8.14	29.70
T05-24	240503	124	241122	327	203	16.40	239	8.08	29.49
T05rorh	221018	291	241122	327	766	53.52	239	6.99	25.50
T06-24	240504	125	241122	327	202	14.63	233	7.24	26.44
T07-24	240503	124	241122	327	203	8.64	240	4.26	15.54
T08-24	240503	124	241122	327	203	0.80	250	0.39	1.43

Appendix E: Melt water runoff to selected rivers in summer 2024, derived from summer surface balance.

ΔS: area in each elevation range where summer balance is negative, **∑ΔS**: cumulative area above a given elevation, **ΔQ_s**: melt water runoff from a given elevation range, **$\sum \Delta Q_s$**: cumulative melt water runoff from an area above given elevation.

Tungnaá water drainage basin

Elevation (m a. s. l.)		ΔS km^2	∑ΔS km^2	ΔQ_s ($10^6 m^3$)	$\sum \Delta Q_s$ ($10^6 m^3$)
1350	1400	0.3	0.3	0.4	0.4
1300	1350	6.0	6.3	9.0	9.4
1250	1300	9.8	16.1	20.2	29.6
1200	1250	10.7	26.8	27.3	56.9
1150	1200	9.5	36.4	27.6	84.5
1100	1150	11.0	47.4	34.4	118.9
1050	1100	10.3	57.7	35.3	154.2
1000	1050	9.5	67.2	36.5	190.7
950	1000	8.8	76.1	37.3	228.0
900	950	8.5	84.6	39.8	267.8
850	900	6.3	90.9	32.6	300.3
800	850	6.3	97.1	34.7	335.0
750	800	4.6	101.8	27.2	362.3
700	750	2.5	104.2	15.3	377.6
650	700	0.1	104.4	0.9	378.5

Sylgja water drainage basin

Elevation (m a. s. l.)		ΔS km^2	∑ΔS km^2	ΔQ_s ($10^6 m^3$)	$\sum \Delta Q_s$ ($10^6 m^3$)
1300	1350	1.1	1.1	1.8	1.8
1250	1300	3.4	4.5	6.9	8.7
1200	1250	5.3	9.7	13.7	22.4
1150	1200	8.0	17.8	23.2	45.6
1100	1150	5.8	23.5	18.2	63.8
1050	1100	6.0	29.5	20.3	84.1
1000	1050	5.7	35.3	21.1	105.3
950	1000	1.8	37.1	7.1	112.3
900	950	0.7	37.8	2.7	115.0

Western Skaftá cauldron water drainage basin

Elevation (m a. s. l.)		ΔS km^2	∑ΔS km^2	ΔQ_s ($10^6 m^3$)	$\sum \Delta Q_s$ ($10^6 m^3$)
1700	1750	2.2	2.2	0.1	0.1
1650	1700	7.1	9.3	0.8	0.9
1600	1650	7.9	17.3	1.9	2.8
1550	1600	5.0	22.3	1.4	4.2
1500	1550	2.6	24.9	0.8	5.1

Eastern Skaftár cauldron water drainage basin

Elevation (m a. s. l.)		ΔS km²	∑ΔS km²	ΔQs ($10^6 m^3$)	∑ΔQs ($10^6 m^3$)
1700	1750	6.9	6.9	0.6	0.6
1650	1700	13.7	20.6	3.6	4.1
1600	1650	9.4	30.0	2.8	7.0
1550	1600	4.0	34.0	1.3	8.3

Grímsvötn water drainage basin

Elevation (m a. s. l.)		ΔS km²	∑ΔS km²	ΔQs ($10^6 m^3$)	∑ΔQs ($10^6 m^3$)
1700	1750	21.8	21.8	3.3	3.3
1650	1700	48.0	69.8	18.2	21.5
1600	1650	30.7	100.5	19.3	40.8
1550	1600	19.6	120.1	15.8	56.5
1500	1550	16.2	136.3	19.1	75.6
1450	1500	9.5	145.8	15.8	91.4
1400	1450	13.7	159.5	28.1	119.5
1350	1400	1.2	160.7	2.6	122.1

Kaldakvísl water drainage basin

Elevation (m a. s. l.)		ΔS km²	∑ΔS km²	ΔQs ($10^6 m^3$)	∑ΔQs ($10^6 m^3$)
1700	1750	3.8	3.8	0.1	0.1
1650	1700	16.7	20.5	1.8	1.9
1600	1650	14.5	35.0	3.8	5.7
1550	1600	18.4	53.4	7.8	13.5
1500	1550	24.1	77.6	13.7	27.2
1450	1500	27.8	105.3	20.7	47.9
1400	1450	22.3	127.7	21.4	69.3
1350	1400	20.5	148.2	25.0	94.3
1300	1350	19.2	167.4	29.8	124.1
1250	1300	20.5	187.9	40.4	164.5
1200	1250	20.0	207.9	48.9	213.4
1150	1200	19.0	226.9	55.0	268.5
1100	1150	17.0	243.9	55.9	324.4
1050	1100	15.7	259.6	58.3	382.7
1000	1050	12.9	272.5	52.9	435.6
950	1000	7.2	279.7	32.8	468.4
900	950	1.2	281.0	5.7	474.1

Jökulsá á Fjöllum water drainage basin

Elevation (m a. s. l.)		ΔS km^2	∑ΔS km^2	ΔQ_s ($10^6 m^3$)	$\sum\Delta Q_s$ ($10^6 m^3$)
1800	1850	0.0	0.0	0.0	0.0
1750	1800	1.9	1.9	0.0	0.0
1700	1750	26.5	28.5	2.4	2.4
1650	1700	79.5	108.0	16.5	18.9
1600	1650	121.1	229.2	31.3	50.2
1550	1600	100.2	329.3	40.3	90.6
1500	1550	92.1	421.5	52.7	143.2
1450	1500	79.3	500.8	58.2	201.5
1400	1450	68.7	569.5	61.2	262.7
1350	1400	54.2	623.7	63.4	326.1
1300	1350	42.7	666.4	66.1	392.2
1250	1300	46.3	712.6	88.7	480.9
1200	1250	49.3	761.9	112.4	593.2
1150	1200	48.7	810.6	133.3	726.5
1100	1150	44.1	854.7	141.1	867.6
1050	1100	31.0	885.6	114.9	982.6
1000	1050	31.1	916.7	131.8	1114.4
950	1000	28.9	945.6	136.8	1251.3
900	950	24.7	970.3	127.0	1378.3
850	900	20.5	990.8	114.1	1492.4
800	850	16.5	1007.3	98.7	1591.1
750	800	8.5	1015.8	53.5	1644.6
700	750	0.3	1016.2	2.2	1646.8

Kreppa and Kverká water drainage basin

Elevation (m a. s. l.)		ΔS km^2	∑ΔS km^2	ΔQ$_s$ (10^{6}m^3)	∑ΔQ$_s$ (10^{6}m^3)
1900	1950	0.0	0.0	0.0	0.0
1750	1800	0.0	0.0	0.0	0.0
1700	1750	1.2	1.2	0.0	0.0
1650	1700	4.5	5.8	0.2	0.2
1600	1650	41.6	47.3	7.2	7.5
1550	1600	20.4	67.7	4.6	12.0
1500	1550	13.4	81.2	4.7	16.7
1450	1500	16.3	97.4	8.5	25.3
1400	1450	20.1	117.5	15.5	40.8
1350	1400	25.9	143.4	26.7	67.5
1300	1350	20.3	163.7	26.3	93.8
1250	1300	15.3	179.0	27.7	121.5
1200	1250	17.7	196.7	41.3	162.8
1150	1200	17.2	213.9	44.5	207.3
1100	1150	16.1	230.0	43.9	251.2
1050	1100	10.4	240.4	29.3	280.5
1000	1050	11.6	252.0	33.7	314.2
950	1000	12.7	264.7	40.8	355.0
900	950	12.8	277.5	45.9	400.9
850	900	11.9	289.4	46.2	447.1
800	850	9.8	299.2	41.5	488.6
750	800	6.7	305.9	31.0	519.6
700	750	3.4	309.3	16.8	536.4
650	700	0.2	309.5	0.8	537.2

Hálslón water drainage basin

Elevation (m a. s. l.)		ΔS km^2	∑ΔS km^2	ΔQ$_s$ (10^{6}m^3)	∑ΔQ$_s$ (10^{6}m^3)
1600	1650	11.2	11.2	2.3	2.3
1550	1600	33.6	44.8	8.1	10.5
1500	1550	65.2	110.0	20.0	30.5
1450	1500	70.0	180.0	36.4	66.9
1400	1450	98.9	278.9	68.3	135.2
1350	1400	132.9	411.8	121.6	256.8
1300	1350	129.1	540.9	141.3	398.0
1250	1300	122.4	663.3	151.8	549.9
1200	1250	97.2	760.5	142.9	692.8
1150	1200	81.9	842.5	150.7	843.5
1100	1150	64.0	906.5	140.0	983.5
1050	1100	54.6	961.0	136.9	1120.4
1000	1050	45.8	1006.9	129.3	1249.7
950	1000	39.1	1046.0	123.9	1373.6
900	950	31.9	1077.9	112.4	1486.1
850	900	26.6	1104.5	103.2	1589.3
800	850	24.4	1128.9	103.7	1693.0
750	800	24.2	1153.1	111.7	1804.6
700	750	22.7	1175.8	112.3	1916.9
650	700	9.4	1185.2	48.7	1965.7
600	650	0.5	1185.7	2.6	1968.2

Jökulsá á Fljótsdal water drainage basin

Elevation (m a. s. l.)		ΔS km^2	∑ΔS km^2	ΔQ_s ($10^6 m^3$)	$\sum\Delta Q_s$ ($10^6 m^3$)
1550	1600	0.0	0.0	0.0	0.0
1500	1550	0.0	0.0	0.0	0.0
1450	1500	0.3	0.4	0.0	0.0
1400	1450	1.2	1.6	0.1	0.1
1350	1400	2.8	4.4	0.6	0.7
1300	1350	5.4	9.8	2.8	3.6
1250	1300	15.8	25.6	15.5	19.1
1200	1250	14.8	40.4	19.2	38.3
1150	1200	16.4	56.9	26.2	64.5
1100	1150	14.0	70.9	27.2	91.7
1050	1100	11.7	82.6	27.7	119.4
1000	1050	10.8	93.4	29.4	148.7
950	1000	8.7	102.1	27.8	176.6
900	950	5.5	107.6	20.6	197.2
850	900	4.2	111.8	17.3	214.5
800	850	2.9	114.8	13.3	227.8
750	800	1.8	116.5	8.7	236.6
700	750	1.6	118.2	8.8	245.3
650	700	0.6	118.8	3.6	249.0

Hornafjarðarfljót water drainage basin

Elevation (m a. s. l.)		ΔS km^2	∑ΔS km^2	ΔQ_s ($10^6 m^3$)	$\sum\Delta Q_s$ ($10^6 m^3$)
1450	1500	0.1	0.1	0.0	0.0
1400	1450	6.5	6.6	3.7	3.7
1350	1400	11.6	18.3	7.3	11.1
1300	1350	18.9	37.2	15.0	26.0
1250	1300	37.3	74.6	36.8	62.8
1200	1250	28.7	103.2	32.2	95.1
1150	1200	19.9	123.1	27.6	122.7
1100	1150	18.3	141.4	30.7	153.4
1050	1100	13.8	155.2	27.9	181.2
1000	1050	10.6	165.8	24.2	205.4
950	1000	10.1	175.9	25.8	231.2
900	950	8.1	184.0	22.7	254.0
850	900	5.1	189.0	15.8	269.8
800	850	4.2	193.2	14.2	284.0
750	800	3.3	196.5	11.5	295.5
700	750	3.1	199.6	11.8	307.3
650	700	3.3	202.9	14.2	321.5
600	650	2.6	205.4	11.9	333.4
550	600	1.9	207.4	9.3	342.7
500	550	1.7	209.1	8.8	351.5
450	500	1.3	210.4	7.3	358.8
400	450	1.0	211.4	5.9	364.6
350	400	1.0	212.4	5.8	370.4
300	350	0.6	213.0	3.7	374.1
250	300	0.7	213.7	4.5	378.7
200	250	0.9	214.5	6.3	384.9
150	200	1.8	216.3	13.4	398.3
100	150	2.4	218.7	18.8	417.1
50	100	2.2	220.9	18.5	435.6
0	50	2.9	223.8	26.9	462.5

Jökulsá á Breiðamerkursandi water drainage basin

Elevation (m a. s. l.)		ΔS km^2	∑ΔS km^2	ΔQ_s ($10^6 m^3$)	$\sum\Delta Q_s$ ($10^6 m^3$)
1650	1700	0.5	0.5	0.1	0.1
1600	1650	2.6	3.1	0.2	0.3
1550	1600	15.3	18.5	1.8	2.1
1500	1550	22.7	41.2	7.4	9.5
1450	1500	36.2	77.4	19.2	28.7
1400	1450	50.9	128.3	35.4	64.2
1350	1400	83.0	211.4	71.9	136.1
1300	1350	82.6	294.0	74.4	210.5
1250	1300	51.0	344.9	48.9	259.4
1200	1250	33.6	378.5	38.2	297.7
1150	1200	27.2	405.7	38.4	336.1
1100	1150	22.1	427.8	37.5	373.6
1050	1100	18.4	446.2	36.1	409.6
1000	1050	14.5	460.7	32.4	442.1
950	1000	15.2	476.0	38.9	481.0
900	950	15.5	491.5	43.9	524.9
850	900	13.1	504.6	40.7	565.6
800	850	15.2	519.8	51.8	617.4
750	800	16.9	536.7	63.5	680.9
700	750	12.9	549.7	52.4	733.3
650	700	20.3	569.9	87.8	821.1
600	650	20.9	590.8	96.3	917.5
550	600	15.9	606.8	78.3	995.8
500	550	14.1	620.8	72.2	1068.0
450	500	4.8	625.6	25.8	1093.8
400	450	6.1	631.8	34.8	1128.6
350	400	5.7	637.5	34.3	1162.9
300	350	4.5	641.9	28.6	1191.5
250	300	4.6	646.5	31.3	1222.7
200	250	4.9	651.5	34.6	1257.3
150	200	4.4	655.8	32.2	1289.5
100	150	4.7	660.5	36.7	1326.2
50	100	4.1	664.6	34.3	1360.5
0	50	1.2	665.8	10.7	1371.3

Breiðárlón/Fjallsárlón water drainage basin

Elevation (m a. s. l.)		ΔS km^2	∑ΔS km^2	ΔQ_s ($10^6 m^3$)	$\sum\Delta Q_s$ ($10^6 m^3$)
1700	1750	0.0	0.0	0.0	0.0
1650	1700	0.0	0.0	0.0	0.0
1600	1650	0.0	0.0	0.0	0.0
1550	1600	1.2	1.2	0.1	0.1
1500	1550	2.5	3.8	0.7	0.9
1450	1500	3.8	7.5	1.2	2.1
1400	1450	4.8	12.3	2.3	4.4
1350	1400	6.3	18.7	5.1	9.5
1300	1350	12.5	31.2	12.8	22.3
1250	1300	6.4	37.6	7.3	29.7
1200	1250	5.5	43.1	7.1	36.7
1150	1200	4.7	47.8	6.8	43.5
1100	1150	4.2	52.0	7.2	50.6
1050	1100	4.6	56.7	8.9	59.5
1000	1050	5.6	62.2	11.8	71.3
950	1000	6.2	68.5	15.9	87.2
900	950	7.2	75.7	20.2	107.3
850	900	5.7	81.4	17.4	124.8
800	850	6.8	88.2	23.3	148.0
750	800	7.9	96.1	29.5	177.5
700	750	6.2	102.4	25.1	202.6
650	700	5.1	107.4	21.9	224.5
600	650	6.2	113.6	28.6	253.1
550	600	7.0	120.7	34.7	287.8
500	550	7.6	128.2	38.8	326.6
450	500	7.9	136.2	42.5	369.1
400	450	8.0	144.2	44.8	413.9
350	400	9.9	154.1	58.7	472.6
300	350	8.0	162.0	50.8	523.4
250	300	6.0	168.1	40.3	563.6
200	250	6.0	174.1	41.9	605.5
150	200	5.6	179.6	40.9	646.4
100	150	5.6	185.2	43.9	690.3
50	100	3.9	189.1	33.3	723.6
0	50	5.0	194.2	46.1	769.7

Skeiðarársandur (Gígja) water drainage basin

Elevation (m a. s. l.)		ΔS km^2	∑ΔS km^2	ΔQ_s ($10^6 m^3$)	$\sum\Delta Q_s$ ($10^6 m^3$)
1700	1750	0.0	0.0	0.0	0.0
1650	1700	15.9	15.9	6.5	6.5
1600	1650	65.3	81.2	19.8	26.3
1550	1600	82.4	163.6	26.4	52.7
1500	1550	110.7	274.3	47.8	100.5
1450	1500	106.4	380.7	69.7	170.2
1400	1450	103.6	484.3	82.6	252.8
1350	1400	90.7	575.0	84.5	337.3
1300	1350	77.4	652.4	83.1	420.4
1250	1300	68.7	721.1	85.9	506.3
1200	1250	59.7	780.8	86.8	593.1
1150	1200	54.1	834.9	91.7	684.8
1100	1150	50.3	885.2	97.4	782.2
1050	1100	45.4	930.6	104.0	886.2
1000	1050	40.0	970.6	104.4	990.6
950	1000	39.4	1010.0	112.4	1103.0
900	950	35.8	1045.8	109.5	1212.5
850	900	37.6	1083.4	123.2	1335.7
800	850	32.1	1115.5	114.8	1450.5
750	800	28.3	1143.8	110.2	1560.7
700	750	23.6	1167.4	98.0	1658.7
650	700	21.9	1189.3	97.3	1756.0
600	650	14.5	1203.8	70.5	1826.5
550	600	20.0	1223.8	103.7	1930.2
500	550	21.9	1245.7	120.8	2051.0
450	500	16.5	1262.2	93.8	2144.8
400	450	11.4	1273.6	68.3	2213.1
350	400	11.5	1285.1	70.7	2283.8
300	350	12.9	1298.0	82.2	2366.0
250	300	13.1	1311.1	88.1	2454.1
200	250	11.6	1322.7	83.0	2537.1
150	200	11.6	1334.3	86.9	2624.0
100	150	9.6	1343.9	75.8	2699.8
50	100	6.8	1350.7	55.6	2755.4
0	50	3.5	1354.2	29.9	2785.3

Djúpá water drainage basin

Elevation (m a. s. l.)		ΔS km^2	∑ΔS km^2	ΔQ_s ($10^6 m^3$)	$\sum\Delta Q_s$ ($10^6 m^3$)
1450	1500	0.1	0.1	0.1	0.1
1400	1450	0.3	0.4	0.4	0.5
1350	1400	0.6	1.0	0.9	1.4
1300	1350	3.4	4.4	5.1	6.5
1250	1300	3.2	7.5	5.2	11.8
1200	1250	2.9	10.4	5.4	17.2
1150	1200	3.2	13.6	7.0	24.2
1100	1150	5.0	18.7	12.5	36.7
1050	1100	5.0	23.6	14.4	51.1
1000	1050	8.4	32.1	26.3	77.4
950	1000	7.3	39.3	24.5	101.9
900	950	7.4	46.7	26.6	128.5
850	900	6.0	52.7	23.4	151.9
800	850	5.8	58.5	23.8	175.7
750	800	5.9	64.4	26.3	202.0
700	750	3.6	68.1	17.4	219.3
650	700	2.0	70.1	10.0	229.3
600	650	0.1	70.1	0.5	229.8

Brunná water drainage basin

Elevation (m a. s. l.)		ΔS km^2	∑ΔS km^2	ΔQ_s ($10^6 m^3$)	$\sum\Delta Q_s$ ($10^6 m^3$)
1000	1050	0.7	0.7	2.1	2.1
950	1000	1.8	2.4	6.0	8.1
900	950	3.8	6.2	13.7	21.8
850	900	3.9	10.1	15.0	36.8
800	850	3.6	13.7	15.0	51.8
750	800	3.9	17.7	17.2	69.1
700	750	4.4	22.1	20.6	89.7
650	700	5.2	27.2	25.9	115.6
600	650	2.5	29.8	13.2	128.9
550	600	0.0	29.8	0.0	128.9

Hverfisfljót water drainage basin

Elevation (m a. s. l.)		ΔS km^2	∑ΔS km^2	ΔQ_s ($10^6 m^3$)	$\sum\Delta Q_s$ ($10^6 m^3$)
1700	1750	0.0	0.0	0.0	0.0
1650	1700	4.6	4.6	1.9	1.9
1600	1650	9.1	13.7	4.7	6.6
1550	1600	10.6	24.3	6.4	13.0
1500	1550	20.8	45.1	15.1	28.1
1450	1500	40.1	85.3	33.8	61.9
1400	1450	26.5	111.8	25.4	87.4
1350	1400	24.0	135.8	29.7	117.1
1300	1350	22.5	158.3	34.5	151.6
1250	1300	17.2	175.5	31.0	182.7
1200	1250	20.3	195.8	40.8	223.4
1150	1200	14.2	210.1	32.5	255.9
1100	1150	10.6	220.7	27.4	283.3
1050	1100	9.4	230.1	27.3	310.6
1000	1050	8.4	238.5	26.6	337.2
950	1000	8.5	247.0	28.9	366.0
900	950	7.5	254.5	26.9	392.9
850	900	7.9	262.4	30.2	423.2
800	850	6.7	269.0	27.4	450.5
750	800	7.5	276.6	32.9	483.5
700	750	9.5	286.0	44.3	527.7
650	700	11.1	297.2	55.9	583.6
600	650	6.3	303.4	33.1	616.8
550	600	0.0	303.5	0.2	617.0

Skaftá water drainage basin

Elevation (m a. s. l.)		ΔS km^2	∑ΔS km^2	ΔQ_s ($10^6 m^3$)	$\sum\Delta Q_s$ ($10^6 m^3$)
1650	1700	2.0	2.0	1.2	1.2
1600	1650	14.9	16.9	9.0	10.2
1550	1600	22.9	39.8	15.7	25.9
1500	1550	31.9	71.7	25.7	51.6
1450	1500	24.6	96.3	21.6	73.3
1400	1450	22.4	118.6	25.1	98.3
1350	1400	20.4	139.0	30.2	128.6
1300	1350	22.1	161.1	40.6	169.2
1250	1300	14.8	175.9	32.5	201.7
1200	1250	20.2	196.1	52.1	253.8
1150	1200	22.0	218.0	64.8	318.7
1100	1150	23.1	241.1	75.7	394.4
1050	1100	21.8	262.9	79.1	473.5
1000	1050	24.8	287.8	99.5	573.0
950	1000	20.0	307.8	88.2	661.1
900	950	16.6	324.5	78.5	739.6
850	900	13.6	338.0	68.0	807.6
800	850	13.5	351.5	71.8	879.4
750	800	12.5	364.0	70.3	949.7
700	750	10.1	374.1	59.7	1009.4
650	700	5.5	379.5	33.9	1043.3
600	650	0.6	380.1	3.5	1046.8

Appendix F: Records of surface elevation change a surface velocity at mass balance survey sites on Vatnajökull.

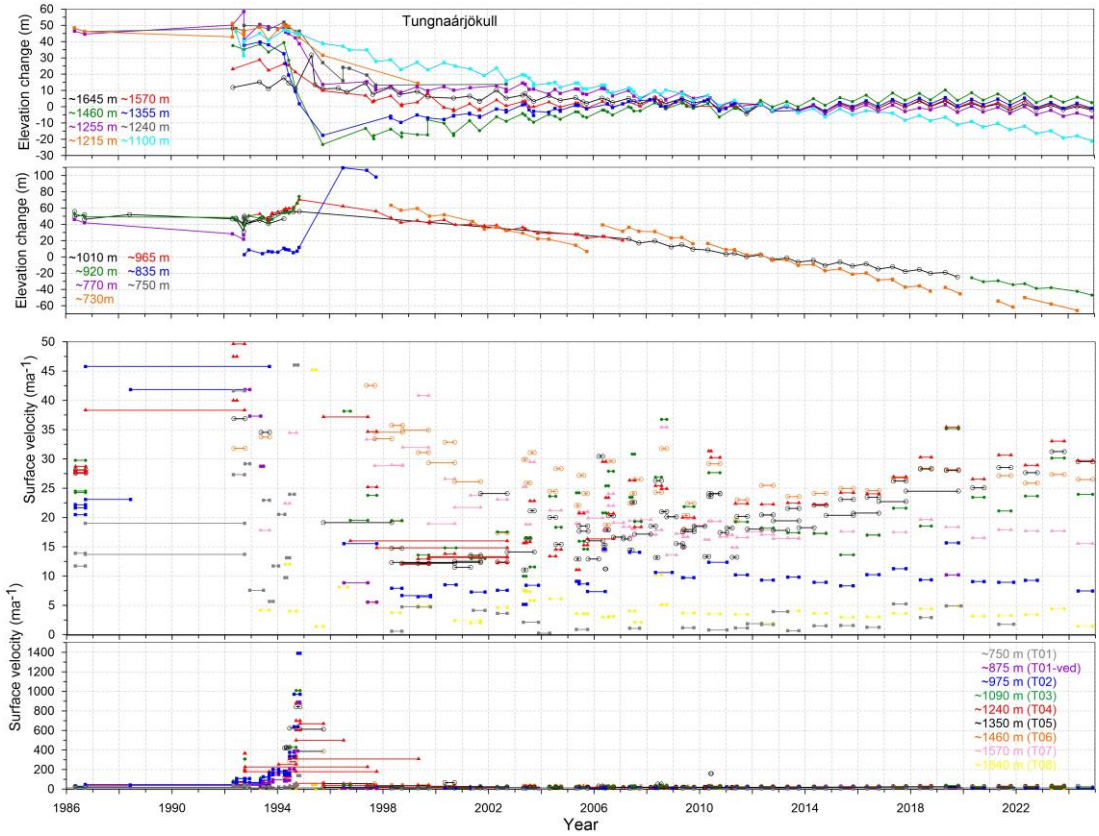

Surface elevation change relative to summer 2012 (upper panel) and average surface velocity (lower panel) at mb sites on Tungnaárjökull in 1986 to 2024.

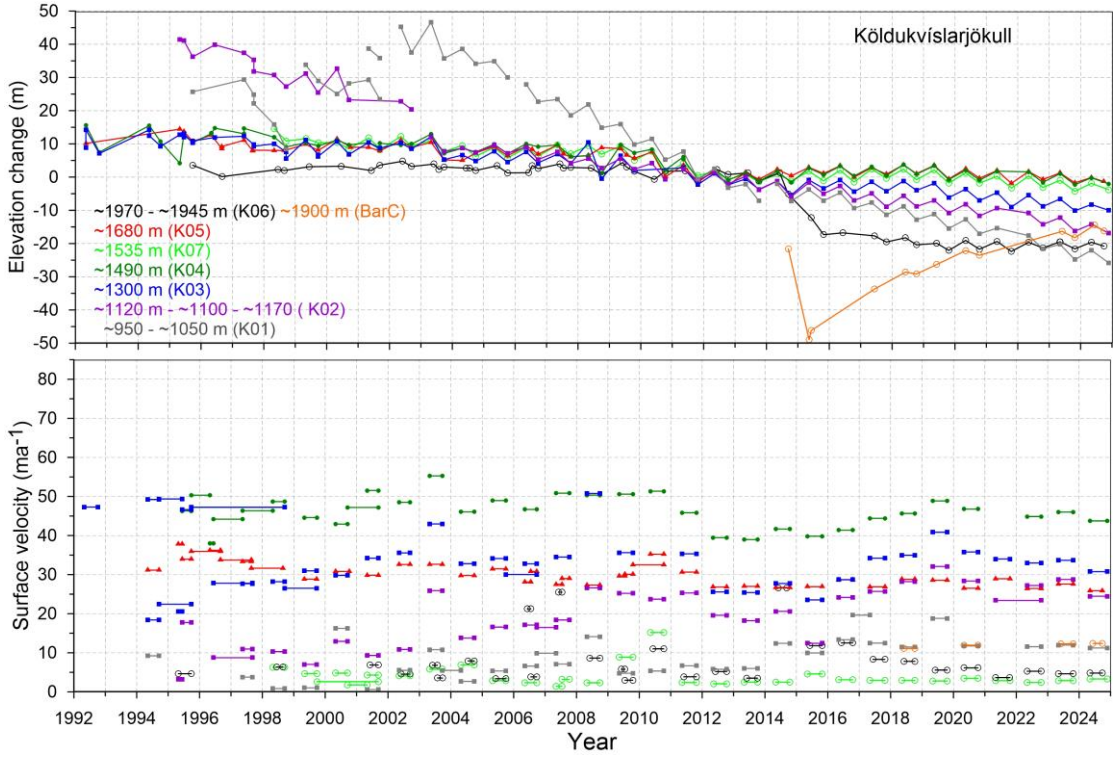

Surface elevation change relative to summer 2011-12 (upper panel) and average surface velocity (lower panel) at mb sites on Köldukvíslarjökull in 1992 to 2024.

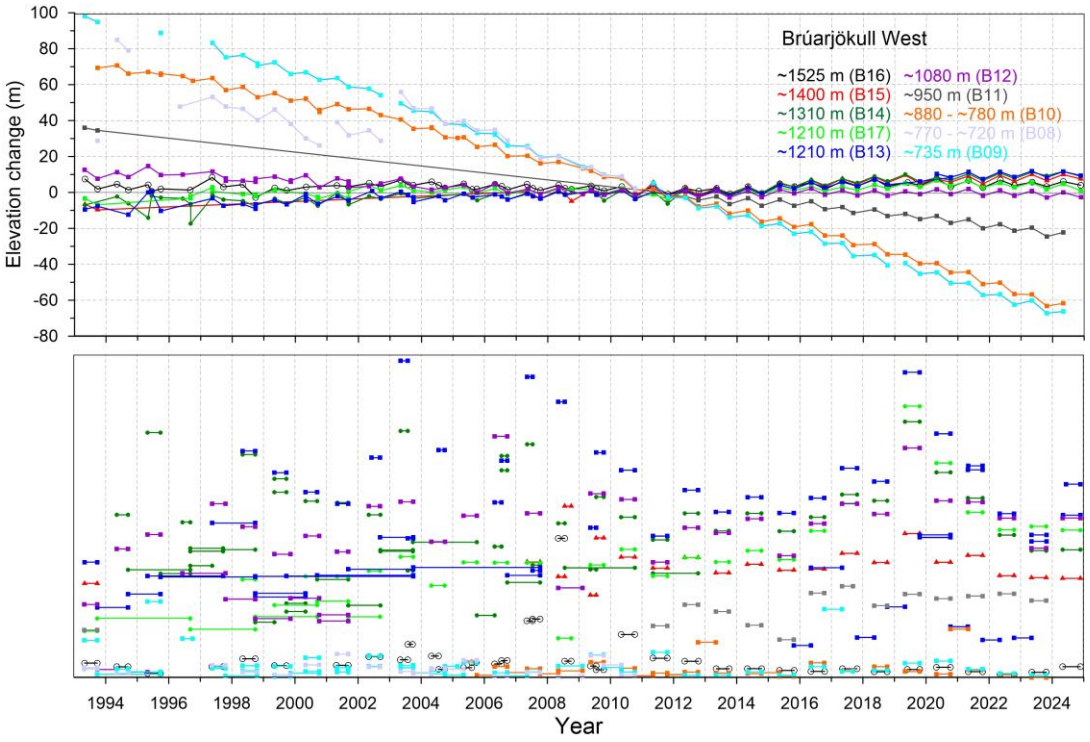

Surface elevation change relative to summer 2011 (upper panel) and average surface velocity at mb sites (lower panel) on W-Brúarjökull in 1993 to 2024.

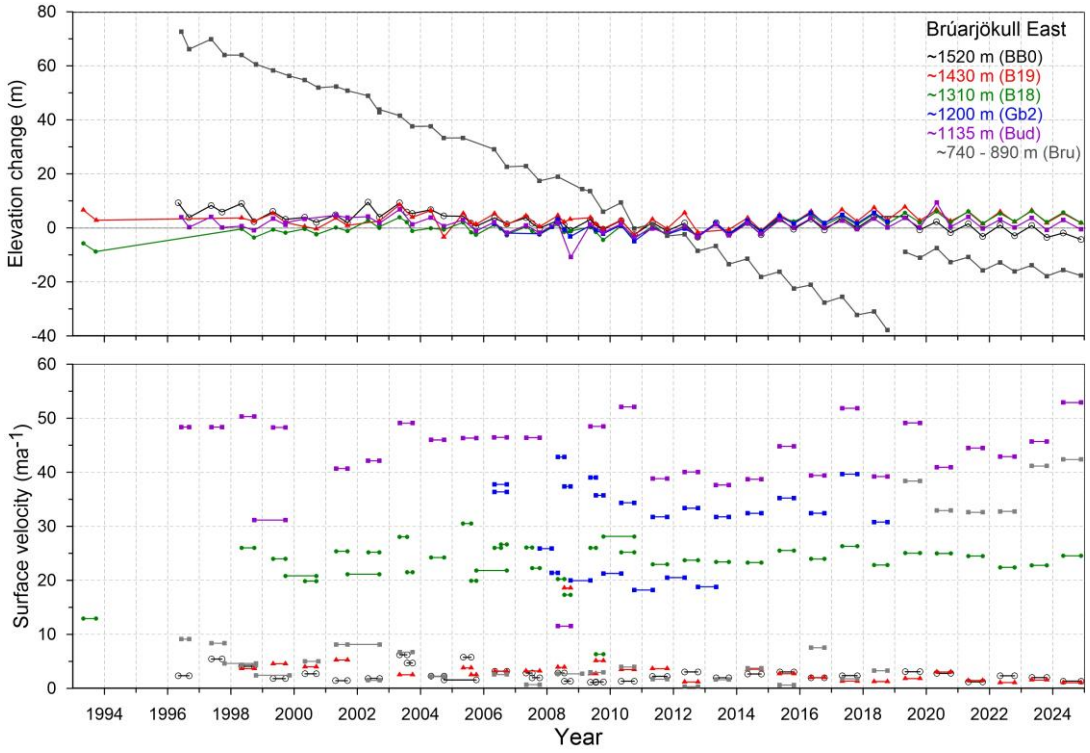

Surface elevation change relative to summer 2010 (upper panel) and average surface velocity at mb sites (lower panel) on E-Brúarjökull in 1993 to 2024.

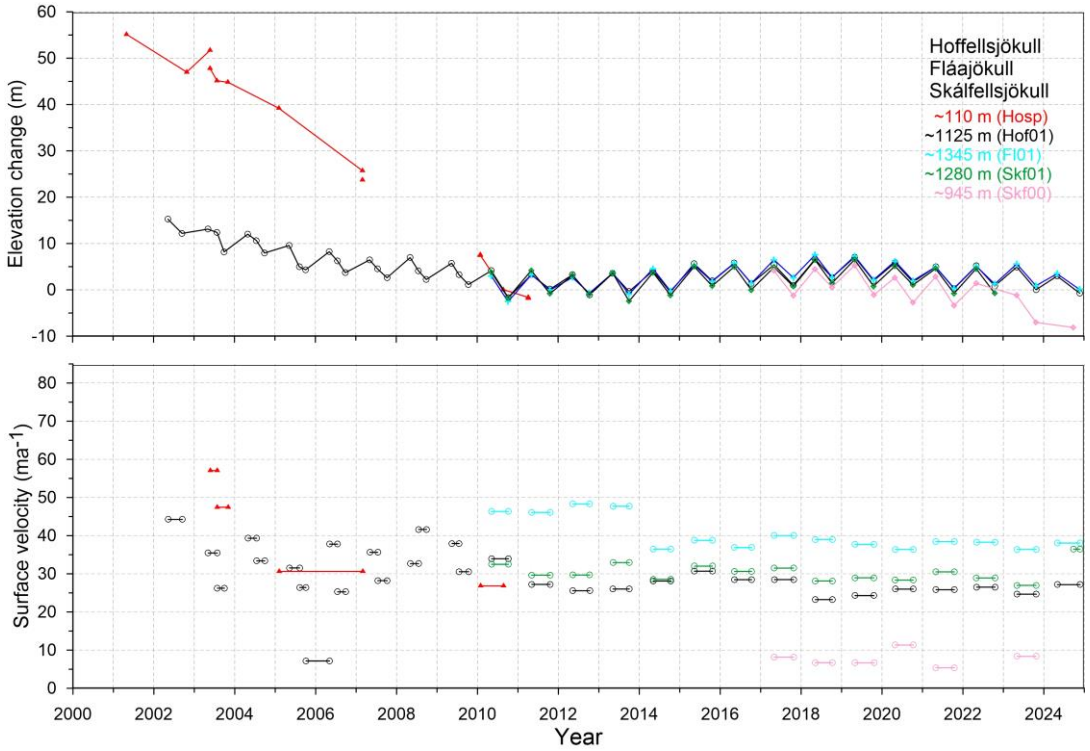

Surface elevation change relative to summer 2010 (upper panel) and average surface velocity) at mb sites (lower panel) on SE-Vatnajökull outlets in 2000 to 2024.

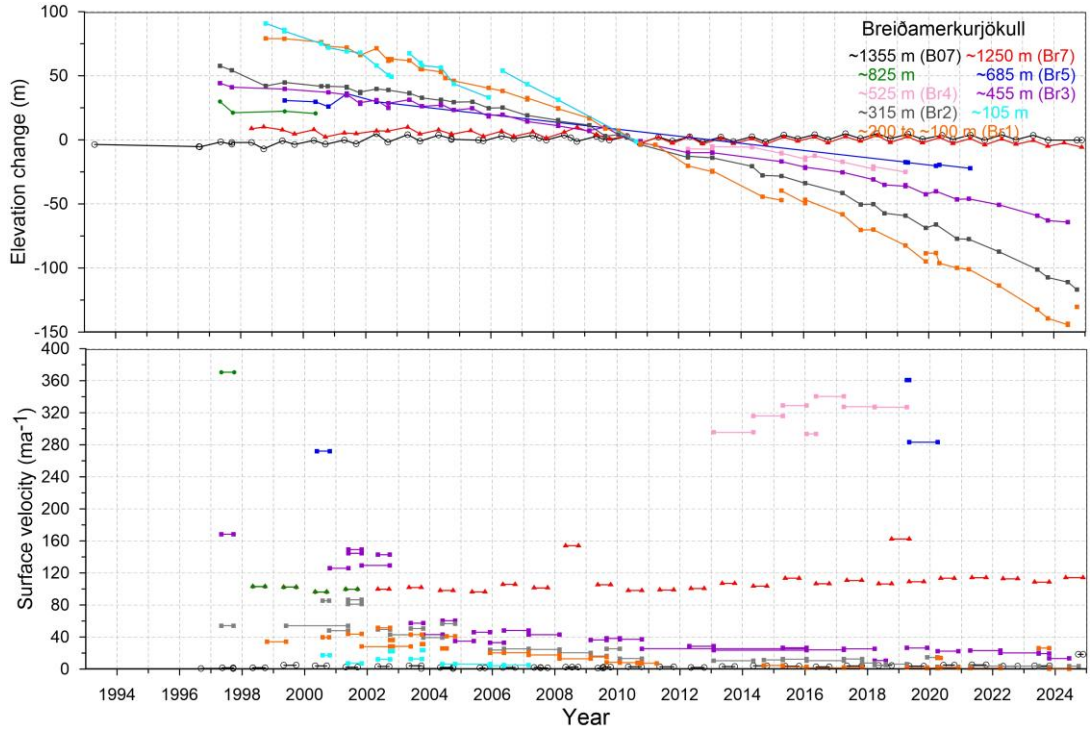

Surface elevation change relative to summer 2010 (upper panel) and average surface velocity at mb sites (lower panel) on Breiðamerkurjökull in 1993 to 2024.

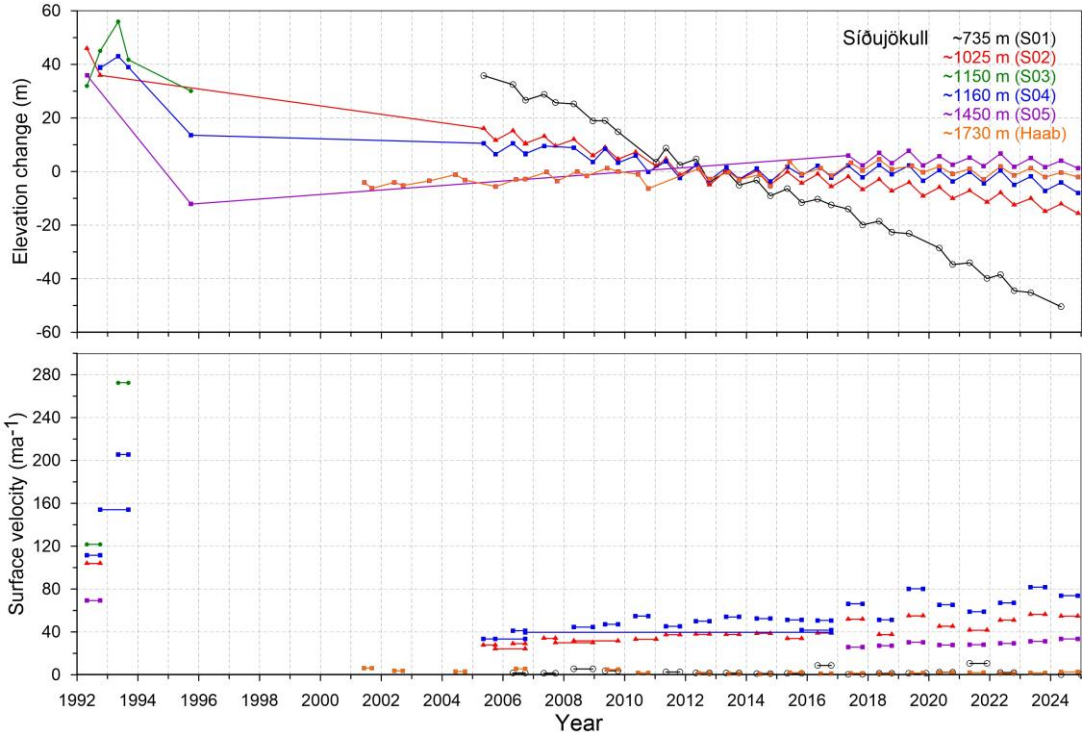

Surface elevation change relative to summer 2012 (upper panel) and average surface velocity at mb sites (lower panel) on Síðujökull in 1992 to 2024.

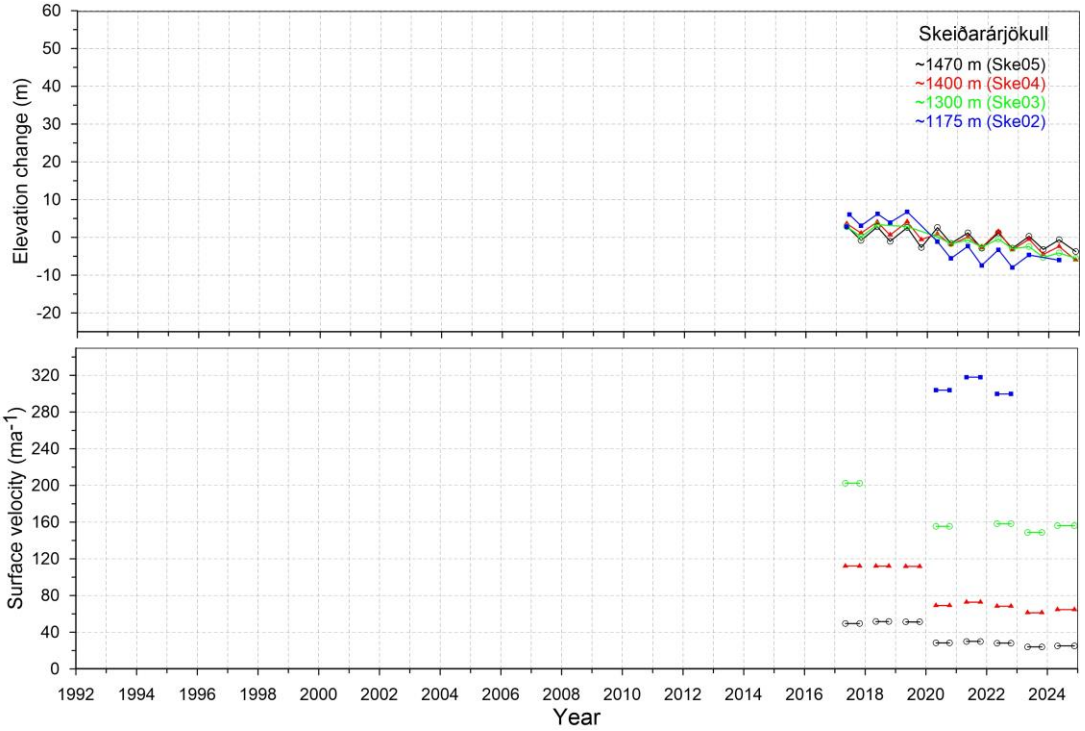

Surface elevation change relative to summer 2011-12 (upper panel) and average surface velocity at mb sites (lower panel) on Skeiðarárjökull in 2017 to 2024.

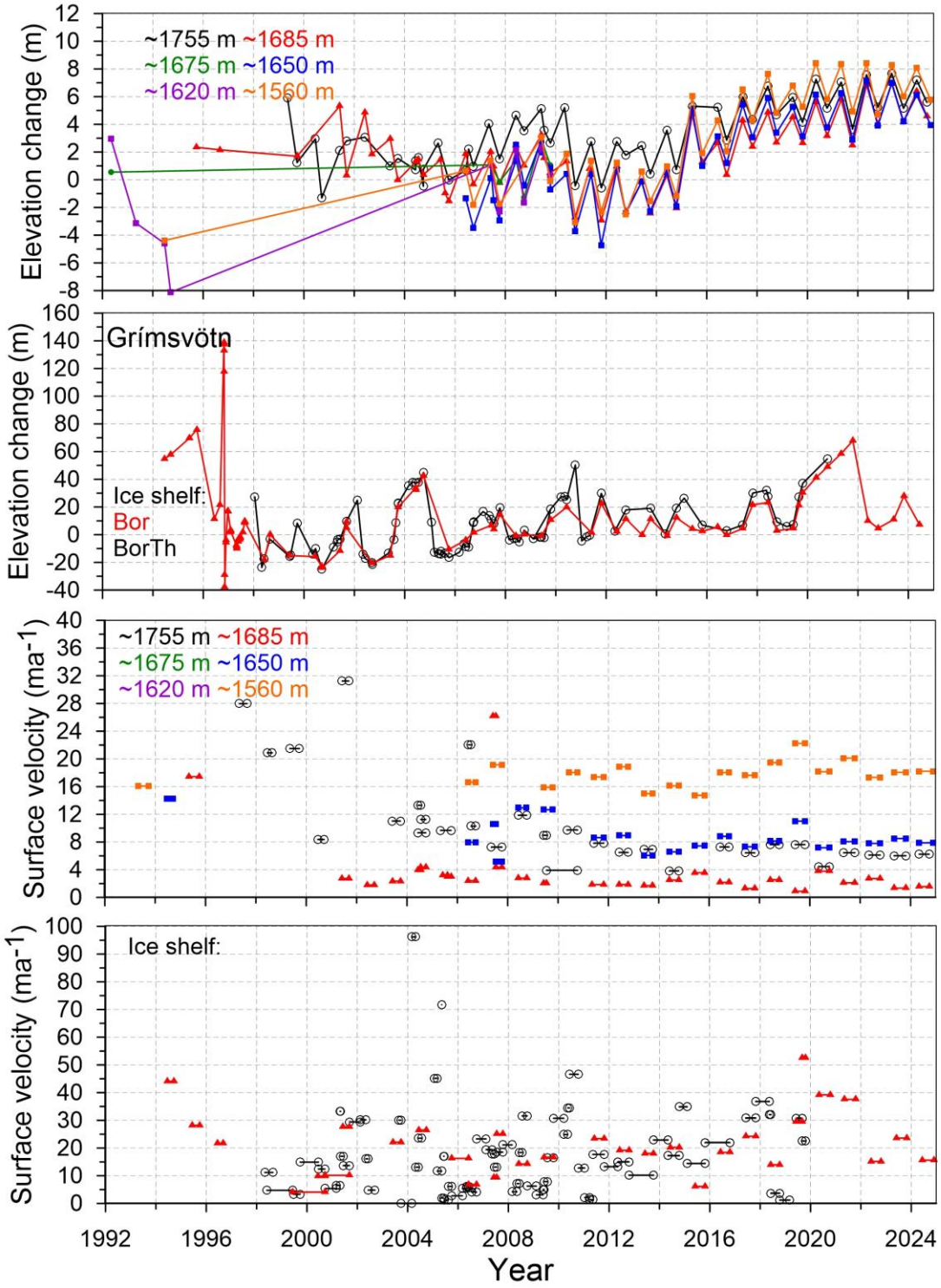

Surface elevation change relative to summer 2012 (upper panels) and average surface velocity at mb sites (lower panels) in Grímsvötn ice catchment in 1993 to 2024.